Monday Morning, October 19, 2015

Energy Frontiers Focus Topic
Room: 211B - Session EN+AS+EM+NS+SE+SS+TF-MoM

Solar Cells I
Moderator: Jason Baxter, Drexel University, Chintalapalle Ramana, University of Texas at El Paso

8:20am EN+AS+EM+NS+SE+SS+TF-MoM1 Elevated Temperature Phase Stability of CZTS-Se Thin Films for Solar Cells, *E. Chagarov, K. Sardashti,* University of California at San Diego, *D.B. Mitzi,* Duke University, *R.A. Haight,* IBM T.J. Watson Research Center, *Andrew C. Kummel*, University of California at San Diego
Density-functional theory simulations of CZTS, CZTSe and $CZTS_{0.25}Se_{0.75}$ photovoltaic compounds have been performed to investigate stability of $CZTS_{0.25}Se_{0.75}$ alloy vs. decomposition to CZTS, CZTSe and other secondary compounds. The Gibbs energy for vibration contribution was estimated by calculating phonon spectra and thermodynamic properties at finite temperatures. It was demonstrated that $CZTS_{0.25}Se_{0.75}$ alloy is stabilized not by enthalpy of formation but by vibration and mixing contributions to the Gibbs energy. A set of phase diagrams was built in multidimensional space of chemical potentials at 300K and 900K temperatures to demonstrate alloy stability and boundary compounds at various chemical conditions. The Gibbs energy gain/loss for several decomposition reactions was calculated as a function of temperature with/without Cu/Zn intermixing and vibration contributions to the Gibbs energy demonstrating $CZTS_{0.25}Se_{0.75}$ that even defect-free (no Cu/Zn intermixing) $CZTS_{0.25}Se_{0.75}$ can be stable at typical processing temperatures.

8:40am EN+AS+EM+NS+SE+SS+TF-MoM2 Chemical and Electrical Characterization of Polycrystalline CZTS,Se and CIGS,Se Grain Boundaries by NanoAuger and Kelvin Probe Force Microscopy (KPFM), *Kasra Sardashti*, UC San Diego, *P.D. Antunez, R.A. Haight,* IBM T.J. Watson Research Center, *A.C. Kummel*, UC San Diego
Polycrystalline Copper-zinc-tin-sulfide/selenide (CZTS,Se) compounds have received wide research interest due to their potential as inexpensive absorber materials composed of earth-abundant elements. Photovoltaic devices fabricated on CZTS,Se have reached conversion efficiencies of 12.6 %. One of the key parameters to further boost the conversion efficiency is to control the concentration of recombination sites at the surface, secondary phase interfaces and in the grain boundaries. To determine the presence of secondary phases on the surface and composition of grain boundaries, this work has employed Auger nanoprobe electron spectroscopy (NanoAuger) with 8nm lateral resolution combined with high resolution ambient Kelvin Probe Force Microscopy (KPFM) with dual-lock-in setup. NanoAuger was performed in planar and cross-sectional modes on CZTS,Se surfaces before and after top surface oxide removal by NH_4OH clean. Elemental maps before and after NH_4OH clean show Sn-/O-rich and Cu-poor grain boundaries suggesting that grain boundaries are terminated by tin-oxide (SnOx). Secondary phases such as SnSe and ZnSe were observed in the cross-sectional maps. Kelvin probe force microscopy (KPFM) on the cleaned surfaces showed that SnOx-terminated grain boundaries have 80-200 mV larger work function than grains, resulting in upward band bending between grains and grain boundaries. The upward band bending accompanied by the large valence band offset between the SnOx and CZTS,Se lead to relatively large energy barriers for both electrons and holes to travel into the grain boundaries and recombine. Comparison with the elemental maps for CIGSe (with device efficiencies as high as 18%) revealed the absence of the grain boundary oxide passivation.

9:40am EN+AS+EM+NS+SE+SS+TF-MoM5 Spin Coating Thin Film CZTS for Efficient, Low-Cost Solar Cells on Flexible Glass Substrates, *D. Kava, J. Galindo, C.O. Sana, S. Shahriar, Deidra Hodges*, University of Texas at El Paso
Photovoltaic's contribution to energy production continues to grow as costs continue to decrease. As silicon cells approach their limits, other materials are emerging. The development of Cu_2ZnSnS_4 (CZTS) thin film solar cells using non-vacuum liquid-based spin coating techniques have been previously investigated. The focus of this paper is the optimization of p-type CZTS thin film solar cells onto flexible substrates. Flexible solar panel costs are higher than their traditional counterparts. CZTS currently reports only a 3.2% efficiency on flexible glass, while the record for CZTS on non-flexible substrates is 12.6%. The cells are created using a single solution ink sol–gel method. All metals are dissolved in a single step prior to deposition onto substrates (nickel foil and corning willow glass) as a thin film. Corning

Willow glass is a new material introduced recently to the market, while nickel is a inexpensive flexible reflective foil. The Corning Willow glass is coated with a molybdenum layer as a reflective back contact layer. By using a single step and a solution deposition method, lower production cost are achievable. For thin film deposition, we used a non-vacuum spin coater (WS650 spin processor, Laurell Technologies) with an optimized spin coat programming. Annealing took place under vacuum in a RTP furnace while time, temperature and ramp functions were varied. The other layers of the device consists of cadmium sulfide n-type window layer and a zinc oxide doped with aluminum transparent top contact layer. Characterization and analysis of the thin films were performed using Raman spectroscopy, scanning election microscope (Zeiss NEON 40), X-ray diffraction (Philipps X'Pert), proflimeter (Veeco Dektak 150), UV-Vis-NIR Spectrophotometer (Carry 5000), Hall Effect measurement system (HMS3000) and 4 point probe (Lucas Labs) measurements. Results show CZTS thin film solar cells on flexible glass is obtainable.

10:00am EN+AS+EM+NS+SE+SS+TF-MoM6 Band Gap Profile of Cu(In,Ga)(Se,S) 2 Thin Films via High-Resolution Reflection Electron Energy Loss Spectroscopy, *Sung Heo*, *H.I. Lee, J.B. Park, G.S. Park,* Samsung Advanced Institute of Technology, Republic of Korea, *D.H. Lee, J.G. Nam,* Samsung, Republic of Korea, *H.J. Kang,* Chungbuk National University, Republic of Korea, *B.D. Choi*, Sungkyunkwan University, Republic of Korea
$Cu(In,Ga)Se_2$ (CIGS)-based solar cells was investigated with an aim of enhancing cell performance because these cells provided high conversion efficiency at relatively low cost. The efficiency of CIGS cells has recently approached 19.7% at small sizes. In general, $Cu(In_{1-x},Ga_x)(Se_{1-y}S_y)_2$(CIGSS) composition profiles are double-graded, and they can improve the open-circuit voltage (V_{OC}) and the efficiency of solar cells because band gaps increase toward both the surface (i.e., with the increase of sulfur) and the bottom (i.e., with the increase of gallium). It is important to accurately measure the band gap at the top and the bottom of the CIGSS cell. Nevertheless, the band gap profile measurement of the CIGSS as a function of depth is challenging.

In this study, we obtained the depth profile of the CIGSS cell using the quantitative Auger Electron Spectroscopy method, for which the relative sensitivity factor was corrected using the inductively coupled plasma-atomic emission spectrometry (ICP-AES) method. We also measured the band gap directly using high-resolution reflection electron energy loss spectroscopy (HR-REELS) with a monochromatic electron gun, which has low electron energy at 300 eV.

For the direct measurement of a band gap profile, HR-REELS spectra were obtained as a function of depth during Ar ion sputtering at 3.0 kV. The band gap profile shows a double-graded band gap as a function of depth. The band gap values are 1.32 eV at the surface (E_{g1}), 1.08 eV at the depth between 0.3 and 0.7μm ($E_{g\ min.position}$), and 1.50 eV at the depth of about 2.2 μm (E_{g2}), respectively. Our findings suggest a new analytical method which directly determines the band gap profile as function of depth.

10:40am EN+AS+EM+NS+SE+SS+TF-MoM8 Spatial Atmospheric ALD of Zinc Oxysulfide Buffer Layers for CIGS Solar Cells, *C. Frijters, P.J. Bolt, P. Poodt, Andrea Illiberi*, Solliance/TNO, Netherlands
Copper Indium Gallium di-Selenide (CIGS) solar cells are a promising approach in photovoltaic technology, having low production costs, high conversion efficiencies (> 20 %), as well as the possibility to manufacture them on flexible substrates. State-of-the-art in CIGS solar cells manufacturing is to use a stack of CdS, intrinsic ZnO (*i-ZnO*) and an Al-doped ZnO TCO on top of the CIGS film. Replacement of CdS by a non-toxic Cd-free layer with wider band gap (> 2.4 eV) would *a)* decrease the production cost by avoiding the expensive treatment of toxic wastes and *b)* increase the overall cell efficiency by enhancing the quantum efficiency in the blue range. Moreover, the use of a "soft" and highly conformal deposition technique is preferred to improve the electrical properties of the buffer layer/CIGS interface.

In this paper we present spatial atmospheric atomic layer deposition of a Zn(O,S) buffer layer as CdS replacement for CIGS solar cells. Spatial ALD is emerging as an industrially scalable deposition technique at atmospheric pressure which combines the advantages of temporal ALD, i.e. excellent control of film composition and uniformity on large area substrates, with high growth rates (up to nm/s). Films are grown by sequentially exposing the substrate to oxygen and sulfur precursors (H_2O, H_2S) and the zinc metal precursor (i.e., DEZn). By controlling the kinetics of surface reactions between evaporated precursors and reactive sites at the film surface, the composition of Zn(O,S) can be precisely tuned. The incorporation of S into

ZnO results in a bowing of the band gap in the range from 3.3 eV (ZnO) to 2.7 (S/O+S ~ 0.5) and 3.4 eV (ZnS), as measured by spectrophotometry. The morphology of the $Zn(O_{x-1},S_x)$ films varies from polycrystalline (for 0<x<30 and 70<x<100) to amorphous (30<x<70), as measured by X-ray diffraction. CIGS solar cells with a Spatial ALD Zn(O,S) buffer layer show an increased spectral response around 400 nm compared to solar cells with a CdS buffer layer. The solar cells with the Zn(O,S) buffer layer had an efficiency of 15.9 %, compared to 15.5 % for the reference solar cells with a CdS buffer layer.

11:00am **EN+AS+EM+NS+SE+SS+TF-MoM9 Deep Level Electron Traps in Epitaxial CuInSe$_2$ Probed using Photo-Modulated X-ray Photoelectron Spectroscopy**, *Nicole Johnson*, University of Illinois at Urbana-Champaign, *P. Aydogan*, Bilkent University, Turkey, *A. Rockett*, University of Illinois at Urbana-Champaign, *S. Suzer*, Bilkent University, Turkey

Performance in a variety of electronic devices is largely controlled by minority carrier charge capture on point defects. To date there is no experimental method to directly identify these point defects in a chemically specific fashion. Photo-modulated X-ray Photoelectron Spectroscopy (XPS) utilizes the chemical and charge sensitivity of XPS to identify changes in peak shape due to changing atomic charge state from capture of light-generated minority carriers. Epitaxial thin films of CuInSe$_2$ (CIS) were chosen as a case study for this technique because their defect chemistry is still relatively unknown as compared to traditional solar cell materials. The 500-1000nm thick films were grown by a hybrid sputtering and evaporation technique on GaAs(001) substrates at600-700°C. Aligned surface morphology features matching the substrate geometry in scanning electron microscopy (SEM) images indicate epitaxial growth, which was confirmed by x-ray diffraction (XRD).A layer of CdS was deposited on the CIS via chemical bath deposition to protect the CIS surface from oxidation in storage and to duplicate the heterojunction used in solar cells. Prior to loading in the XPS, the CdS was etched off to expose a Cd doped CIS surface for analysis. The photo-modulated XPS used monochromatic AlKα x-rays with a 532 nm laser as the illumination source. Under illumination, each film constituent was observed to exhibit unique binding energy shifts. Based on their peak shifts relative to the surface photovoltage profile, Cd and In were found to be right at the surface while Cu and Se were deeper into the film, consistent with a Cd-doped, In-rich surface. The technique is therefore shown to provide a chemically-sensitive depth profile non-destructively that can be obtained even on a relatively rough sample. Additionally, shape changes in the Se 3d doublet spectra indicate electron capture in a deep trap state that is likely due to cation vacancies. Measurements at varying temperatures indicate air-induced surface recombination states are passivated by annealing at 80C, allowing the surface photovoltage to persist. At 230C, an irreversible change happens in the surface properties such that the surface photovoltage gets much smaller and reverses sign. This work was supported by a joint NSF-TUBITAK collaborative research project (NSF Grant No: 1312539 TUBITAK Grant No: 212M051).

11:20am **EN+AS+EM+NS+SE+SS+TF-MoM10 The Role of ZnTe Buffer Layers on the Performance and Stability of CdTe Solar Cells**, *Jiaojiao Li*, Colorado School of Mines, *A. Abbas*, Loughborough University, UK, *D.M. Meysing, J.D. Beach, D.R. Diercks*, Colorado School of Mines, *M.O. Reese, T.M. Barnes*, National Renewable Energy Laboratory, *C.A. Wolden*, Colorado School of Mines, *J.M. Walls*, Loughborough University, UK

The use of ZnTe buffer layers at the back contact of CdTe solar cells has been credited with contributing to recent improvements in both record cell efficiency and module stability. To better understand the underlying reasons high resolution transmission microscopy (HR-TEM) and atom probe tomography (APT) were used to study the evolution of the back contact region before and after rapid thermal activation of this layer. During activation the 150 nm ZnTe layer, initially nanocrystalline and homogenous, transforms into a bilayer structure consisting of an amorphous region in contact with CdTe characterized by significant Cd-Zn interdiffusion, and a crystalline layer that shows evidence of grain growth and twin formation. This graded layer may passivate interface defects and account fo the improved open circuit voltage and fill factor that accompanies the RTP activation step. Copper, co-evaporated uniformly within ZnTe, is found to segregate dramatically after rapid thermal activation, either collecting near the ZnTe|Au interface or forming Cu$_x$Te clusters in CdTe at defects or grain boundaries near the interface. Further examination of the Cu$_x$Te clusters revealed that they are encased in a thin layer of Zn, and it is postulated that this structure may limit the extent of diffusion into CdTe and play an important role in device stability.

11:40am **EN+AS+EM+NS+SE+SS+TF-MoM11 The Performance and Durability of Broadband Anti-Reflection Coatings for Thin Film CdTe Solar Cells**, *G. Womack, P.M. Kaminski, **John Walls***, Loughborough University, UK

Light reflection from the glass surface of a photovoltaic (PV) module is a significant source of energy loss for crystalline silicon and all types of thin film PV devices. The reflection at the glass and air interface accounts for ~4% of the total energy. Single layer anti-reflection coatings using magnesium fluoride or porous silica with sufficiently low refractive index have been reported but these are only effective over a narrow range of wavelengths. In this paper we report on the design, deposition and testing of multilayer broadband anti-reflection coatings that reduce the weighted average reflection over the wavelength range used by thin film CdTe devices to ~1.22% resulting in a useful 3.6% increase in photocurrent. In this study we have used multilayer stacks consisting of silica and zirconia layers deposited using a reactive magnetron sputtering process. Details of the stack design, sputtering process parameters and the optical and micro-structural properties of the layers are provided.

Thin film CdTe devices pose a special problem because the anti-reflection coating is applied to one side of the glass while device layers are deposited directly on to the opposite glass surface in the superstrate configuration In thin film CdTe production, the glass is exposed to high temperature processes during the absorber deposition and during the cadmium chloride activation treatment. If glass pre-coated with a broadband anti-reflection coating is to be used then the coating must withstand temperatures of up to ~550°C. Surprisingly, our studies have shown that multilayer silica/zirconia anti-reflection coatings on soda lime glass remain unaffected by temperatures up to 600 °C at which point mild crazing is observed. This is an important observation since it means that low cost glass which is pre-processed with a broadband anti-reflection coating by glass manufacturers is potentially useable in thin film CdTe module production

Surface Science
Room: 113 - Session SS+AS+EN-MoM

Synthesis, Structure and Characterization of Oxides
Moderator: Sylvie Rangan, Rutgers, the State University of New Jersey

8:20am **SS+AS+EN-MoM1 Oxygen Uptake on Rh(111)**, *Daniel Killelea, J. Derouin, R.G. Farber*, Loyola University Chicago

Rhodium surfaces are of high utility for the partial oxidation of small molecules. We present results from a study of the uptake of gas-phase oxygen atoms on the Rh(111) surface. A combination of temperature programmed desorption (TPD), Auger electron spectroscopy (AES), and scanning tunneling microscopy (STM) were used to determine the total amount of oxygen, the oxygen surface coverages, and the surface structures, respectively. Our findings suggest that oxygen atoms are readily incorporated in to the near-surface region on Rh(111) while retaining low oxygen surface coverages and structures. We further studied how the surface changes when the subsurface oxygen atoms emerge to the surface. These finding provide insight to the formation of bulk oxides, and show that high-coverages of oxygen are not necessary for absorption of oxygen into the selvedge.

8:40am **SS+AS+EN-MoM2 Formation of Subsurface Oxygen and Surface Oxides on Ag(111) by Atomic Oxygen**, *Jonathan Derouin*, R.G. Farber, D.R. Killelea*, Loyola University Chicago

Understanding the interaction of oxygen with transition metal surfaces is important in many areas including corrosion and catalysis. The oxygen/silver system in particular has been studied extensively both experimentally and theoretically. Interest is driven largely by the role of silver in two widely used industrial reactions: the epoxidation of ethylene to produce ethylene oxide and the partial oxidation of methanol to produce formaldehyde. In addition, the oxygen/silver system can serve as a model for the dissociative chemisorption of diatomic molecules on close packed metal surfaces. Despite extensive research, the oxygen/silver system is still not well understood. To better understand this system, we use UHV-STM, AES and TPD to study the adsorption of atomic O on an Ag(111) crystal. Atomic O is generated by thermally cracking molecular O. By varying the power of the thermal cracker we are able to change the flux of atomic O reaching the Ag surface. Higher atomic O fluxes produce O structures

* Morton S. Traum Award Finalist

which desorb at significantly higher temperatures than structures produced with lower O fluxes. We then use UHV-STM to further characterize the various oxide structures produced.

9:00am SS+AS+EN-MoM3 Surface and Bulk Properties of Pure and Mixed Titania, *Matthias Batzill*, University of South Florida **INVITED**
Titanium oxide in its different polymorphs remains a model system for structure property relationships in simple oxides. In this talk we address issues related to both the bulk and the surface properties of TiO2. Measuring the photocatalytic activity of anatase- and rutile- epitaxial films we conclude that charge carriers excited deeper in the bulk contribute to the surface photocatalytic activity for anatase compared to rutile [1]. This difference may be an important factor for explaining the generally higher photocatalytic activity of anatase-TiO_2. In the second part of the talk, surface properties are presented on the example of rutile $TiO_2(011)$. The (011) surface orientation is less frequently studied compared to the (110) surface. Under UHV-conditions the (011) surface reconstructs into a complex 2x1 structure. We investigate the stability of this reconstruction under chemical adsorption. We find that for strongly adsorbing molecules the surface restructures to enable stronger adsorption. We show that this restructuring is strongly anisotropic resulting in quasi-1D adsorbate structures [2]. The instability of the rutile $TiO_2(011)$-2x1 surface may also be exploited for the formation of unique mixed oxide surfaces. This we demonstrate with iron oxide, which forms an ordered mixed TiFeOx surface oxide layer. Such mixed oxide surface may also form by impurity segregation from the bulk and thus may be a common surface structure in Fe-doped TiO_2.

[1] "Why is anatase a better photocatalyst than rutile? - Model studies on epitaxial TiO_2 films" T. Luttrell, S. Halpegamage, J.G. Tao, A. Kramer, E. Sutter, M. Batzill Sci. Rep. 4, 4043 (2014).

[2] "Adsorbate Induced Restructuring of $TiO_2(011)$-(2×1) Leads to One-Dimensional Nanocluster Formation" Q. Cuan, J. Tao, X.Q. Gong, M. Batzill Phys. Rev. Lett. 108, 106105 (2012).

9:40am SS+AS+EN-MoM5 Characterizations of Non-polar Polar Interfaces: Cr_2O_3 on ZnO (0001) and (000-1), *Xiaodong Zhu, M.D. Morales-Acosta, J. Shen, F.J. Walker, J. Cha, E.I. Altman*, Yale University
The growth of non-polar Cr_2O_3 on oppositely poled ZnO surfaces was characterized to determine how the polar substrate influences the properties of the non-polar film. Photoelectron spectroscopy (XPS and UPS), electron diffraction (RHEED and LEED), High-resolution transmission electron microscopy (HRTEM), X-ray diffraction (XRD) and X-ray reflectivity (XRR) have been performed to determine the growth mode, film quality and interfacial electronic properties are influenced by the substrate polarization. The growth is 2D; however, the films appear initially disordered on both substrates. With increasing film thickness, the films ordered with a well-defined epitaxial relationship. The HRTEM and XRD/XRR results for thicker films confirm a clear interface and well-defined lattice structure near the interface and throughout the film, indicating that above a critical thickness the entire film reorganizes into an ordered structure. The polar interfaces show a small but noticeable band offset that decayed with increasing film thickness. Statistical analysis of UPS valence band spectra revealed an enhanced density of states near the Fermi level for Cr_2O_3 on the positive surface consistent with stabilization of the positive interface by charge transfer; in contrast, no significant valence band differences were observed between bulk Cr_2O_3 and thin Cr_2O_3 thin layers on the negative surface. The results will be compared with those obtained for $ZnO/Cr_2O_3/$ ZnO (0001) and (000-1) to determine if the interfacial properties are sensitive to how the interface is formed.

10:40am SS+AS+EN-MoM8 Exploring Iron Oxide Clusters and Films Supported on HOPG with HREELS and AES, *Joel Langford*, University of California, Irvine, *F. Rosner*, Technical University of Munich, Germany, *J. Kwon, J.C. Hemminger*, University of California, Irvine
We are using High Resolution Electron Energy Loss Spectroscopy (HREELS) and Auger Electron Spectroscopy (AES) to investigate nanoclusters and films of iron oxide supported on highly oriented pyrolytic graphite (HOPG). For the films, two AES oxidation profiles were generated by annealing in oxygen. One profile was at a constant sample temperature of 500 K with varying exposure, the other by varying sample temperature while keeping exposure at a constant 1000 L. Both oxidation profiles saturate at an AES O/Fe ratio of 1.2. This ratio is below the O/Fe ratio of magnetite (Fe_3O_4), and hematite (Fe_2O_3) indicating incomplete oxidation of the film. Additional evidence for incomplete film oxidation comes from the absence of Fuchs-Kliewer phonons in the HREEL spectra. For the nanoclusters we are investigating two systems; polydispersed iron oxide nanoclusters on HOPG, and platinum nanoclusters supported on iron oxide nanoclusters. The polydispersed nanoclusters are more susceptible to oxidation than the film as evident by the higher AES O/Fe ratio and the

presence of Fuchs-Kliewer phonons in the HREEL spectra. The platinum nanoclusters are synthesized on the iron oxide nanoparticles by an ex-situ photodeposition technique and therefore adventitious carbon is adsorbed prior to transfer into the UHV chamber. To remove the adventitious carbon we annealed in oxygen at a sample temperature of 1000 K. HREEL spectra show that the annealing procedure removes adventitious carbon because of the absence and appearance of a CO resonance before and after cleaning, respectively. HREEL spectra after low temperature CO adsorption and as a function of subsequent anneal temperature will be presented.

11:00am SS+AS+EN-MoM9 Computational Materials Design®: Ionic Conduction in Rare-Earth-Metal Oxides from the First Principles-based Studies, *Susan Aspera, M. Sakaue, M. Alaydrus, T.P.T. Linh, N.H. Linh, H. Nakanishi*, Osaka University, Japan, *H. Kasai*, Akashi College, Japan
Solid oxide fuel cells (SOFC) have been one of the most promising technologies to tap alternative sources of energy. This technology utilizes abundant fuel materials such as H_2, CH_4 and other hydrocarbon materials to lessen our dependence on non-renewable fossil fuels that are nearly depleting. It takes into advantage the efficiency brought about by high kinetics of reaction at the electrolyte sides occurring at high working temperature. With this, ceramic based materials are often used as electrolyte and electrode materials. However, the working temperature of SOFCs is often too high (700˚C to 1000˚C). This limits the application of SOFCs and consequently high cost of producing durable materials for high working temperature. Recently, research related to this technology focuses on materials that work at intermediate temperature (IT-SOFC). This entails finding/designing materials that have high ionic conductivity at IT-SOFC working temperature.

Recent developments in computational simulation techniques, coupled with the rapid progress in computer efficiency, make first principles-based COMPUTATIONAL MATERIALS DESIGN (CMD®) a relevant field in the world of surface science and condensed matter physics. In this scheme, quantum mechanical calculations are performed to design promising materials and, understand the necessary mechanisms for the realization of an efficient technological device. Here, we employed the CMD® process and density functional theory-based analysis to study the atomic and electronic properties of several rare-earth-metal oxides (Pr_2NiO_2, La_2GeO_5, $LaGaO_3$ and CeO_2) which has potential application in IT-SOFC. These materials are known to have different structures according to symmetry, and the mechanism by which O ion conducts, i.e. via oxygen vacancies (O_{vac}) migration or O interstitial migration. The O ion migration path is dependent on the structure of the material, and the corresponding activation energy barrier for oxygen ion migration (E_{ac}) is affected by the concentration of O_{vac} and the presence of dopants, for O ion conduction via vacancies. In most of these systems, dopants with the same ionic radius as the host materials create high probability for O_{vac}, which then affects ionic conductivity, and the E_{ac} is found to be least for dopants with ionic radius near to that of the host material. Furthermore, as ionic migration is sensitive to the atomic structure, E_{ac} is party due to the structural alteration brought about by the presence of impurities such as dopants and creation of heterostructure interfaces. With these understanding, we can comment on the methods by which ionic conductivity can be enhanced in these materials.

11:20am SS+AS+EN-MoM10 Modeling and Characterization of Exemplar Sealing Glasses to Develop Chemistry-Structure-Property Relationships, *Michael Brumbach, T. Zeitler, T. Alam, M. Rodriguez, L. Criscenti, M. Kalan, A. Mirabal, D. Bencoe, K. Ewsuk*, Sandia National Laboratories
The performance of joining materials in many applications, such as glass-to-metal seals in solid oxide fuel cells and medical devices, require improvements in glass properties for greater reliability. In this work, simple sealing glass compositions have been used to develop experimentally-validated molecular models. The goal is to understand glass chemistry and structure such that modeling can be used to guide glass design, for manufacturability, and optimized performance. The coupled modeling and experimental work will be discussed.

Technological glasses are used in many applications where inorganic joining is required. Applications of joining glasses include glass in glass-to-metal seals (in solid oxide fuel cells or medical components), glass-bonded ceramics (such as debased aluminas), and low temperature co-fired ceramic (LTCC) packaging for microelectronics. For these applications, well-controlled processing conditions and high reliability in the end-product are of paramount importance. To better understand materials performance and reliability our objective is to develop experimentally-validated simulation tools to predict and control glass chemistry-structure property relationships. These tools will be used to predict structure-function relationships in bulk glasses and at joining interfaces.

Results from experimental characterization of several barium aluminosilicate glasses will be discussed. Solid-state NMR, lab-based and synchrotron X-ray scattering, and EXAFS have been used to determine structural characteristics of the exemplar glasses. Comparison of experimental results to molecular dynamics modeling of the three-component glass will be presented. Additional simulations of glass properties and comparisons to measurements will also be discussed.

Energy Frontiers Focus Topic
Room: 211B - Session EN+AS+EM+NS+SE+SS+TF-MoA

Solar Cells II
Moderator: Adrie Mackus, Stanford University

2:20pm **EN+AS+EM+NS+SE+SS+TF-MoA1 Influence of Annealing Temperature in the Bulk Defect Formation in Perovskite Thin Films**, *Weina Peng, B.X. Anand, L.-H. Liu, S.C. Sampat, B.E. Bearden, A.V. Malko, Y.J. Chabal*, University of Texas at Dallas
Perovskites are emerging as front-runners for solar cell applications because of their superior optoelectronic properties. Over the past few years the grain size of perovskites has been continuously improved from several hundred of nanometers to a few millimeters which resulted in better solar conversion efficiencies. In addition to surface and grain boundary related defects, perovskites are prone to the formation of bulk defects as well. However the role of bulk defects in the determination of photovoltaic performance of perovskites is rarely explored. To this end we investigate the impact of annealing temperature on the defect density in polycrystalline $CH_3NH_3PbI_3$ thin films of ~1 micron average grain size prepared using vapor assisted solution process (VASP). The photoluminescence (PL) intensity and lifetime show systematic reduction when the annealing temperature is increased from 150°C to 200°C. A rough estimate of the defect state density obtained using fluence dependent PL measurements reveal a 5 fold increase in defect density for a 25°C increase in annealing temperature although the average grains size stays unchanged. Furthermore, surface passivation of perovskite films using Al_2O_3 via atomic layer deposition leads to an improvement in PL intensity and lifetime. But the PL quantum efficiency, as well as the lifetime, of the surface passivated 200°C annealed sample remains significantly lower than that of the un-passivated 150°C annealed sample indicating that the majority of the defects states we observe in the high temperature annealed samples originate from bulk defects. Thus the present study shows that minimizing the number of bulk defects, in addition to surface defects, is very important in the realization of highly efficient perovskite solar cells.

3:00pm **EN+AS+EM+NS+SE+SS+TF-MoA3 Tandem Solar Cells Using Perovskites, Silicon and CIGS**, *M.D. McGehee, Tomas Leijtens*, Stanford University **INVITED**
The efficiency of perovskite solar cells has soared from a few percent to over 20% in the last 3 years. They are very attractive for multijunction solar cell applications because the bandgap of perovskite semiconductors can be easily tuned in the range of 1.55 to 2.2 eV and the open circuit voltage of the cells is large. We have made highly efficient semitransparent perovskite solar cells using silver nanowire meshes as the top electrode. These cells can be used in combination with either silicon or copper indium gallium diselenide solar cells to make four-terminal and two-terminal tandems. We will also present detailed characterization of perovskite semiconductors made with different processing conditions to show what needs to be done to minimize recombination and make the solar cells stable.

3:40pm **EN+AS+EM+NS+SE+SS+TF-MoA5 Lifetime, Mobility, and Diffusion of Photoexcited Carriers in Ligand-Exchanged Lead Selenide Nanocrystal Films Measured by Time-Resolved Terahertz Spectroscopy**, *G.W. Guglietta*, Drexel University, *B.T. Diroll, E.A. Gaulding, J.L. Fordham*, University of Pennsylvania, *S. Li*, Drexel University, *C.B. Murray*, University of Pennsylvania, *Jason Baxter*, Drexel University
Colloidal semiconductor nanocrystals have been used as building blocks for electronic and optoelectronic devices ranging from field effect transistors to solar cells. Properties of the nanocrystal films depend sensitively on the choice of capping ligand to replace the insulating synthesis ligands. Thus far, ligands leading to the best performance in transistors result in poor solar cell performance, and vice versa. To gain insight into the nature of this dichotomy, we used time-resolved terahertz spectroscopy measurements to study the mobility and lifetime of PbSe nanocrystal films prepared with five common ligand-exchange reagents. Non-contact terahertz spectroscopy measurements of conductivity were corroborated by contacted van der Pauw measurements of the same samples. The films treated with different displacing ligands show more than an order of magnitude difference in the peak conductivities and a bifurcation of time-dynamics. Inorganic chalcogenide ligand-exchanges with sodium sulfide (Na_2S) or ammonium thiocyanate (NH_4SCN) show high THz mobilities above 25 $cm^2V^{-1}s^{-1}$, which is desirable for transistors, but nearly complete decay of transient photocurrent within 1.4 ns. The high mobility with NH_4SCN and Na_2S exchanges is more than offset by their short lifetimes and results in diffusion lengths of only ~200 nm. In contrast, ligand exchanges with 1,2-ethylenediamine (EDA), 1,2-ethanedithiol (EDT), and tetrabutylammonium iodide (TBAI) show ~5x lower mobilities but much longer carrier lifetimes, with ~30% of photoexcited carriers remaining for >10 ns. The long lifetimes with EDA, EDT, and TBAI yield diffusion lengths of at least 500 nm, which is approaching the film thickness desired for strong light absorption in solar cells. This bifurcated behavior may explain the divergent performance of field-effect transistors and photovoltaics constructed from nanocrystal building blocks with different ligand exchanges.

4:00pm **EN+AS+EM+NS+SE+SS+TF-MoA6 iCVD Synthesis and Integration of Poly(vinylpyrrolidone) and Poly(4-vinylpyridine) as Polymer Electrolytes in Dye Sensitized Solar Cells**, *Yuriy Y. Smolin, S. Janakiraman, A.J. Sauter, M. Soroush, K.K.S. Lau*, Drexel University
Initiated chemical vapor deposition (iCVD) is used to synthesize and integrate poly(4-vinylpyridine) (P4VP) and polyvinylpyrrolidone (PVP) as polymer electrolytes within the mesoporous TiO_2 photoanode of dye sensitized solar cells (DSSCs). DSSCs with conventional liquid electrolytes are prone to leakage and evaporation, which hinders DSSC durability and field implementation. In addition, liquid electrolytes lead to significant electron recombination within the cells that limit DSSC performance. In contrast, polymer electrolytes do not suffer from the practical disadvantages and could potentially enhance the cell's I-V behavior.

However, in order to enable good contact between the TiO_2 electrode and the polymer electrolyte, a major obstacle is the difficulty in achieving good pore filling of the polymer into the mesoporous TiO_2 layer. Mesoscale pore diameter, high aspect ratio, and tortuous pore structure of the photoanode along with liquid surface tension, poor wettability, and solute steric hindrance make pore filling extremely limited when using liquid techniques. This leads to poor electrical contact and lower efficiency. To overcome the challenges of pore filling, we directly synthesized polymer electrolytes inside the pore volume of the photoanode using the solvent-free technique of iCVD. iCVD relies on the vapor delivery of monomer and initiator, which facilitates infiltration into the porous TiO_2 substrate, and by controlling the relative rates of diffusion and surface polymerization through iCVD process parameters, uniform and conformal growth of polymer is achieved. The pore filling of the polymer electrolyte into 5–10 µm photoanodes using iCVD is typically 90–100% which is significantly better than that achievable with liquid techniques like spin coating.[1]

In this work, we will show that iCVD P4VP and PVP polymer electrolytes can be effectively integrated within TiO_2 mesoporous photoanodes to produce enhanced DSSCs. By varying the polymer electrolyte chemistry including the use of a crosslinking agent during iCVD to stabilize the resulting polymer structure, DSSC I-V characteristics, such as open-circuit voltage, short-circuit current density and fill factor, are tuned.[2] To gain a better understanding on the effect of the polymer electrolyte, experimental techniques such as linear sweep voltammetry, intensity modulated spectroscopy, and impedance spectroscopy are used. Mathematical modeling of DSSC behavior is also performed to relate these experimental observations with the dynamics of the operation of the cell.

1. S. Nejati and K. K. S. Lau, *Nano Lett.*, 2010, 11, 419-423.

2. Y. Y. Smolin et al., *J. Power Sources*, 2015, 274, 156-164.

4:20pm **EN+AS+EM+NS+SE+SS+TF-MoA7 Interfacial Effects on Device Performance in Organic Solar Cells**, *Huanxin Ju, J.F. Zhu*, University of Science and Technology of China, *D.S. Ginger*, University of Washington
The better understanding of the underlying mechanisms is essential for the further development of highly efficient organic photovoltaics (OPVs) devices. In this paper, the transient photovoltage (TPV) and charge extraction (CE) measurements in combination with the synchrotron radiation photoemission spectroscopy (SRPES) were used to gain insights intothe correlation between the microscopic interfacial properties and macroscopic device performance. The OPV devices based on PCDTBT: $PC_{70}BM$ with Ca interlayer were studied as a reference system to investigate the interfacial effects on device performance. The charge carrier decay dynamics demonstrated that the device with the Ca interlayer exhibited a lower recombination constant (k_{rec}) than that only with the Al cathode at a given charge carrier density (n). In addition, the interfacial energy band structures indicated that the strong dipole moment produced by the Ca interlayer can facilitate electron extraction as well as drive hole away at the cathode/polymer interface, resulting in retarding interfacial recombination losses. Finally, we examined the device performance with the Ca interlayer to find that the efficiency is improved by 28% as compared to that without

the Ca interlayer, which shows good correlation with the observed interfacial properties.

4:40pm EN+AS+EM+NS+SE+SS+TF-MoA8 Tungsten-Titanium Mixed Oxide Thin Films for Improved Structural and Optical Properties for Solar Driven Applications, *Mirella Vargas*, The University of Texas at El Paso, *N.R. Murphy*, Air Force Research Laboratory, *R.V. Chintalapalle*, The University of Texas at El Paso

Tungsten oxide (WO_3) is a well-established n-type semiconductor possessing unique optical and electronic properties. WO_3 has become the most interesting inorganic material for electrochromic applications due to the reversible spectral absorption properties associated with WO_3. WO_3 thin films and nanostructures exhibit an optical band gap that permits efficient use of the solar spectrum including absorption in the blue part of the visible region and the ultraviolet region, as well as a high transmission region that extends from the near-infrared (IR) to the visible spectrum. Coupled with good electronic transport properties, photosensitivity, and chemical integrity, WO_3-based materials are attractive for applications related to sustainable energy production including energy efficient windows and architecture, photoelectrochemical (PEC) water-splitting, photocatalysis and solar cells. Anion or cation doping into WO_3 has been extensively studied as this offers the opportunity to tailor the transport properties that may influence the efficiency of solar driven devices. Titanium doping into WO_3 has proven to enhance the electrochromic response and the cyclic lifetime by a factor of five in PEC devices. In the present case a systematic investigation of progressively increasing the Ti content in the W-Ti target for reactive sputtering has been employed to tune the structure, chemistry, and properties of the films. Tungsten-titanium (W-Ti) mixed oxide thin films were fabricated using reactive sputtering of W-Ti alloy targets with Ti content ranging from 0 to 30 wt.%. X-ray photoelectron spectroscopy confirms the existence of W and Ti in their highest oxidation state of +6 and +4, respectively. Quantification of binding energy shifts for W and Ti core-level transitions confirms the formation of WO_3-TiO_2 composite oxide films. Optical analyses made from spectrophotometry measurements indicate a decrease in band gap with a discrete amount of Ti incorporation. The band gap decreases with increasing Ti from 3.0 eV to 2.5 eV. Such films are expected to have the possibility for tuning the electrical conductivity while retaining the optical transparency to make them efficient for photoelectrochemical cells and photovoltaics.

5:00pm EN+AS+EM+NS+SE+SS+TF-MoA9 Potential Resolution to the "Doping Puzzle" in Pyrite FeS₂, *X. Zhang, M. Li, L. O'Brien, J. Walter, M. Manno, F. Mork, J. Kakalios, Eray Aydil, C. Leighton*, University of Minnesota

In principle, pyrite FeS_2 is one of the most suitable photovoltaic materials for sustainable low-cost, large-scale solar cell manufacturing because it has high absorbance in the visible and comprises earth-abundant inexpensive elements. However, current efficiencies of solar cells based on pyrite FeS_2 have not exceeded 2.8%. Early research on this material concluded that unintentionally doped FeS_2 thin films are *p*-type and subsequent solar cell work evolved based on this presumption. In fact, it is now widely accepted that FeS_2 thin films almost always exhibit *p*-type conduction even though single crystals are typically found to be *n*-type. This discrepancy between single crystals and thin films is perplexing and to date this puzzle remains unexplained. In this talk we reexamine the conclusion that undoped FeS_2 films are predominantly *p*-type and provide an explanation for this "doping puzzle" in pyrite. Using a combination of Hall effect, thermopower, and temperature-dependent resistivity measurements on a large set of well characterized single crystals and thin films, we show that the widely accepted predominant *p*-type behavior in pyrite films may, in fact, be an artifact of hopping conduction and should be revisited. Specifically, both Hall effect and thermopower measurements establish that all of our high-mobility (>1 cm^{2}V^{-1}s^{-1}) films and single crystals are *n*-type. Temperature-dependent resistivity measurements on these high mobility films and crystals establish diffusive electronic transport. We find that films with lower mobility (4×10^{-3}-1 cm^{2}V^{-1}s^{-1}) also show *n*-type Hall effect but exhibit a *p*-type Seebeck coefficient, leading to a discrepancy in the measured carrier type. Temperature-dependent resistivity measurements on these intermediate mobility films show a transition from diffusive to hopping transport. Finally, both Hall and Seebeck coefficients are strongly suppressed and invert in the lowest mobility thin films ($<4 \times 10^{-3}$ cm^{2}V^{-1}s^{-1}) indicating apparent *p*-type conduction. Temperature-dependent resistivity measurements establish unambiguous hopping behavior in these lowest mobility films. Based on this evolution of Hall and Seebeck coefficients with carrier mobility, and the well-known suppression of the Hall and Seebeck effects in conductors with hopping electronic transport, we conclude that the apparent crossover from *n*-type to *p*-type with decreasing mobility is, in fact, an artifact of hopping conduction.

5:20pm EN+AS+EM+NS+SE+SS+TF-MoA10 Interparticle Contact Radius and Electron Transport in Thin Films Comprised of Nanocrystals, *Elijah Thimsen, D. Lanigan*, Washington University, St. Louis

Thin films comprised of nanocrystals are being explored for a variety of applications that involve electron transport. For traditional applications such as photovoltaic solar cells, the goal is often to utilize solution processing to make an inexpensive thin film that essentially behaves as a bulk material with diffusive transport. For other applications, such as neuromorphic computing, variable range hopping (VRH) transport is more desirable because it enables a given nanocrystal to have orders of magnitude more nearest neighbors than it physically touches. It is of paramount importance that the structure-property relationships that control electron transport mechanism be elucidated. Previous work has demonstrated that interparticle separation distance affects charge carrier mobility. However, for films comprised of nanocrystals that are physically touching, what is the effect of contact radius? In this work, we present a systematic experimental study of the effect of interparticle contact radius on the electron transport mechanism in thin films comprised of heavily-doped ZnO nanocrystals embedded in Al_2O_3. As the contact radius increased, the electron transport mechanism crossed over from VRH to diffusive conduction. For large contact radius between nanocrystals, the room-temperature electron mobility in the film approached the local mobility within a nanocrystal, approximately 10 cm^{2}V^{-1} s^{-1}. The conclusion is that for nanocrystals that are physically touching, the interparticle contact radius determines the transport mechanism. With the ability to control the electron transport mechanism in films comprised of ZnO nanocrystals, we performed an exploratory study of the Hall effect in these materials. Hall effect measurements are of great utility and are routine for determining charge carrier mobility and type, but the interpretation of data for materials that exhibit VRH has been difficult in the past. For well-connected ZnO nanocrystals that exhibit diffusive conduction, the Hall coefficient was independent of temperature, as expected for the high doping level. Alternatively, for films with small contact radius between nanocrystals, which exhibited a VRH transport mechanism, we observed an anomalous behavior of the Hall coefficient at low temperature (100 to 200 K). Surprisingly, for films that exhibited VRH, the magnitude of the Hall coefficient increased exponentially with decreasing temperature, in stark contrast to the conventional wisdom that the Hall effect is suppressed for VRH.

Advanced Surface Engineering
Room: 212A - Session SE+EM+EN-MoA

Thin Film Technologies for Energy Storage, Conversion and Harvesting
Moderator: Michael Stueber, Karlsruhe Institute of Technology, Andrey Voevodin, Air Force Research Laboratory

2:20pm SE+EM+EN-MoA1 Properties of Zinc Oxide Thin Films Grown on Silicon Wafers by Pulsed Laser Deposition, *Yilu Li, J.W. Wrobel, M.K. Michael*, University of Missouri-Kansas City

Pulsed ultraviolet light from a XeF excimer laser was used to grow thin films of zinc oxide on (111) p-type silicon wafers within a versatile high vacuum laser deposition system. Pressure, target temperature and distance from the target to the substrate can be adjusted in the system. Scanning electron microscopy, energy dispersive X-ray spectroscopy, X-ray diffraction spectroscopy and ellipsometry had been used to analyze the structures and properties of ZnO thin film products.

3:00pm SE+EM+EN-MoA3 Synthesis of Crystallized and Nanostructured TiO₂ Thin Films by Reactive Magnetron Sputtering for Application as Photoanode in Dye Sensitive Solar Cells, *J. Dervaux, P.-A. Cormier, S. Konstantinidis*, Université de Mons, Belgium, *P. Moskovkin, S. Lucas*, University of Namur, Belgium, *Rony Snyders*, Université de Mons, Belgium

Nowadays, the efficient use of renewable energies, and more specifically of solar energy, represents a major economic and environmental issue. Among the potential solutions, the Dye Sensitive Solar Cells (DSSC) present many advantages. In order to improve the efficiency of DSSC, TiO_2 nanoparticles, which are usually used as photo-anode, could be replaced by nanostructured TiO_2 thin films. Indeed, a photo-anode of ordered porous nano-columnar TiO_2 would provide large surface area for dye absorption, fast electron transfer path, enhanced light trapping, and tight interfaces to conducting electrodes and contributes to a high fill factor and an overall higher cell efficiency. In view of this application, the anatase phase of TiO_2 is usually

the preferred polymorph as electron acceptors in DSSCs even if a synergistic effect exists between anatase and rutile with an optimal rutile content of around 13 wt%.

In this work, nanostructured and crystallized TiO_2 thin films are synthesized by reactive magnetron sputtering combined with Glancing Angle Deposition (GLAD). The substrate temperature, the substrate bias voltage and the rotation speed were varied in order to determine the best experimental conditions leading to (nano-)porous films with anatase TiO_2 columns. The chemical composition, the crystalline structure and the microstructure of the films were analyzed by XPS, XRD, SEM and TEM, respectively while the surface area is evaluated by the BET method.

It is demonstrated that many type of microstructures (tilted columns, straight pillars, chevrons,…) are obtained by combining the GLAD parameters and the sputtering conditions. On the other hand, depending on these growth conditions, the phase constitution can be tuned from amorphous to pure rutile or anatase phases including mixtures of both polymorphs. The surface area of the synthesized layer strongly depends on the experimental conditions and on the associated microstructure. The highest obtained value is of ~ 140 m^2/g for a tilted columnar amorphous/anatase sample which is significantly better than the values reported for TiO_2 nanoparticules systems (~ 60 m^2/g). On the other hand, a clear correlation between the surface area and the dye absorption is demonstrated revealing a good impregnation of the layer. It is also demonstrated that this impregnation behaviour is depending on the size of the dye molecule revealing different populations of pores as a function of their size. This is supported by TEM and modelling data using NASCAM, a 2D-3D Kinetic Monte Carlo code for the simulation of deposition, diffusion, nucleation and growth of films on a surface.

3:20pm SE+EM+EN-MoA4 Silver-Carbon-Nanotube Metal Matrix Composites for Metal Contacts on Space Photovoltaic Cells, *Omar K. Abudayyeh, C. Nelson, S.M. Han,* University of New Mexico, *N. Gapp, D.M. Wilt*, Air Force Research Laboratory
The advanced solar cells used in space vehicles today are rapidly moving towards thin-film-based inverted metamorphic multijunction (IMM) solar cells mounted on flexible substrates. However, the IMM cells are more prone to cracking than state-of-the-art triple junction cells. The cell cracking can lead to metal contact failure on IMM cells, compromising the power generation. To mitigate the power loss and increase the lifetime of IMM cells, silver metal films imbedded with carbon nanotubes (CNTs), otherwise known as metal matrix composites, have been developed and investigated for the reinforced mechanical strength against stress-induced cracking. We have primarily focused on (1) surface functionalization of CNTs to make their surface more hydrophilic and wetting to metals, (2) optimization of a cyanide-free electrochemical deposition of silver, (3) electrochemical deposition, drop casting and nanospreader technique to control the composite microstructure, and (4) mechanical and electrical characterization of the composite films. We observe that carboxylation of CNTs produces a stable, homogeneous suspension of negatively charged CNTs at pH > 6. Lustrous-mirror-finish silver films are also successfully deposited, using a commercial cyanide-free silver-plating solution with precise control of current density. Currently, one of the microstructures being explored is a silver-carbon-nanotube layer-by-layer structure, where the surface coverage of CNTs is an important parameter that directly affects the CNT packing fraction and metal intercalation through the CNT network. We quantify the CNT surface coverage as a function of different deposition variables by digitally analyzing scanning electron microscopy images. In this presentation, we will further discuss how this surface coverage correlates to the mechanical and electrical properties of the MMC films. We characterize the mechanical properties, using nanoindentation and strain failure tests. The initial nanoindentation analysis reveals that the composite film has a lower elastic modulus (10 GPa) than pure silver (73 GPa) or CNT (1000 GPa). The lower elastic modulus is attributed to the electroplating process of silver, in which hydrogen is incorporated and trapped within the composite. Our finite element analysis also corroborates this speculation, where the elastic modulus near 10 GPa is predicted with approximately 4% void fraction. While the composite elastic modulus is lower than that of pure silver, the strain failure tests show that carbon nanotubes can bridge 20 to 50-mm-wide microcracks, maintaining electrical conductivity of the composite.

3:40pm SE+EM+EN-MoA5 Laser Liftoff of Single Crystal GaAs Thin Films and Energy Conversion Devices, *Bruce Clemens, G. Hayes, V. Parameshwaran, A. Jan, J.B. Reeves*, Stanford University **INVITED**
GaAs and related III-V sphalerite materials offer a wide array of tunable characteristics that lend themselves to many advanced device technologies. However, the cost of GaAs substrates limits their use, specially for photovoltaics. Separating epitaxially-grown layers from a growth substrate can reduce costs, however the current approach, which uses an acid to laterally etch an epitaxial sacrificial layer, is slow and can damage other device layers. Here, we demonstrate laser lift-off as a new approach that is orders of magnitude faster, and that enables more freedom in the selection of other device layers. We grow a structure with a spatially-tuned optical absorption coefficient by growing a small-band-gap, pseudomorphic layer between the GaAs substrate and a GaAs film and device structure. By using InGaAsN with a band gap of 0.9 eV for this layer, we achieve high absorption of 1064 nm (1.17 eV) light from a Nd:YAG nanosecond laser pulse, while GaAs is essentially transparent for this wavelength. Illumination through the back of the GaAs substrate with laser fluences of about 0.7 J/cm^2 achieves transfer of the GaAs layer to a flexible polymer substrate. Transmission electron microscopy and x-ray diffraction show that the initial InGaAsN layer is coherently strained to match the GaAs substrate, and that the GaAs film is strain-free and free of dislocations, both before and after lift-off. Thermal modeling shows only modest heating outside of the InGaAsN layer, so that the film or device above the InGaAsN layer experiences minimum thermal exposure. Examination of the lift-off interfaces shows evidence of melting and re-solidification. We demonstrate a process using additional InGaP etch layers that allow for quick and easy clean-up of this melted region, resulting in restoration of the original GaAs wafer surface to a condition suitable for re-use. Thus our process can transform the GaAs substrate from a consumable to a manufacturing tool. Device performance and material properties of lifted-off devices will be reported.

4:20pm SE+EM+EN-MoA7 Optical and Structural Properties of Metal-dielectric Composite Films, *Lirong Sun, N.R. Murphy, J.G. Jones, J.T. Grant*, Air Force Research Laboratory
In this work, the metal - metal oxide composite films were prepared in multilayer stacks. A medium layer of silver or a mixture of silver and oxide (SiO_2, Al_2O_3, ZnO and ITO) was embedded between the host (SiO_2, Al_2O_3, ZnO and ITO) materials. The mixture of silver and oxide was deposited by co-sputtering the silver target and one oxide target in pure argon simultaneously using DC and pulse DC magnetron sputtering techniques. The optical constant of composite films was tailored by varying deposition time of the medium layer, deposition conditions and host material. The absorbing spectral peaks were influenced by silver content, silver particle sizes and oxide matrix. The *in situ* spectroscopic ellipsometry data was performed in real time during film growth to derive film thickness and optical constants. The dispersion results were further correlated with absorption spectra, film density, grain sizes and surface morphology by UV-Vis-NIR spectra, X-ray diffraction, X-ray reflectivity and scanning electron microscope measurements.

5:00pm SE+EM+EN-MoA9 Atomic Layer Deposition of Alumina and Titania Passivation Layers in Microchannel Reactors for Coke Suppression, *Hao Feng*, Xi'an Modern Chemistry Research Institute, China
Alumina and titania thin films are deposited inside the channels of stainless steel tubes by atomic layer deposition to deactivate the metal surface for the purpose of coke suppression. The ALD equipment is modified to incorporate the high-aspect-ratio metal tubes into the flow path. Experiment parameters are adjusted to ensure complete and uniform coverage of the internal surface areas of the metal tubes. The thicknesses of the passivation layers are precisely controlled by adjusting the number of ALD cycles. In coking experiments the passivated metal tubes are used as reactors for thermal cracking of a hydrocarbon fuel composed of C_{12}-C_{16} paraffins. The lifetime of the experiment system passivated by ALD alumina films can be up to 5 times longer compared to the system using bare metal tubes as the reactor. By analyzing the tested metal tube samples it is discovered that the ALD alumina film remains intact after the coking experiment so that the metal catalyzed filament coke formation can be completely inhibited by the alumina passivation layer. The anti-coking performances of ALD titaina passivation layers are also noticeable but not as stable. The formation of filament cokes can also be suppressed by titania passivation layers. However, the ALD titania films tend to crack during the coking experiments. This could lead to failures of the passivation layers and acceleration of coke formation.

Energy Frontiers Focus Topic
Room: 211B - Session EN+AS+EM+SE+SS-TuM

Photocatalysis
Moderator: Jason Baxter, Drexel University, Manjula Nandasiri, Pacific Northwest National Laboratory

8:00am EN+AS+EM+SE+SS-TuM1 Ultra-dense Hydrogen and Low Energy Nuclear Reactions, *Sveinn Olafsson*, Science Institute, Physics department University of Iceland, *L. Holmlid*, University of Gothenburg, Sweden

For over the last 25 years the science of cold fusion/LENR has been researched around the world with slow pace of progress. Modest quantity of excess heat and signatures of nuclear transmutation and helium production have been confirmed in experiments and theoretical work has resulted in a flora of possible theoretical scenarios. [1-2]

Here we present energy production in several stages of surface processes that result first in the formation of Rydberg matter of Hydrogen [3] that can later condense in a new ultra-dense Hydrogen phase with 2.3 pm short bond distances. This phase is nuclear active showing break-even fusion reaction [7] under 100mW laser pulsing and slow spontaneous fusion occurring without laser pulsing[4,5,6]. The experimental work in around 30 publications is briefly reviewed and latest experimental results presented and discussed.

In that work high-energy particles are detected from the spontaneous processes using scintillation and other similar detectors. Both spontaneous line-spectra and a spontaneous broad energy distribution similar to a beta-decay distribution are observed indicating detection of particles such as muons. The broad distribution is concluded to be due to nuclear particles, giving straight-line Kurie-like plots. They are observed even at a distance of 3 m in air and have a total rate of 10^7-10^{10} s^{-1}. In the talk the link of these observation to Low energy nuclear reactions (LENR) or so called cold fusion will be discussed experimentally and theoretically.

1. The science of low energy nuclear reaction.

Storms E. World Scientific Publishing Company; **2007**.

2. The explanation of low energy nuclear reaction.

Storms E. Ienergy Press; **2014**.

3. Review paper: Experimental Studies and Observations of Clusters of Rydberg Matter and Its Extreme Forms Leif Holmlid. J Clust Sci (**2012**) 23:5–34

4. Spontaneous ejection of high-energy particles from ultra-dense deuterium D(0)

Leif Holmlid and Sveinn Ólafsson

Volume 40, Issue 33, 7 September **2015**, Pages 10559–10567)

5. Charged particle energy spectra from laser-induced processes: nuclear fusion in ultra-dense deuterium D(0) Leif Holmlid and Sveinn Ólafsson submitted **2015**.

6. Muon detection studied by pulse-height energy analysis: Novel converter arrangements

Leif Holmlid and Sveinn Ólafsson. Rev. Sci. Instrum. 86, 083306 (**2015**);

7. Heat generation above break-even from laser-induced fusion in ultra-dense deuterium

Leif Holmlid. AIP Advances 5, 087129 (**2015**);

8:20am EN+AS+EM+SE+SS-TuM2 Optical and Surface Properties of Semiconductor Nanowires for Solar Fuels, *Eleonora Frau, J. Vukajlovic, A. Dalmau-Mallorqui, A. Fonctuberta i Morral, E. Alarcon Llado*, Ecole Polytechnique Fédérale de Lausanne (EPFL), Switzerland

Semiconductor nanowires (NWs) are filamentary crystals with new properties from their bulk counterparts. Their large versatility makes them excellent candidates as building blocks for contributing to solving the energy problem in the near future. In this work, we will assess two main properties of semiconductor NWs that have an impact to solar energy conversion.

First, it is known that light is strongly absorbed by NW arrays since light resonances give rise to effective absorption cross-sections that are much larger than the geometrical ones. Optical resonances depend on NW geometry and dielectric environment, and can result into absorption effective diameters up to 25 times larger than the geometrical for certain wavelengths. We have used finite-difference time-domain (FDTD)

electromagnetic simulations to understand and design NW-based sunlight scavengers. For instance, a GaAs NW array that is only covering 3% of the surface can generate more photocurrent than a planar film, considering a 30% reflectivity (see figure1). Also that thanks to optical resonances, an indirect-bandgap material such as Si is capable of absorbing most of the light within a 2um long NW array that only covers 7% of the device surface.

On the other hand, it is also known that surface states and traps detriment device performances. However, in case where solar energy is directly converted into fuel (such as hydrogen) in a photoelectrochemical (PEC) cell, the large surface-to-volume ratio of NW forests is an important asset. Since the electrochemical reactions happen at the semiconductor surface, NWs enable the use of low-cost catalysts (e.g. MoSx) even though they exhibit lower performances than noble metals (e.g. Pt). In order to assess the effects of nanostructuring photo-electrodes for solar fuel generation, we have studied photo-cathodes based on Silicon nanopillar structures. The photo-cathodes were fabricated by using a top-down approach and their diameters range from ~200 to 900nm and lengths ~2um. We observe that reducing the size of the nanostructure, increases the overpotential, and thus the overall efficiency (see figure 2). By coating the surface with thin TiO_2 layers, the performance is improved in terms of overpotential and fill factor. We explain these findings by using an electrico-kinetic model of the semiconductor-water junction. We find that the TiO_2 layers actually act as a hole blocking layer, preventing recombination.

8:40am EN+AS+EM+SE+SS-TuM3 Engineering Surfaces and Interfaces for Photoelectochemical (PEC) Water-Splitting, *Thomas Jaramillo, J.D. Benck*, Stanford University, *J. Kibsgaard*, SLAC National Accelerator Laboratory, *T.R. Hellstern, C.J. Hahn, P. Chakthranont, R. Britto, K.D. Fong*, Stanford University **INVITED**

The talk will focus on engineering surfaces and interfaces for solar photoelectrochemical (PEC) water-splitting for the direct, renewable production of H_2. In particular, this talk begin by describing research efforts to develop H_2 evolution catalysts that are active, stable, and comprised of only earth-abundant elements, including transition metal sulphides, phosphides, and phosphosulfides.[1-3] Next, we will describe recent efforts to integrate these catalysts onto semiconductor surfaces to provide corrosion protection as well as enhanced interfacial catalysis for PEC water-splitting.[4] This talk will focus on the need for high turnover frequency (TOF) catalysts, which ultimately enable the greatest flexibility in designing optimum interfaces for high performance devices.

[1] J. Kibsgaard, T.F. Jaramillo, F. Besenbacher, "Building an appropriate active site motif into a hydrogen evolution catalyst with thiomolybdate $[Mo_3S_{13}]^{2-}$ clusters," *Nature Chemistry*, **6** (2014) 248.

[2] J.D. Benck, T.R. Hellstern, J. Kibsgaard, P. Chakthranont, T.F. Jaramillo, "Catalyzing the Hydrogen Evolution Reaction (HER) with Molybdenum Sulfide Nanomaterials," *ACS Catalysis*, **4** (2014) 3957.

[3] J. Kibsgaard and T.F. Jaramillo, "Molybdenum Phosphosulfide: An Active, Acid-Stable Earth-Abundant Catalyst for the Hydrogen Evolution Reaction," *Angewandte Chemie*, **53** (2014) 14433.

[4] J.D. Benck, S.C. Lee, K.D. Fong, J. Kibsgaard, R. Sinclair, T.F. Jaramillo, "Designing active and stable silicon photocathodes for solar hydrogen production using molybdenum sulfide nanomaterials," *Advanced Energy Materials*, **4** (2014) 1400739.

9:20am EN+AS+EM+SE+SS-TuM5 Bulk and Surface Effects of Incorporating Titanium Into Hematite Thin Films to Improve Photoelectrochemical Water Splitting, *Anthony Abel, A.M. Patel*, Drexel University, *I.G. Torregrosa*, Utrecht University, Netherlands, *B. Opasanont, J.B. Baxter*, Drexel University

Hematite (α-Fe_2O_3) has emerged as a promising photoanode material for photoelectrochemical (PEC) water splitting due to its chemical stability, earth-abundance, low cost, and suitable band gap for both water splitting and visible light absorption. However, poor charge separation due to low hole mobility and high recombination rate, and sluggish oxygen evolution reaction kinetics have limited its potential as an economical water-splitting catalyst. Here, we investigate titanium incorporation into hematite photoanodes and provide insight into the role of Ti^{4+} in improving PEC performance. Planar hematite thin films (~45 nm thick) were deposited by successive ionic layer adsorption and reaction (SILAR) of FeOOH on an FTO/glass substrate and subsequent annealing to induce phase transition to α-Fe_2O_3, and titanium was incorporated up to 10% Ti/(Ti+Fe) by either modification of the SILAR solution (SM:α-Fe_2O_3) or solid-state diffusion (SSD:α-Fe_2O_3) during the annealing process. PEC measurements revealed substantial improvements in both charge separation efficiency and hole injection into the electrolyte, increasing photocurrent from nearly zero to

~0.6 mAcm^{-2} under 1-sun irradiation at 1.23 V$_{RHE}$. Mott-Schottky analysis indicated a 100 mV cathodic shift in the flat band potential upon doping with Ti^{4+} regardless of fabrication method, but a 100-fold increase in carrier density only in SM:α-Fe$_2$O$_3$ films, resulting in a high 20 % separation efficiency at 1.23 V$_{RHE}$ with optimized 5 % Ti/(Ti+Fe) in the modified SILAR solution. Electrochemical impedance spectroscopy showed a 4x increase in the surface state capacitance peak near the water oxidation onset potential, possibly due to reduced Fermi level pinning as a result of more efficient hole injection into the electrolyte . More importantly, doping with titanium resulted in a 100-fold decrease in the charge transfer resistance from surface states to the electrolyte, revealing the strong influence of Ti^{4+} on interfacial kinetics . Further surface modification with an ultrathin FeOOH surface passivation layer raised the plateau photocurrent to ~0.8 mAcm^{-2} at 1.23 V$_{RHE}$, representing a 3x improvement over previous reports of SILAR-deposited hematite films and comparable with record performance for planar hematite deposited using high vacuum synthesis techniques.

9:40am EN+AS+EM+SE+SS-TuM6 Iron Oxide Nanoparticle Growth on Highly Oriented Pyrolytic Graphite (HOPG) and Photocatalytic Properties of Pt on Iron Oxide, *Jayde Kwon, J.C. Hemminger*, University of California, Irvine

Highly oriented pyrolytic graphite (HOPG) is an ideal substrate to study the fundamental growth mechanism of iron oxide independent from substrate effects. Platinum on iron oxide is a model heterogeneous catalyst with importance to biotechnology and solar cell applications. Selective growth of iron oxide nanoparticle (NP) either on step edges of HOPG or oxygen plasma treated HOPG by physical vapor deposition (PVD) will be presented. The successful selective iron oxide NP growth was validated by scanning electron microscopy (SEM), transmission electron microscopy (TEM), and X-ray photoelectron spectroscopy (XPS). The development of the NP array system is highly significant in that it can provide an ideal template for theoretical calculations for fundamental metal growth studies. Pt nanoparticles was subsequently deposited on the iron oxide nanoparticles using a selective photodeposition technique. The application of these nano-systems (Pt nanoparticles on iron oxide nanoparticles) towards photocatalysis of methylene blue will be presented. Although iron oxide is a promising semiconductor photocatalyst, it suffers from a short hole diffusion length, low electrical conductivity and a high rate of electron hole recombination. However, this bimetallic system using platinum deposited on iron oxide overcomes these barriers. A novel method was developed using small quantities of Pt on iron oxide to significantly enhance methylene blue decomposition. This system is also being explored as a catalytic model for water-gas shift reactions.

11:00am EN+AS+EM+SE+SS-TuM10 Interface Design for Efficient and Stable Photoelectrochemical Water Splitting, *Joel Ager*, Lawrence Berkeley National Laboratory INVITED

Solar photoelectrochemical (PEC) water splitting is potential future carbon-neutral energy source which could dramatically change the landscape of global energy generation and storage. The half reactions for water splitting are as follows:

2H$^+$ + 2 e$^-$ <-> H$_2$ (1)

H$_2$O <-> 2e$^-$ +2H$^+$ + 1/2O$_2$. (2)
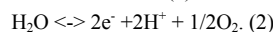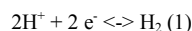
The free energy change for the overall reaction, H$_2$O <-> H$_2$ + 1/2O$_2$ corresponds to 1.23 eV per electron transferred; however, typically >1.5 V is required to overcome kinetic limitations, particularly for the O$_2$ evolution reaction. The most commonly used approach for integrated solar water splitting employs photocathodes (H$_2$ or hydrocarbon producing) and photoanodes (O$_2$ producing) linked in a tandem geometry [1].

The interface challenges required to demonstrate a practical system which is both efficient and stable under operation are substantial and severe. In addition to constructing interfaces, either solid-solid or solid liquid, which achieve the desired photovoltaic charge separation, the surfaces of these photoelectrodes can be a failure point under sustained operation due to corrosion. We have found that the use of nanoscale conformal oxide layers can greatly reduce corrosion rates. Moreover, it is possible to achieve both high performance and lifetime by the use of protection layers which are also tuned for selective carrier contact.

Examples of such a strategy will be shown for photocathodes [2-5] and for photoanodes [5]. Recent work on p-type transparent oxides (p-TCOs) used as selective hole contacts for photoanodes will be emphasized. For example, it will be shown that using NiCo$_2$O$_4$ as the p-TCO and n-type Si as a prototypical light absorber, a rectifying heterojunction capable of light driven water oxidation can be created. By placing the charge separating junction in the Si using a np$^+$ structure and by incorporating a highly active Ni-Fe oxygen evolution catalyst, efficient light-driven water oxidation can be achieved. The generality of the p-TCO protection approach is demonstrated by multi-hour, stable, water oxidation with n-InP/p-NiCo$_2$O$_4$ heterojunction photoanodes.

References.

1. J. W. Ager *et al.*, Energy Environ. Sci. (2015). DOI:10.1039/C5EE00457H

2. M. H. Lee *et al.*, *Ang. Chemie Int. Edition***51** 10760 (2012).

2. Y. Lin *et al.*, *Nano Letters***13** 5615 11 (2013)

3. Y. Lin *et al.*, *J. Phys. Chem.* C **119**, 2308 (2015).

4. J. Yang *et al.*, *J. Amer. Chem. Soc.***136** 6191 (2014).

11:40am EN+AS+EM+SE+SS-TuM12 Buried, Hetero, and p-i-electrolyte III-V Photoelectrochemical Junctions with Significantly Enhanced Photocurrent Onset Potentials, *James Young, H. Doscher, J. Turner, T. Deutsch*, National Renewable Energy Laboratory

To approach the maximum achievable solar-to-hydrogen (STH) conversion efficiencies with photoelectrochemical (PEC) devices, it is necessary to employ the lowest possible band gap (E$_g$) absorbers that can still provide sufficient voltage to drive water splitting at high rates (1.7-1.8 V for 25% STH). The record 12.4% STH was achieved by a GaInP$_2$/GaAs PEC/photovoltaic (PV) tandem device while an all solid state GaInP$_2$/GaAs PV/PV tandem produces an open-circuit voltage that approaches 2.4 V. Since GaAs (E$_g$ = 1.4 eV) is the current-limiting junction in these devices, it can be substituted by InGaAs with E$_g$ = 1.0 eV to reach 25% STH. The current-for-voltage tradeoff of using lower-E$_g$ absorbers moves toward the constraint of insufficient voltage for spontaneous water splitting. To address this approaching constraint, we investigate several alternative device structures at the III-V/electrolyte interface that show photocurrent onset potential enhancements of a few hundred mV. We will present band diagram calculations and electrochemical measurements to discuss the voltage performance of these structures.

12:00pm EN+AS+EM+SE+SS-TuM13 X-ray Absorption Studies on the Li-S Battery Cathode Side, *Yifan Ye*, University of Science and Technology of China, *A. Kawase*, Lawrence Berkeley National Laboratory, *H.X. Ju*, University of Science and Technology of China, *E. Cairns*, Lawrence Berkeley National Laboratory, *J.-H. Guo*, Lawrence Berkeley Lab, University of California, Berkeley, *J.F. Zhu*, University of Science and Technology of China

As increasing global energy consumption in the coming days, sustainable, clean energy technologies are highly desirable. The high theoretical specific capacity of 1675 mA·h/g for elemental S has prompted intense effort to study the Lithium-Sulfur batteries. With the application of cetyltrimethyl ammonium bromide (CTAB), modified sulfur-graphene oxide (S-GO) nano-composite based Li/S batteries exhibited a very high initial discharge capacity of 1440 mA·h/g of sulfur at 0.2C with excellent rate capability of up to 6C for discharge and 3C for charge while still maintaining high specific capacity. And the batteries demonstrated cycling performance up to 1500 cycles with extremely low decay rate of 0.039% per cycle. With the introduction of CTAB, the performance of the GO-S based Li-S battery has been improved significantly, thus it is important to figure out the role of CTAB played in the system. During the synthesis process of the cathode materials, S and Na$_2$S were used as the precursors, the ratio of S/Na$_2$S is crucial to the components of the precursors. Moreover, the sequence of mixing GO/CTAB solution with precursor solution is a key point to effective cathode synthesis procedure. Understanding these information helps to optimize the methodology for the controllable synthesis of desired cathode material that can be used to fabricate an efficiency and well-performed Li/S battery. S K-edge X-ray absorption spectroscopy (XAS) is applied to study the chemical species evolution during the GO-S-CTAB cathode material synthesis. The influences on the cathode materials related to the battery performance are monitored by S K-edge XAS. The research revealed the interaction between CTAB and GO, S, Na$_2$S and Na$_2$S$_x$. It indicated that CTAB can physical absorbed on Na$_2$S$_x$ molecules by bonding with the terminal S atoms of Na$_2$S$_x$ chains, and this kind of bonding can convert to chemical C-S bonding with heating treatment. Thus the interaction of CTAB with GO, formed C-S between CTAB and S and interaction of GO and S provided a tight tri-layer structure which can immobilize the S particles on GO sheet and finally enhanced the battery performance. The information from this work proved the importance of Na$_2$S:S ratio, CTAB/GO adding procedure in the fabrication process, and we can easily apply XAS to optimize these recipe. And moreover, this work proved strong evidence that XAS tools can be used to do the initial characterization on the battery performance before real cycling procedure.

Surface Science
Room: 112 - Session SS+AS+EN+NS-TuM

Nanostructures, Nanoplasmonics and Surface Reactions

Moderator: Bruce Koel, Princeton University

8:20am SS+AS+EN+NS-TuM2 ENDOM: A Simple Method to Deposit Nanostructures from Nanowires to Nanopores, *Ashley Ellsworth, A.V. Walker*, University of Texas at Dallas

A key challenge in the practical application of nanostructures is their effective integration through assembly, patterning and alignment on technologically relevant substrates. We have recently demonstrated a new technique, electroless nanowire deposition on micropatterned substrates (ENDOM), by which to simultaneously synthesize and place nanowires on chemically patterned substrates. The nanowires can be precisely oriented on the surface in arbitrary shapes, such as an arch and around a right angle bend. In ENDOM, the shape of the deposit is controlled by the substrate pattern while its width is controlled by the reaction conditions. By employing longer deposition times and the appropriate substrate patterns, nanopores and nanochannels can be produced. However for sensing and nanoelectronic applications, free standing nanopores and nanochannels are generally employed. We have observed that the nanostructure adhesion to the surface is dependent upon the reagent concentrations. For example in Cu ENDOM, upon reduction of triethanolamine (complexing agent and buffer) concentration, nanowires no longer adhere strongly to the substrate and can be transferred to another substrate. In this presentation, we shall discuss the mechanisms of adhesion, transfer of these nanostructures to other substrates and proof-of-concept studies to synthesize free-standing nanostructures.

8:40am SS+AS+EN+NS-TuM3 Chemical Reaction on Photo-excited Plasmonic Nanostructures, *Sulio Linic*, University of Michigan **INVITED**

We will also show that plasmonic silver nanoparticles, optically excited with low intensity visible light, exhibit direct photo-catalytic activity in a number of oxidation reactions.[1] We will discuss underlying mechanisms associated with these phenomena and predictive models that can capture the outcome of chemical transformations on these materials.[2,3,4] We propose that this new family of plasmonic metal photo-catalysts could prove useful for many heterogeneous catalytic processes that cannot be activated using conventional thermal processes on metals or photo-catalytic processes on semiconductors. I will show an example of such a process.[5]

1. D. B. Ingram, S. Linic, JACS, 133, 5202, 2011

2. Suljo Linic, Phillip Christopher and David B., Nature Materials, 10, 911, 2011.

3. Ingram P. Christopher, H. Xin, S. Linic, Nature Chemistry, 3, 467, 2011.

4. P. Christopher, H. Xin, M. Andiappan, S. Linic, Nature Materials, 11, 1044, 2012.

5. M. Andiappan, J. Zhang, S. Linic, Science, 339, 1590, 2013

9:20am SS+AS+EN+NS-TuM5 Structured Noble Metal Nanosurfaces for Biosensing and Bioanalysis (4): TLC-SERS and *In Situ* Monitoring of Surface-Adsorbed Target Molecules, *Hiroyuki Takei, J. Saito, K. Watanabe*, Toyo University, Japan, *T. Okamoto*, Riken, Japan, *H. Vieker, A. Beyer, A. Gölzhäuser*, Bielefeld University, Germany

Surface-enhanced Raman spectroscopy, SERS, is a powerful technique for in-situ characterization of chemical species. Requisite noble metal nanosurfaces can be prepared with a variety of techniques, ranging from simple vacuum deposition of a metal followed by annealing to intricate processing by electron beam lithography. Some commercial SERS plates are now available, and it is sometimes possible to detect signals from even single molecules if pure. However, in real-world applications, target molecules are often found in mixtures, either containing other Raman-active chemical species or a background material that can overwhelm the target molecule. It can also happen that one might be interested in directly obtaining SERS spectra of chemical species adsorbed on a solid surface.

When faced with a mixture sample, we can carry out separation before SERS measurement. To do so, we incorporated a SERS layer into a thin layer chromatographic plate. While a number of workers have reported applying noble metal nanoparticles after separation with a conventional TLC plate, we feel that such an additional step is cumbersome and does not guarantee uniformity in SERS signals. Our TLC-SERS is prepared with the following procedure; (1) adsorption of 100 nm diameter SiO_2 nanospheres as a dense monolayer on a glass slide, (2) evaporation of gold or silver with thicknesses up to 100 nm, and (3) spreading of chromatography silica gels. Steps (1) and (2) give rise to surface-adsorbed cap-shaped noble metal nanoparticles. We demonstrate that the TLC-SERS can actually separate mixture samples and provide in-situ SERS spectra. Two examples will be used to demonstrate the utility of our TLC-SERS plates. One deals with a mixture of roughly equal portions of Raman-active chemical species, rhodamine 6 G, crystal violet and BPE. The other is skim milk to which a trace amount of melamine has been added. We show that the three-component mixture could be separated and SERS spectra of all three components could be obtained separately and that melamine added to skim milk could be detected after separation but not before.

For detection of surface-adsorbed chemical species, we prepared silver nanoparticles on a PDMS sheet, using the same protocol as above. The PDMS sheet can be made less than 1 mm thick so that with an appropriate pressurization system, pressure can be applied to the PDMS sheet in order to press the silver nanoparticles against a near-by solid surface to which target molecules are adsorbed. Such a system can be utilized to detect, for example, residual pesticides on agricultural produces. We will demonstrate direct detection of ferbam on a grapefruit.

9:40am SS+AS+EN+NS-TuM6 Growth and Intercalation of Cu and Dy on the Basal Plane of Graphite, *Patricia A. Thiel, D. Appy, E.J. Kwolek, D. Shao, M. Wallingford, M.C. Tringides, J.W. Evans, Y. Han*, Iowa State University, *H. Lei*, Institute of Solid State Physics, CAS, China, *C.-Z. Wang*, Iowa State University

Graphite, and surface processes on graphite, serves as a valuable benchmark for carbon-based materials such as graphene. We have studied copper and dysprosium on graphite, deposited by an e-beam evaporator in UHV and imaged with STM, to determine the characteristic features of nucleation and growth of metal islands. One of the fundamental questions that arises naturally is whether metal nucleates homogeneously on the terraces or whether it nucleates heterogeneously at defect sites. To answer this question we employ several tools, especially a comparison between high-level van der Waals theory for single atom diffusion, and measured island density. We also present evidence for unexpected metal intercalation at the surface of graphite, after treatment at elevated temperature.

11:00am SS+AS+EN+NS-TuM10 Surface-Mediated Self-assembly of a Flexible Nucleoside Analogue into Micron-sized Hydrogen-bonded Polymers, *Jun Wang, P. Bonnesen*, Oak Ridge National Laboratory, *E. Rangel, E. Vallejo, A. Sanchez-Castillo*, Universidad Autónoma del Estado de Hidalgo, Mexico, *H.J. Cleaves*, Tokyo Institute of Technology, Japan, *A.P. Baddorf, B. Sumpter, M. Pan, P. Maksymovych, M. Fuentes-Cabrera*, Oak Ridge National Laboratory

We report on an extraordinary large-scale surface-mediated molecular self-assembly of a flexible nucleoside analogue into a well-organized hydrogen-bonded polymer on Au(111). The nucleoside analogue is (RS)-N^9-(2,3-Dihydroxypropyl)Adenine $(R,S$-DHPA), and it consists of the Adenine nucleobase and a tethered glycol group. Employing scanning tunneling microscopy and density functional theory calculations we show that the polymer primarily self-assembles along the Au(111) herringbone reconstruction pattern and extends to the micrometer scale and beyond. The profound propensity toward self-assembly in this case arises from the properties of the glycol moiety of the R,S-DHPA molecule: it is linear and flexible, and these features, together with the specific ways in which the glycol and the Adenine moieties can hydrogen bond, confer R,S-DHPA with a superior self-assembly ability. Our results suggest that nucleoside analogues with flexible acyclic groups could provide the means for synthesizing substrate-supported mesoscale hydrogen-bonded polymers.

11:20am SS+AS+EN+NS-TuM11 Nanowire Kinking during Vapor-liquid-solid Growth: Experiments and Simulations, *Yanming Wang, Y. Li*, Stanford University, *S. Ryu*, Korea Advanced Institute of Science and Technology, *P.C. McIntyre, W. Cai*, Stanford University

Nanowires (NWs) are promising components for next-generation electronic and optical devices, and the vapor-liquid-solid (VLS) growth is a widely studied method for NW fabrication. However, many fundamental questions regarding the VLS mechanism are still not understood, such as NW kinking during growth. Kinking, a sudden change in axial orientation of nanowires during growth, is a common defect that complicates the directed synthesis of these nanocrystals. Understanding such defects is important for better control of the NW orientation, yield and quality required for applications.

Experimental studies of coherent kinking of germanium nanowires detect two different kinking structures. One structure, which is most pronounced for Ge NW's of diameter close to 20 nm, involves kinking from a vertical <111> to <110> growth axis on Ge (111) single crystal substrates. The other involves kinking from the vertical [111] axis to an inclined <111> growth direction for NWs of > 30 nm diameter.

The balance of capillary forces driving these two modes of kinking are analyzed quantitatively. We developed a 3D multi-phase field model for VLS NW growth. The model captures the NW tapering and sidewall facets in good agreement with experimental observations. The model predicts the steady-state NW growth velocity is a linear function of the vapor chemical potential and the inverse of catalyst diameter, providing a confirmation of the Gibbs-Thomson effect in nanowire growth. With anisotropic interfacial energies, the model shows the NW growth orientation dependence on catalyst diameter and hence it provides an explanation of the NW kinking in the steady-state growth regime. In this model, we introduce a perturbation force to induce the NW structural transition and the free energies are evaluated at different stages during the droplet movement. It enables us to discuss the instability of the catalyst droplet for different pedestal structures, which is important for understanding the onset of the kinking at the NW base.

11:40am SS+AS+EN+NS-TuM12 Adsorption of Water and Bromine on Gold Nanoclusters Investigated by Neutralization in Low Energy Alkali Ion Scattering, *Christopher Salvo*, *J. Keagy*, *J.A. Yarmoff*, UC Riverside

Small gold (Au) nanoclusters have been heavily studied because of their intriguingly high catalytic activity, especially when compared to bulk gold. We employ a specialized method of Low Energy Ion Scattering (LEIS) to probe the electronic properties of nanoclusters prepared with a variety of methods. The experiments measure the neutralization probability of singly scattered alkali ions, which is acutely sensitive to the local electrostatic potential a few Å's above the surface. Because the Au atoms are much more massive than the substrate atoms, this method allows the signal from the nanoclusters to be separated from that of the substrate so that the neutralization reflects the local properties of the cluster surfaces. Earlier work had demonstrated that the neutralization is a function of cluster size, and that it is enhanced for the smallest clusters presumably because they are negatively charged [1]. The work presented here investigates the adsorption of water and Br on Au nanoclusters grown on TiO_2 or SiO_2. There are multiple factors that can contribute to a change in the neutralization of the scattered ions, such as the cluster size, shape, or charge state. When Br attaches to a nanocluster, the neutralization decreases presumably due to charge transfer from the cluster to the electronegative Br atom. Surprisingly, it is found that the neutralization of scattered K^+ ions increases in the presence of adsorbed water at liquid nitrogen temperatures. Furthermore, the increase of neutralization for adsorbed water is independent of whether the water or the Au is deposited first. Possible explanations for these observations will be discussed.

[1] G.F. Liu, Z. Sroubek and J.A. Yarmoff, Phys. Rev. Lett., **92**, 216801 (2004).

12:00pm SS+AS+EN+NS-TuM13 Optical Constants Measured for Fe, Ni and Pd by Reflection Electron Energy-Loss Spectroscopy Spectra, *H. Xu, B. Da, S.F. Mao*, University of Science and Technology of China, *J. Toth, K. Tokesi*, Institute for Nuclear Research, Hungarian Academy of Sciences (ATOMKI), *Zejun Ding*, University of Science and Technology of China

The energy loss function (ELF), which is directly related to optical constants of a solid, dominates the energy loss process of an electron moving inside or flying nearby a solid. It is therefore able to obtain optical constants by surface electron spectroscopy technique. Accurate measurement of optical data by optical methods in a photon energy range up to 10^2 eV is still insufficient; delicate experimental conditions are required when measuring data in vacuum ultraviolet region (20-50 eV). Fortunately, such information is essentially contained in and, therefore, can be extracted from a reflection electron energy loss spectroscopy (REELS) spectrum due to the shorter information depth of signal electrons compared with that of photons.

In the present work, reflection electron energy loss spectra of transition metals, Fe, Ni and Pd, were measured at several primary energies ranging from 0.5 keV up to 5 keV and in a wide energy-loss range. Prior to the measurements in situ cleaning of the sample surface was performed using Ar+ ion sputtering with proper current density and time. Vacuum was kept as 1.5×10^{-9} mbar in the measurement chamber during the REELS measurements. Surface cleanness was checked by XPS in several cases after the REELS measurements. An improved reverse Monte Carlo simulation for determination of optical constants via accurate description of electron inelastic transport process was performed. ELF of those metals were extracted from experimental REELS spectra. The accuracy of the obtained optical data has been confirmed by f-sum and ps-sum rules. Comparisions of our data with other sources from either experimental measurements or density functional theory calculation are given.

Mechanistic Insight of Surface Reactions: Catalysis, ALD, etc. - I
Moderator: Ludwig Bartels, University of California - Riverside

8:00am SS+AS+EN-TuM1 Active Sites of Nitrogen-Doped Carbon Materials for Oxygen Reduction Reaction, *Takahiro Kondo*, *D. Guo, R. Shibuya, C. Akiba, S. Saji, J. Nakamura*, University of Tsukuba, Japan

Nitrogen-doped carbon materials have been found to demonstrate high electrocatalytic activity for oxygen reduction reaction (ORR) as the non-metal catalysts but the active site is still under debate. This is due to the complexity of the real catalysts, such as mixing of different type of N and inhomogeneity in both structure and conductance. Here we designed the nitrogen doped graphite (HOPG) model catalysts with different type of N dominance and its concentration to directly clarify the ORR active site. ORR measurements showed that active site was created by pyridinic N (N bonded to two carbon atoms). The ORR active site was ascribed to the carbon atom with Lewis base property created by neighbour pyridinic N based on the investigations of intermediate state of ORR, localized electronic states at carbon next to pyridinic N and CO_2 adsorption property by X-ray photoelectron spectroscopy (XPS), scanning tunneling spectroscopy (STS) and temperature programmed desorption (TPD), respectively. The ORR activity of model catalyst per pyridinic N concentration was then found to be in good agreement with that for real nitrogen-doped graphene catalyst.

8:20am SS+AS+EN-TuM2 Cerium Oxide-Induced Intercalation of Oxygen on Supported Graphene, *Zbynek Novotny*, Pacific Northwest National Laboratory, *F.P. Netzer*, Karl-Franzens University, Austria, *Z. Dohnalek*, Pacific Northwest National Laboratory

Cerium oxide is an important catalytic material known for its ability to store and release oxygen, and as such, it has been used in a range of applications, both as an active catalyst and as a catalyst support. Using scanning tunneling microscopy and Auger electron spectroscopy, we investigated oxygen interactions with CeO_x clusters on a complete graphene monolayer-covered Ru(0001) at elevated temperatures (550 – 700 K). Under oxidizing conditions (~10^{-7} Torr of O_2), oxygen intercalation under the graphene layer is observed. Time dependent studies demonstrate that the intercalation starts in the vicinity of the CeO_x clusters and extends until a completely intercalated layer is observed. Atomically resolved images further show that oxygen forms p(2×1) structure underneath the graphene monolayer. Temperature dependent studies yield an apparent kinetic barrier for the intercalation of 0.9 eV. This value correlates well with the theoretically determined value for the reduction of small CeO_2 clusters reported previously. At higher temperatures, the intercalation is followed by a slower etching of the intercalated graphene (apparent barrier of 1.1 eV). The intercalated oxygen can also be released through the CeO_x clusters by annealing in vacuum. In agreement with previous studies, no intercalation is observed on a complete graphene monolayer without CeO_x clusters, even in the presence of a large number of point defects. These studies demonstrate that the easily reducible CeO_x clusters act as intercalation gateways capable of efficiently delivering oxygen underneath the graphene layer.

8:40am SS+AS+EN-TuM3 Dissociation Dynamics of Energetic Water Molecules on $TiO_2(110)$: Combined Molecular Beam Scattering and Scanning Tunneling Microscopy Study, *Z.-T. Wang, Y.-G. Wang, R.T. Mu, Y. Yoon, G.A. Schenter, R. Rousseau, I. Lyubinetsky, Zdenek Dohnalek*, Pacific Northwest National Laboratory

Molecular beam scattering techniques have proven extremely useful in determining the dynamics of energy flow in the course of chemical reactions. We have successfully designed and constructed a unique, state of the art instrument combining a molecular beam scattering source coupled with a low temperature scanning tunneling microscope (STM). The combination of these techniques allows us to follow the same area during adsorption and image surface species as a function of incident energy of reacting molecules. Our first study focuses on reversible water dissociation on Ti rows of $TiO_2(110)$, which leads to the formation of pairs of terminal and bridging hydroxyl species, $H_2O \leftrightarrow HO_t + HO_b$. The results of our measurements show the onset of H_2O dissociation at 0.2-0.3 eV of incident energy, independent of whether the molecules impinge along or across the Ti rows at an incident angle of 60° relative to surface normal. Following the onset, the dissociation probability increases linearly with increasing incident energy. Ensembles of *ab initio* molecular dynamics (AIMD) simulations at several incident energies reproduce the product distribution seen in the

STM. Additionally, these studies show that the dissociation occurs only for the impacts in the vicinity of surface Ti ions with an activation energy of 0.3 eV and that the O-H bond cleavage is accomplished within the time of a single vibration. The AIMD simulations were further used to construct a classical potential energy surface for water/TiO$_2$(110) interactions and execute non-equilibrium classical MD simulations that closely reproduce the onset and linear energy dependence of the dissociation probabilities.

9:00am SS+AS+EN-TuM4 Tracking Site-Specific C-C Coupling of Formaldehyde Molecules on Rutile TiO$_2$(110), *Zhenrong Zhang*, K. Zhu, Y. Xia, Baylor University, *M. Tang*, Southern Illinois University Carbondale, *Z.-T. Wang, I. Lyubinetsky*, Pacific Northwest National Laboratory, *Q. Ge*, Southern Illinois University Carbondale, *Z. Dohnálek*, Pacific Northwest National Laboratory, *K. Park*, Baylor University

We report the direct visualization of molecular coupling of the smallest aldehyde, formaldehyde, on reduced rutile TiO$_2$(110) surfaces using scanning tunneling microscope (STM). Images from the same area at viable temperatures (75 ~ 170 K) show that formaldehyde preferably adsorbs to bridging-bonded oxygen vacancy (V$_O$) defect site. V$_O$-bound formaldehyde couples with Ti-bound CH$_2$O form a diolate species, which stays stable at room temperature. In addition, two V$_O$-bound formaldehyde molecules can couple and form Ti-bound species, which desorbs above ~215 K. This coupling reaction heals both the V$_O$ sites indicating formation and desorption of ethylene. We also directly observed the diffusion of methylene groups to nearby empty V$_O$ sites formed upon dissociation of the C-O bond in V$_O$-bound formaldehyde, which suggests that the ethylene formation is via coupling of the methylene groups.

9:20am SS+AS+EN-TuM5 AVS 2014 Gaede-Langmuir Invited Talk: Models for Heterogeneous Catalysts: Complex Materials at the Atomic Level, *Hajo Freund**, Fritz Haber Institute of the Max Planck Society, Germany   **INVITED**

Our understanding of catalysis, and in particular heterogeneous catalysis, is to a large extend based on the investigation of model systems. The enormous success of metal single crystal model surface chemistry, pioneered by physical chemists, is an outstanding example. Increasing the complexity of the models towards supported nanoparticles, resembling a real disperse metal catalyst, allows one to catch in the model some of the important aspects that cannot be covered by single crystals alone. One of the more important aspects is the support particle interface. We have developed strategies to prepare such model systems based on single crystalline oxide films, which are used as supports for metal, and oxide nanoparticles, which may be studied at the atomic level using the tools developed in surface science. However, those oxide films may also serve as reaction partners themselves, as they are models for SMSI states of metal catalyst. Using such model systems, we are able to study a number of fundamental questions of potential interest, such as reactivity as a function of particle size and structure, influence of support modification, as well as of the environment, i.e. ultra-vacuum or ambient conditions, onto reactivity. The thin oxide film approach allows us to prepare and study amorphous silica as well as 2D-zeolites. Those systems, in spite of their complexity, do lend themselves to theoretical modelling as has been demonstrated.

11:00am SS+AS+EN-TuM10 The Solid State Li-CoO Conversion Reaction Studied by ARXPS and STM, *Ryan Thorpe*, S. Rangan, Rutgers, the State University of New Jersey, *A. Howansky*, Stony Brook University, *R.A. Bartynski*, Rutgers, the State University of New Jersey

Cobalt (II) oxide is a promising electrode material for Li-ion conversion batteries, undergoing the following reversible redox reaction upon exposure to lithium:

$$2Li + CoO \leftrightarrow Li_2O + Co^0$$
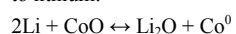
In order to characterize the phase progression and morphology of the Li-CoO reaction, epitaxial CoO(100) and (111) films were exposed to lithium in an ultra-high vacuum chamber. The early stages of the reaction were then characterized with scanning tunneling microscopy (STM), while the diffusion of Li into the films and resultant reduction of CoO was quantified using angle-resolved x-ray photoemission spectroscopy (ARXPS). From these measurements, a model of the Li-CoO reaction was constructed for each orientation.

For CoO(111) films, the conversion reaction initiated at step edges and defect sites before proceeding across the surface of the film. STM images of CoO(111) after 0.2 ML of Li exposure suggest that the conversion reaction products initially assumed a periodic structure which was in registry with the CoO(111) surface. For larger Li exposures, ARXPS measurements indicated that the reaction proceeded in a layer-by-layer fashion into the bulk, maintaining a planar interface between reacted and unreacted CoO.

---

* Gaede Langmuir Award Winner

The reaction of the CoO(100) surface with 0.1 ML of Li resulted in the formation of 2-3 nm Co metal nanoparticles which decorated the CoO step edges. Upon further lithiation, the conversion reaction proceeded into the film preferentially at step edges. ARXPS measurements suggested that the reaction penetrated deep into the CoO film from these nucleation points before spreading across the rest of the surface. These combined results show the importance of crystallographic orientation in determining the reaction kinetics in a Li-ion battery.

11:20am SS+AS+EN-TuM11 Imaging Water Adsorption and Dissociation on RuO$_2$ (110) Surfaces, *Rentao Mu*, D.C. Cantu, X. Lin, V.A. Glezakou, Z.-T. Wang, I. Lyubinetsky, R. Rousseau, Z. Dohnálek, Pacific Northwest National Laboratory

Understanding water/solid interactions is a current critical scientific challenge with important implications for a variety of fundamental and applied processes. Here we study the interactions of water with RuO$_2$, which has a wide range of applications in photocatalytic water splitting, heterogeneous catalysis, electrochemistry and many other energy-related areas. We prepared stoichiometric (*s*-), reduced (*r*-) and oxidized (*o*-) RuO$_2$(110) surfaces and studied water adsorption, dissociation, and diffusion using time-lapsed scanning tunneling microscopy and density functional theory calculations. On *s*-RuO$_2$(110) we show that water monomers become mobile above 238 K and form dimers which are immobile below 273 K. More importantly, we find that the mobile water dimers dissociate readily to form Ru-bound H$_3$O$_2$ and hydroxyl species (HO$_b$) on bridging oxygen (O$_b$) rows. The onset for diffusion of H$_3$O$_2$ on *s*-RuO$_2$(110) is observed at ~273 K, indicating a significantly higher diffusion barrier than that for water monomers. The experimentally determined diffusion barriers are in agreement with those obtained from the DFT calculations. The observed behavior is compared and contrasted with that observed for water on isostructural rutile TiO$_2$(110) where both molecularly-bound monomers and dimers are in equilibrium with their deprotonated states. In contrast with TiO$_2$(110), the larger separation of Ru atoms induces the segmentation of water chains at high water coverages. On slightly oxidized *o*-RuO$_2$(110), water molecules react with oxygen adatoms (O$_a$'s) on Ru rows and form pairs of terminal hydroxyl groups which can reversibly dissociate back to a water molecule and O$_a$. This process results in the displacement of O$_a$'s along the Ru rows. Along- and across-row diffusion of isolated water molecules is tracked at room temperature on both slightly, and heavily oxidized *o*-RuO$_2$(110) by following the position of hydroxyl pairs. On *r*-RuO$_2$(110), we find that water molecules readily dissociate at bridging oxygen vacancies and form bridging hydroxyl groups. The mechanism of along- and across-row diffusion of the bridging hydroxyl protons is also studied at room temperature. The atomically-detailed, quantitative assessment of binding and diffusion of the surface species formed upon water adsorption on RuO$_2$(110) represent a critical step in achieving fundamental level understanding of the role RuO$_2$ plays as H$_2$ and O$_2$ evolution co-catalysts in photocatalytic water splitting reactions.

11:40am SS+AS+EN-TuM12 Surface Reaction Kinetics during Low Temperature ALD of Al$_2$O$_3$ Studied by Broadband Sum-frequency Generation, *Vincent Vandalon*, W.M.M. Kessels, Eindhoven University of Technology, Netherlands

The nonlinear optical technique of broadband sum-frequency generation (BB-SFG) has been used to study the surface reactions during atomic layer deposition (ALD). Vibrational BB-SFG spectroscopy is excellently suited for *in-situ* studies of the surface chemistry governing ALD because of its inherent interface selectivity, submonolayer sensitivity, and short acquisition times. In contrast to BB-SFG, conventional absorption spectroscopy, based on the so called "differential" measurements, monitors only changes on the surface. On the other hand, due to its surface selectivity, BB-SFG reveals information about both *persistent* and *changing* surface groups. Therefore, with this technique, open questions can be addressed such as the origin of the decrease in growth per cycle (GPC) at low temperatures of the ubiquitous process of thermal ALD of Al$_2$O$_3$ from Al(CH$_3$)$_3$ and H$_2$O. So far, a complete picture of the surface chemistry explaining the reduced GPC is missing and the exact cause of the limited growth at low temperatures remains unclear.

More particularly, the surface chemistry of thermal ALD Al$_2$O$_3$ was followed by monitoring the density of the -CH$_3$ surface groups. In contrast to ALD at high temperatures, below 200ºC it was observed that a significant amount of -CH$_3$ could not be removed during the water half-cycle. The observed kinetics could not be explained by a thermally-activated first-order reaction with a constant cross section. We investigated the temperature dependence of the reaction kinetics further by measuring the -CH$_3$ coverage as a function of precursor and co-reactant exposure at different temperatures. It found that the absolute cross section obtained for the TMA half-cycle was independent of temperature, indicating that the chemisorption of TMA is not a thermally activated process. The behavior during the water half-cycle was found to be more complex showing a strong

dependence on temperature; it cannot be described as a reaction simply obeying Arrhenius behavior. This is in line with the more complex behavior predicted by recent DFT work carried out by Shirazi and Elliott [Nanoscale 2015] where a so-called "cooperative" effect was observed leading to a coverage dependent reactivity. The observations presented in this work are direct experimental evidence of such a "cooperative" effect and were only possible due to the inherent surface selectivity of BB-SFG.

12:00pm **SS+AS+EN-TuM13 The Preparation and Redox Properties of Cu/Al$_2$O$_3$/ZnO(0001) Model Surfaces**, *J. Hu, J.J. Huang, H. Zhang,* ***Mingshu Chen***, Xiamen University, China

The Cu/Al$_2$O$_3$/ZnO(0001)-Zn ternary model catalysts were prepared and characterized by XPS and LEISS. The Al$_2$O$_3$/ZnO was prepared by depositing Al onto the ZnO surface in O$_2$ atmosphere at 523 K, and Cu/ZnO was prepared by depositing Cu onto ZnO surface at room temperature. It was found that Al$_2$O$_3$ grew on the ZnO surface by a layer-by-layer model, while Cu formed two-dimensional islands only at low coverage and three dimensional clusters at high coverage. For Cu/Al$_2$O$_3$/ZnO(0001)-Zn, the XPS and LEIS spectra showed that the copper islands were preferred on the interfaces of Al$_2$O$_3$/ZnO. Comparing to the Cu/ZnO binary model catalyst, the addition of Al$_2$O$_3$ obviously slowed down the reduction of Cu/Al$_2$O$_3$/ZnO by H$_2$. More significantly, the existence of Al$_2$O$_3$ in the ternary model catalyst leaded to an increase of Cu$^+$ concentration. The enhancement of Al$_2$O$_3$ in Cu/Al$_2$O$_3$/ZnO(0001)-Zn for methanol synthesis may origin from that the Al$_2$O$_3$ helps to stabilize the surface Cu$^+$ which has been proposed as one of the active sites.

Energy Frontiers Focus Topic
Room: 211B - Session EN+EM+NS+SE+SS+TF-TuA

Batteries and Supercapacitors
Moderator: Elijah Thimsen, Washington University, St. Louis, Andrew C. Kummel, University of California at San Diego

2:20pm EN+EM+NS+SE+SS+TF-TuA1 Behavior of Layered Cathode Materials: A Route to Higher Energy Density for Li-Ion Batteries, *Marca Doeff, F. Lin,* Lawrence Berkeley National Laboratory*, I. Markus,* Lawrence Berkeley Lab, University of California, Berkeley **INVITED**
The most promising cathode materials for Li-ion batteries geared towards vehicular applications are the so-called NMCs ($LiNi_xMn_yCo_zO_2$), based on cost and performance considerations. NMCs exhibit a slightly sloping voltage profile in lithium half-cells, with typical utilizations significantly lower than the theoretical capacity of about 280 mAh/g. An attractive strategy for increasing the energy densities of devices meant for traction applications would be to cycle NMCs to a higher potential than is currently used (usually about 4.3V vs. Li^+/Li) so that more lithium can be extracted and cycled. For this approach to be viable, the cathodes must exhibit excellent structural stability and good reversibility over a wide composition range. Our recent work has been directed towards understanding the high-potential behavior of NMCs, using an array of synchrotron x-ray techniques as well as transmission electron microscopy. These techniques show that surface reconstruction to rock salt and spinel phases occur during high voltage cycling, and result in impedance rises and apparent capacity losses. The degree to which this occurs is a function of how the material is made and its electrochemical history. Partial substitution of Ti for Co in NMCs not only increases the capacities obtained during cycling to 4.7V in lithium half-cells compared to baseline materials, but appears to improve the cycling behavior as well. First principles calculations show that the aliovalent substitution lowers the voltage profile slightly. This allows a greater amount of lithium to be extracted and cycled below 4.7V, resulting in higher practical capacities. The Ti-substitution also delays the formation of rock salt during charging, resulting in better capacity retention. These observations suggest that optimizing the synthesis and judicious substitution can mitigate deleterious structural changes of the NMCs due to high potential operation in Li-ion cells. These strategies should be combined with those designed to prevent side reactions with electrolytic solutions during high potential operation, such as new electrolytic solutions with improved oxidative stability, or atomic layer deposition coatings on electrode surfaces, to further ensure stable cycling.

3:00pm EN+EM+NS+SE+SS+TF-TuA3 Next-Generation Electrolytes for Lithium-Ion Batteries, *Sarah Guillot,* University of Wisconsin - Madison*, M. Usrey, A. Pena-Hueso,* Silatronix, Inc.*, R.J. Hamers,* University of Wisconsin-Madison and Silatronix, Inc.
Current-generation electrolytes for lithium-ion batteries are limited in electrochemical stability and thermal stability. Over the last several years, researchers at University of Wisconsin and at Silatronix, inc. have developed several new generations of electrolytes based upon incorporation of organosilane groups into the molecular structure. A recently developed class of compounds shows unprecedented enhancements in performance, including the ability to cycle full cells over 400 times at 70 degrees C, and the ability to reduce or eliminate "gassing" at cathode surfaces. In this talk we will discuss the molecular structure of these organosilane-based compounds, quantitative measurements of the decomposition pathways, and the resulting mechanistic insights into the molecular properties that gives rise to their outstanding performance characteristics.

3:20pm EN+EM+NS+SE+SS+TF-TuA4 Physico-Chemical Properties of Polyamidoamine Dendrimer-Based Binders for Carbon Cathodes in Lithium-Sulfur Batteries, *Manjula Nandasiri, P. Bhattacharya, A. Schwarz, D. Lu,* Pacific Northwest National Laboratory*, D.A. Tomalia,* NanoSynthons LLC*, W.A. Henderson, J. Xiao,* Pacific Northwest National Laboratory
Lithium-sulfur (Li-S) batteries are one of the most promising energy storage systems, offering up to five-fold increase in energy density as compared with state-of-the-art lithium-ion batteries to meet the growing demand for environmentally benign energy storage devices with high energy density, low cost, and long life time. For practical applications, high sulfur (active material) loading (> 2 mg/cm^2) within the carbon cathode in Li-S batteries is essential. Most reports on engineered cathode materials for Li-S batteries are based upon low sulfur loadings (typically ~1 mg/cm^2), which are

impractical and often give misleading results. It is unknown how these novel engineered cathodes behave under high sulfur loading conditions. The binder is perhaps the most critical material in achieving a high sulfur loading in carbon cathodes. We have recently used dendrimers with various surface chemistries as functional binders in Li-S cells with SuperP-carbon/S as the cathode material. Even without engineering the cathode, very favorable cycling stability and electrolyte wetting were obtained with these binders. It was attributed to the high density of surface functional groups on the dendrimers, high curvature of the binder and its porosity, and the interactions between the large number of basic nitrogen and oxygen atoms on the dendrimers and lithium polysulfides.

Here, we will discuss the fundamental properties of dendrimers as aqueous binders for Li-S battery cathodes and compare their performance with other aqueous, commonly used linear polymeric binders such as styrene butadiene rubber (SBR) and sodium carboxyl methyl cellulose (CMC). Specifically, generation 4 polyamidoamine (PAMAM) dendrimers with hydroxyl (OH), 3-carbomethoxypyrrolidinone (CMP), and sodium carboxylate (COONa) surface functional groups served as good, electrochemically stable binders at high S loadings (~3-5 mg/cm^2) with high initial capacities (> 1000 mAh/g). In comparison to CMC-SBR binder-based electrodes which failed at high C-rates (0.2C) after 40 cycles**,** dendrimer-based binders showed a capacity retention of >85% for more than 100 cycles. It was also observed that acidic groups and all-NH_2 surface groups are poor binders, whereas binders with COO^- and neutral surface groups (OH, CH_3) show better performance. X-ray photoelectron spectroscopy was used to identify different surface functional groups in these dendrimers and understand their interactions with SuperP-carbon/S cathode. In addition, a detailed physico-chemical characterization using IR spectroscopy and XANES/EXAFS will be presented to substantiate the superior dendrimer-carbon/S interactions.

4:20pm EN+EM+NS+SE+SS+TF-TuA7 The Road beyond Lithium Batteries is Paved — In Three Dimensions — With Rechargeable, Dendrite-Free Zinc, *Debra Rolison, J.F. Parker, C.N. Chervin, I.R. Pala, M.D. Wattendorf, J.W. Long,* U.S. Naval Research Laboratory **INVITED**
Lithium-ion batteries dominate the energy-storage landscape, but do so with the ever-present threat of thermal runaway and conflagration courtesy of flammable electrolytes and oxygen-releasing electrode materials. Fortunately, Zn-based batteries offer a compelling alternative grounded in the innate safety and cost advantages of aqueous electrolytes augmented by the high earth-abundance of Zn and the high energy density of Zn-based batteries (comparable to Li-ion). Traditional Zn-based batteries provide suboptimal utilization of the zinc (typically <60% of theoretical capacity) and poor rechargeability—thanks to the complex dissolution/precipitation processes that accompany Zn/Zn^{2+} cycling of conventional powder-bed Zn electrode structures in alkaline electrolyte. We address these limitations by redesigning the zinc anode as a porous, 3D-wired "sponge" architecture. Zinc sponge electrodes achieve >90% Zn utilization when discharged in primary Zn–air cells, retaining both the 3D framework of the Zn sponge and an impedance characteristic of the metal thanks to an inner metallic core of 3D zinc. When cycled in Ag–Zn and Ni–Zn cells, the Zn sponges retain monolithicity and reveal uniform deposition of charge/discharge products at the external and internal surfaces, even to deep depth-of-discharge of the zinc. These results show that all Zn-based chemistries can now be reformulated for next-generation rechargeable, Li-free batteries

5:00pm EN+EM+NS+SE+SS+TF-TuA9 Porous Silicon Electrochemical Capacitor Devices for Integrated On-Chip Energy Storage, *Donald Gardner, C.W. Holzwarth III, Y. Liu, S. Clendenning, W. Jin, B.K. Moon, Z. Chen, E.C. Hannah, T.V. Aldridge,* Intel Corp*, C.P. Wang, C. Chen,* Florida International University*, J.L. Gustafson,* Intel Corp
Integrated on-chip energy storage is increasingly important in the fields of internet of things (IoT), energy harvesting, and sensing. Silicon is already the materials of choice for the integrated circuits found in every IoT device; however, the efforts to integrate electrochemical (EC) capacitors on a silicon die have been limited. Unlike batteries, EC capacitors are electrostatic devices and do not rely on chemical reactions enabling cycle lifetimes of >1M. This is especially important for off-power-grid IoT devices where difficulty associated with regularly replacing the batteries of billions of devices is prohibitive. This work demonstrates electrochemical capacitors fabricated using porous Si nanostructures with extremely high surface-to-volume ratios and an electrolyte. Devices were fabricated with tapered channels sized from 100 nm at the top to 20 nm and with aspect ratios greater than 100:1. Surface coatings were necessary for long-term stability because unpassivated silicon structures react with the electrolytes. To obtain uniform coatings using stop-flow atomic layer deposition (ALD), efficient surface reactions are needed between high volatility, low molecular

weight, small molecular diameter precursors without chemical vapor deposition side reactions. $TiCl_4$ and NH_3 precursors were found to coat porous Si with TiN uniformly. Measurements of coated P-Si capacitors reveal that an areal capacitance of up to 6 mF/cm^2 can be achieved using 2 μm deep pores, and scales linearly with depth with 28 mF/cm^2 measured for 12 μm deep pores. Three-terminal CV measurements with EMI-BF$_4$ ionic electrolyte were used to examine the stability of different pore sizes and TiN coating thicknesses. Pores with an average 50 nm width and 100:1 aspect ratio were stable to ±1.2 V when cycled at 10 mV/s and stable to ±1.0 V when cycled at 1 mV/s. Different ionic liquids were studied to determine the ionic liquid best suited to TiN coated porous Si including TEA-BF$_4$/AN, EMI-BF$_4$, EMI-Tf, and a 3M EMI-BF$_4$/propylene carbonate (PC) mixture. Using impedance spectroscopy, the time constant for a 2 μm deep porous Si EC capacitor with a high conductivity TiN coating was found to be 17.6 ms which is fast enough that this can be used for applications involving AC filtering for AC-DC conversion. Measurements of volumetric energy density versus power density of porous Si devices versus other devices show several orders of magnitude higher energy density than electrolytic capacitors with a similar voltage range. These results are also between one to two orders of magnitude higher than other studies utilizing porous silicon and are comparable to commercial carbon-based EC capacitors.

5:20pm EN+EM+NS+SE+SS+TF-TuA10 Investigations of Magnesium Stripping and Deposition using *Operando* Ambient Pressure X-ray Photoelectron Spectroscopy, *Yi Yu*, Lawrence Berkeley National Laboratory, *Q. Liu*, Shanghai Tech University, China, *B. Eichhorn*, University of Maryland, College Park, *E.J. Crumlin*, Lawrence Berkeley National Laboratory

Since the first demonstration of rechargeable magnesium battery, magnesium metal has been considered as an attractive battery anode due to its high volumetric energy density, high negative reduction potential, natural abundance in the earth crust, and relatively good safety features due to its dendrite-free formation. Although it is well accepted that the dissolution and plating of metal plays an important role in the electrochemical properties related to the discharge and charge of the battery, the nature of metal-electrolyte chemical and electrochemical interaction is still not fully established. In an effort to elucidate the interfacial electrochemical mechanisms, we present the studies of magnesium deposition and stripping using *operando* ambient pressure X-ray photoelectron spectroscopy (AP-XPS). Synchrotron X-rays at the Advanced Light Source, Lawrence Berkeley National Laboratory and our 'tender' X-ray AP-XPS endstation allow for probing the liquid-solid interface at pressures up to 20 Torr. Cyclic voltammetry is employed to examine the reversibility of electrochemical magnesium deposition. This talk will provide details on how *operando* AP-XPS coupled with electrochemistry allows for studying electrochemical processes of magnesium deposition and stripping at the liquid-solid interface and yields chemical information relevant to real-world applications.

5:40pm EN+EM+NS+SE+SS+TF-TuA11 Atomic Layer Deposition of Solid Electrolytes for Beyond Lithium-Ion Batteries, *Alexander Kozen*, *G.W. Rubloff*, University of Maryland, College Park **INVITED**
Solid Li-based inorganic electrolytes offer profound advantages for energy storage in 3-D solid state batteries: (1) enhanced safety, since they are not flammable like organic liquid electrolytes; and (2) high power and energy density since use of the 3D geometry can maximize the volume of active material per unit area, while keeping the active layer thickness sufficiently small to allow for fast Li diffusion. The quality of thin solid electrolytes is currently a major obstacle to developing these solid state batteries, restricting electrolyte thickness to >100 nm to control electronic leakage, consequently slowing ion transport across the electrolyte and impeding 3-D nanostructure designs that offer high power and energy.

Furthermore, the ion-conducting, electron-insulating properties of solid electrolytes are promising for their use as protection layers on metal anodes (e.g., Li, Na, Mg) and on cathodes in proposed "beyond-Li-ion" battery configurations such as Li-NMC, Li-O$_2$, and Li-S to prevent electrolyte breakdown.

Atomic layer deposition (ALD) is well suited to the challenge of solid electrolytes, providing ultrathin, high quality films with exceptional 3-D conformality on the nanoscale. We have developed a quaternary ALD processes for the solid electrolyte LiPON, exploiting *in-operando* spectroscopic ellipsometry and *in-situ* XPS surface analysis for process development. ALD LiPON has tunable morphology, and a nitrogen-dependent tunable ionic conductivity as high as 3.5×10^{-7} s/cm.

We explore the potential of ALD solid electrolytes for the fabrication of solid, 3D microbatteries, as we as the use of thin ALD solid electrolyte coatings on metal anodes to improve interfacial stability against organic electrolytes and thus prevent SEI formation. We demonstrate and quantify

protection of lithium metal anodes with low ionic conductivity ALD Al$_2$O$_3$ coatings to prevent degradation reactions, and probe the surface chemistry and morphology of these anodes. Finally, we demonstrate that protection of Li metal anodes using ALD protection layers can improve the capacity of Li-S batteries by 60% by preventing anode corrosion by dissolved sulfur species in the electrolyte.

This work has implications beyond the passivation of lithium metal besides its focus and greatest impact on the Li-S battery system, as ALD protection layers could also be applied to other promising metal anode battery systems such as Mg and Na, and other beyond Li-ion technologies such as Li-NMC or- Li-Air where similar reactivity issues prevent adoption.

Nanometer-scale Science and Technology
Room: 212B - Session NS+EN+SS-TuA

Nanophotonics, Plasmonics, and Energy
Moderator: David Wei, University of Florida

2:20pm NS+EN+SS-TuA1 Subnanoscale Exciton Dynamics of C$_{60}$-based Single Photon Emitters Explored by Hanbury Brown Twiss Scanning Tunneling Microscope, *Pablo Merino Mateo*, C. Grosse, A. Rosławska, K. Kuhnke, K. Kern, Max-Planck-Institut für Festkörperforschung, Germany
Electron-hole pair (exciton) creation and annihilation by charges are crucial processes for technologies relying on efficient charge-exciton-photon conversion. Photoluminescence has been instrumental for this purpose with near-field techniques approaching 20 nm spatial resolution. However, molecular resolution is still out of reach and individual charge carriers cannot be addressed with these methods. In the present contribution we show how to overcome these limitations by using scanning tunneling microscopy (STM) to inject current at the atomic scale and Hanbury Brown-Twiss (HBT) interferometry to measure photon correlations in far-field electroluminescence.

Quantum systems like molecules or quantum dots cannot emit two photons at the same time which results in an antibunching of the emitted photon train and a dip in the photon-photon correlation function. Such single photon emitters are key elements for quantum cryptography and their miniaturization to the nanoscale would be desirable. This requires reproducible emitter separations typically below the optical diffraction limit and has imposed strong limitations on suitable structures and materials.

Using our HBT-STM setup on localized trap states in C$_{60}$ multilayers we were able to study single photon emission at the ultimate molecular scale. Controlled injection allows us to generate excitons in C$_{60}$ and probe them with charges one by one. We demonstrate electrically driven single photon emission and determine exciton lifetimes in the picosecond range. Monitoring lifetime shortening and luminescence saturation for increasing carrier injection rates provides access to charge-exciton annihilation dynamics with Ångstrom spatial resolution. Comparison with theory reveals exciton quenching efficiencies close to unity. Our approach introduces a unique way to study single quasi-particle dynamics on the ultimate molecular scale.

2:40pm NS+EN+SS-TuA2 Low-Damage Etching Process for the Fabrication of GaAs based Light-Emitting Devices, *Cedric Thomas*, A. Higo, Tohoku University, Japan, T. Kiba, Hokkaido University, Japan, Y. Tamura, Tohoku University, Japan, N. Okamoto, I. Yamashita, Nara Institute of Science and Technology, Japan, A. Murayama, Hokkaido University, Japan, S. Samukawa, Tohoku University, Japan
Fabrication of quantum dots (QD) and their use for optical devices are still facing big challenges, for instance a high-density and three-dimensional array of QDs is hardly achieved. We report here the fabrication of stacked layers of GaAs QDs (called nanodisks, NDs) of less than 20 nm in diameter by a top-down approach and their optical characteristics when embedding in light emitting device.

The fabrication process consists of a bio-template [1] used to create a high density etching mask coupled to a low-damage etching process using neutral beam (NB) [2]. The bio-template is realized by a self-assembled monolayer (SAM) of proteins called ferritins (cage like proteins) of 12 nm outside diameter with a 7 nm iron oxide core. The proteins are functionalized with poly-ethylene glycol (PEG) to control the ferritin-to-ferritin distance and avoid any ND coupling after fabrication. After removing the protein shell by oxygen based treatment, a high-density (ca. 1×10^{11} cm^{-2}) nano-pattern of cores is used as etching mask. The NB etching consists of an inductively couple plasma chamber separated from the process chamber by a carbon electrode with a high aspect-ratio aperture

array. Therefore, the charged particles are efficiently neutralized and the UV photons from the plasma almost completely screened

Stacks of GaAs and AlGaAs layers were grown by metalorganic vapor phase epitaxy (MOVPE), with a GaAs cap layer of a few nanometer thick. SAM of ferritins was done by spin-coating. After removing protein shell by oxygen annealing in vacuum, a hydrogen radical treatment was performed to remove to remove the oxide layer. Etching was then realized by pure chlorine NB. Regrowth of AlGaAs barrier was done by MOVPE. Finally, temperature dependence of photoluminescence emission and ND light emitting diode were measured and results discussed [3].

[1] I. Yamashita et al., Biochim. Biophys. Acta 1800 (2010) 845

[2] S. Samukawa et al., Jpn. J. Appl. Phys. 40 (2001) L997

[3] A. Higo et al., Sci. Reports 5 (2015) 9371

3:00pm NS+EN+SS-TuA3 Surface Plasmon-Mediated Selective Deposition of Au Nanoparticles on Ag Bowtie Nano-Antennas, *Jingjing Qiu, D. Wei*, University of Florida
Utilizing intrinsic surface properties to selectively direct and control nanostructure growth on a nanostructure is fundamentally interesting and holds great technological promise. We observed a surface plasmon resonance (SPR)-induced selective deposition of gold nanoparticles (Au NPs) at the tip of a silver (Ag) bowtie nanostructure using 532 nm laser excitation. Nanoscale secondary ion mass spectrometry (NanoSIMS) was applied to chemically image the distribution of elements after deposition, reaching a spatial resolution of ~50 nm and an elemental analysis sensitivity of 50 ppm. Possible mechanisms underlying this selective deposition were proposed based on the experimental evidence and theoretical discrete dipole approximation (DDA).

3:20pm NS+EN+SS-TuA4 Broadband Light Trapping in Nanopatterned Substrates for Photovoltaic and Photonic Applications, *Carlo Mennucci*, Department of Physics, University of Genova, Genova, Italy, *C. Martella, M.C. Giordano, D. Repetto, F. Buatier de Mongeot*, University of Genova, Italy
Here we report on self-organised nanofabrication method applied to substrates of relevance in the field of optoelectronic and photonics in view of light trapping applications. We demonstrate the optical functionalization of glass [1], crystalline semiconductor (GaAS and Si [2]) and TCO substrates recurring to a self-organised pattern formation based on low-energy Ion Beam Sputtering (IBS). High aspect ratio nanoscale features are formed recurring to defocused IBS through a self-organised sacrificial Au nanowire stencil mask. Ion-beam irradiation at grazing angle leads to the formation of quasi-periodic one-dimensional nanostructures with a characteristic lateral size in the range of 200nm and a root-mean-square roughness (σ) of the surface, measured by Atomic Force Microscope, ranging from 80 to 150nm.

These nanostructures confer broadband anti-reflective bio-mimetic functionality to crystalline semiconductor substrates (GaAs and Si [2]) as well as to glass and TCO substrates in the Visible and Near Infra-Red part of the spectrum. In fact, suppression of the reflected light intensity is due to high aspect ratio sub-wavelength features which leads to a progressive transition of the refractive index from the value of air to that of the substrate (index grading) analogous to that observed in the corneas of nocturnal moths. At the same time the patterned substrates have shown enhanced broadband light scattering due to the extended vertical dynamic of the surface corrugations with lateral size comparable or bigger than light wavelength. Moreover, Angular Resolved Scattering measurements has recently proved that nanostructured glasses can scatter light in the Visible and Near Infra-Red range of spectrum more efficiently and at wider angles with respect to standard Ashai-U substrates commonly used in optoelectronic device applications.

In order to asses the light trapping effect, identical amorphous thin film silicon solar cells (p–i–n single junctions) are grown on nano-patterned and on reference flat glass superstrates. Their performance is assessed by measuring their I–V characteristic and EQE under standard AM1.5g test conditions. The first encouraging results demonstrated that solar cells grown on patterned substrates with RMS roughness σ around 80 nm exhibit a 15% relative enhancement in photocurrent.

References:

[1] C. Martella, D. Chiappe, P. Delli Veneri, L.V. Mercaldo, I. Usatii, F.Buatier de Mongeot, Nanotechnology 24 (22), 225201 (2013).

[2] C. Martella, D. Chiappe, C. Mennucci, F. Buatier de Mongeot ,J.Appl.Phys. 115,194308 (2014).

4:20pm NS+EN+SS-TuA7 *In Situ* Visualization of Intercalation-Driven Nanoparticle Phase Transitions using Plasmon-EELS, *Jennifer Dionne*, Stanford University INVITED
A number of energy-relevant processes rely on nanomaterial phase transitions induced by solute intercalation. However, many of these phase transitions are poorly understood, since observing them in nanomaterials – and in particular in individual nanoparticles – can be extremely challenging. This presentation will describe a novel technique to investigate intercalation-driven phase transitions in individual nanoparticles, based on *in-situ* environmental transmission electron microscopy (TEM) and plasmon electron energy loss spectroscopy (EELS). As a model system, this presentation will focus on the hydrogenation of palladium nanoparticles. We use the plasmon-EEL signal at varying hydrogen pressures as a proxy for hydrogen concentration in the particle. First, we investigate the hydriding properties of single-crystalline particles, free from defects and grain boundaries, and free from elastic interactions with the substrate. We obtain single particle loading and unloading isotherms for particles ranging from approximately 10 nm to 100 nm, allowing us to address outstanding questions about the nature of phase transitions and surface energy effects in zero-dimensional nanomaterials. We find that hydrogen loading and unloading isotherms of single crystals are characterized by abrupt phase transitions and macroscopic hysteresis gaps. These results suggest that thermodynamic phases do not coexist in single-crystalline nanoparticles, in striking contrast with ensemble measurements of Pd nanoparticles. Then, we extend our single-particle techniques to explore the hydriding properties of polycrystalline and multiply-twinned nanoparticles, including Pd nanorods and icosahedra. In contrast to single crystalline nanoparticles, these particles exhibit sloped isotherms and narrowed hysteretic gaps. Based on these results, we develop a model to deconvolve the effects of disorder and strain on the phase transitions in nanoscale systems. Lastly, we describe techniques to generate high-resolution plasmon-EELS (and hence phase) maps of nanoparticles. These mapping studies promise unprecedented insight into the internal phase of nanomaterials, and can be complemented with diffraction and dark-field imaging studies. We will discuss how these results could be used to interpret the thermodynamics of Li-ion insertion in battery electrodes, hydrogen absorption in state-of the-art metal hydride catalysts, or ion exchange reactions in quantum dot syntheses.

5:00pm NS+EN+SS-TuA9 Pulsed Laser-Induced Self-Assembly of Noble Metal Nanoparticles and an EELS Characterization, *Yueying Wu*, University of Tennessee, *G. Li*, University of Notre Dame, *C. Cherqui, N. Bigelow*, University of Washington, *J.P. Camden*, University of Notre Dame, *D. Masiello*, University of Washington, *J.D. Fowlkes*, Oak Ridge National Laboratory, *P.D. Rack*, University of Tennessee
Controlled nanoscale synthesis of plasmonic nanostructures based on noble metals is critical for realizing many important applications such as surface-enhanced Raman spectroscopy (SERS), subwavelength waveguides, plasmonically enhanced photovoltaics, and photocatalysis. Recently pulsed laser induced dewetting (PLiD) has been shown to be an intriguing self and directed assembly technique for elemental and alloyed metallic nanoparticles. The liquid-phase assembly takes place in single to tens of nanoseconds and is governed by liquid phase instabilities and hydrodynamics of liquid thin films which produce arrays of random or highly ordered nanoparticles. In our recent studies, the PLiD of un-patterned, as well as nanolithographically pre-patterned thin films of various shapes and sizes was investigated for the purpose of understanding how initial boundary conditions facilitate precise assembly. The resultant ultra-smooth and metastable nanoparticles (~20nm to 1μm) are expected to be ideal building blocks for plasmonic applications. Based on this, we present a study on the self-assembly of gold and silver alloy thin films and also provide a comprehensive characterization of the resultant nanoparticles using electron energy loss spectroscopy (EELS) and through simulation using full-wave electron-driven discrete-dipole approximation (e-DDA). The study provides for the first time a thorough mapping of the plasmonic modes of synthesized Au-Ag alloy nanoparticles over a large size range.

5:20pm NS+EN+SS-TuA10 Flexible, Adaptive Optoelectronic Camouflage Skins Using Concepts Inspired by Cephalopods, *Cunjiang Yu*, University of Houston
Octopus, squid, cuttlefish and other cephalopods exhibit exceptional capabilities for visually adapting to or differentiating from the coloration and texture of their surroundings, for the purpose of concealment, communication, predation and reproduction. Long-standing interest in and emerging understanding of the underlying ultrastructure, physiological control and photonic interactions has recently led to efforts in the construction of artificial systems that have key attributes found in the skins of these organisms. In spite of several promising options in active materials for mimicking biological color tuning, such as cholesteric liquid crystals, electrokinetic and electrofluidic structures, colloidal crystals and

plasmonics, existing routes to integrated systems do not include critical capabilities in distributed sensing and actuation.

The results reported here show that advances in heterogeneous integration and high performance flexible/stretchable electronics provide a solution to these critical sub-systems when exploited in thin multilayer, multifunctional assemblies. The findings encompass a complete set of materials, components, and integration schemes that enable adaptive optoelectronic camouflage sheets with designs that capture key features and functional capabilities of the skins of cephalopods. These systems combine semiconductor actuators, switching components and light sensors with inorganic reflectors and organic color-changing materials in a way that allows autonomous matching to background coloration, through the well-known working principle of each device.

Demonstration devices capable of producing black-and-white patterns that spontaneously match those of the surroundings, without user input or external measurement, involve multilayer architectures of ultrathin sheets of monocrystalline silicon in arrays of components for controlled, local Joule heating, photodetection and two levels of matrix addressing, combined with metallic diffuse reflectors and simple thermochromic materials, all on soft, flexible substrates. Systematic experimental, computational and analytical studies of the optical, electrical, thermal, and mechanical properties reveal the fundamental aspects of operation, and also provide quantitative design guidelines that are applicable to future, scaled embodiments.

5:40pm **NS+EN+SS-TuA11 Controlled Deposition of High Quality Nanocrystal Multilayer Structures for Optoelectronic Applications**, *Sara Rupich*, *A.V. Malko, Y.N. Gartstein, Y.J. Chabal*, University of Texas at Dallas
In order to meet the world's growing energy demand, harvesting energy from the sun is necessary. While silicon-based solar cells remain the industry standard, hybrid Si/nanocrystal (NC) structures exhibit significant promise for the development of the next generation of photovoltaic devices. In most current NC-based photovoltaics, photons are absorbed, separated and extracted in the NC layer; however, conversion efficiencies are limited by interface quality and carrier mobility. Hybrid Si/NC structures offer an alternative approach. In these structures, light is absorbed in the NC layer and transferred via efficient excitonic radiative (RET) and non-radiative (NRET) energy transfer into the underlying Si substrate where charge extraction and collection occurs. In order to utilize such structures, the controllable deposition of tens of layers of NCs needs to be realized where the composition of each layer can be varied. While many techniques exist to deposit NCs on substrates (i.e. spin coating, dropcasting), these methods result in thick films with limited control over the composition. Composition controlled structures need to be built up one layer at a time.

Here, we present the controllable deposition of dense, NC multilayer structures on Si and SiO$_2$ substrates via evaporation-driven self-assembly at the air-liquid interface. Using a layer-by-layer approach, CdSe/ZnS NC multilayers were assembled, up to 15 layers in thickness. Extensive spectroscopic (UV-vis absorbance, photoluminescence (PL), ellipsometry) and microscopic (scanning electron microscopy and atomic force microscopy) characterization provided evidence for the successful deposition of high quality NC multilayers in each cycle. Additionally, the NCs were found to retain their quantum yields in the multilayers structures indicating that the deposition process does not introduce additional interface trapping centers and showing their promise for integration into optoelectronic devices. Using time-resolved PL measurements, a gradual increase in the average measured NC PL lifetime was observed as a function of layers for NC multilayers on Si surfaces. This behavior was confirmed by theoretical modeling and is indicative of the gradual reduction in ET efficiency as a function of distance and.

As this process is applicable to NCs of different size, shape and composition, the fabrication of band gap graded multilayers structures is possible, which would enable energy harvesting schemes based on directed energy flows.

6:00pm **NS+EN+SS-TuA12 Efficient Coupling of Visible Light to Thin Film Waveguides; FDTD Field Model Results for Nanometer Scale Graded Index/Waveguide Structures.**, *Adam Lambert*, *E. Demaray*, AVS
Previous work utilizing Finite Difference Time Domain (FDTD) models with 20 nm resolution demonstrated normal incident plane wave AM 1.5 solar light could be coupled and concentrated into modes of a lateral duct with ~ 91% efficiency for tapered concentrator with spatially uniform refractive index. However, for efficient coupling and mode compression into high index waveguides in advanced devices, continuously graded index films on the order of 150-200nm with nonlinear profiles have been shown to be near ideal anti-reflective coatings which Antropy Technology can now produce at high volume using modern sputter coating processes. Such devices could be revolutionary not only in the field of photonics, but could also open the path for an wide variety of green energy and advanced

lighting applications. This presentation focuses on current advances in the parametric investigation of nonlinear refractive index profiles and related sputter coating production processes. The FDTD problem solving framework provides the fully resolved time dependent propagation of the electromagnetic field, accounting for the nonlinear influence of subwavelength structures and allowing for detailed design of the thin film product. We are reporting resolution capabilities are in the 1-5nm range depending on the relevant length scales for the process. Quantification of power, absorption/heat, and other variables relevant to R&D can easily be extracted during post processing. Parallel Monte Carlo simulations predict the refractive index profile resulting from dual source, inline, biased pulse DC sputter coating. The combination allows for highly accurate feasibility studies and front end process design. Both quantified numerical results as well as qualitative animations of the influence of the subwavelength devices are presented for both processes, as well as a detailed overview of the potential applications.

Surface Science
Room: 113 - Session SS+AS+EN-TuA

Mechanistic Insight of Surface Reactions: Catalysis, ALD, etc. - II
Moderator: Bruce D. Kay, Pacific Northwest National Laboratory

2:20pm **SS+AS+EN-TuA1 How does Absorbed Hydrogen Drive Olefin Hydrogenation on Pd?**, *Satoshi Ohno*, *M. Wilde, K. Fukutani*, The University of Tokyo, Japan
Pd-dissolved hydrogen is an essential ingredient in the highly selective hydrogenation of olefinic C=C double bonds catalyzed by Pd, yet the particular role played by H below the surface has long been debated controversially. Some proposed that absorbed H atoms become directly involved in hydrogenation reactions after they emerge from the metal interior onto the catalyst surface in an energetic state. Others considered that sizeable populations of subsurface sites by absorbed hydrogen indirectly activate surface-adsorbed hydrogen by altering the electronic structure of the catalyst.

To resolve this dispute we have studied the hydrogenation reaction of cis-2-butene to butane on a Pd(110) model catalyst surface with temperature-programmed desorption (TPD) and ^{1}H(^{15}N, ag)^{12}C nuclear reaction analysis (NRA) that reveals the hydrogen distribution on and beneath the surface. TPD demonstrates that the catalytic hydrogenation reaction proceeds efficiently between 160 and 250 K. NRA under the hydrogenation reaction condition, on the other hand, shows that the H concentration in the Pd subsurface region is as small as 0.5 at. %. Thus, the scenario of indirect surface-hydrogen activation through large quantities of H in the subsurface sites appears rather unrealistic for our experimental conditions. We furthermore elucidate that the butane reaction yield scales linearly with the number of Pd-dissolved H atoms that reach the surface after diffusion from the Pd bulk. This observation clarifies that the Pd-catalyzed olefin hydrogenation is triggered by the emergence of bulk-dissolved hydrogen onto the Pd surface. Our NRA H profiles also demonstrate that the catalytic reaction proceeds on the Pd surface fully saturated with chemisorbed hydrogen. This surface hydrogen is considered important, as it possibly prevents deactivation of reactive surface hydrogen species in vacant chemisorption sites.

Finally, the TPD spectrum of butene shows four peaks at 140, 165, 190, and 225 K, suggesting multiple butene-adsorption modes onto Pd(110) surfaces. Reactive TPD experiments in presence of absorbed hydrogen exhibit a significant decrease in the 165 K peak, identifying this feature as the reactive butene species in the catalytic hydrogenation reaction.

2:40pm **SS+AS+EN-TuA2 CO Oxidation over Pd Catalysts Supported on Different Low-Index Surfaces of CeO$_2$: A Combined Experimental and Computational Study**, *Xiao Liu*, *Y.W. Wen, Z.Z. Chen, B. Shan, R. Chen*, Huazhong University of Science and Technology, China
Pd/CeO$_2$ has attracted much attention on the low temperature CO oxidation due to the strong metal-support interactions. In this study, we have systematically investigated the interface properties and CO oxidation activities of Pd catalysts supported on different low-index surfaces of CeO$_2$. The Pd/CeO$_2$ nanorods have been prepared by incipient wetness impregnation method and the exposed surfaces of CeO$_2$ nanorods have been controlled by changing the calcination temperature after their successful synthesis by hydrothermal method. Their catalytic activities in CO oxidation have been tested and the results show that Pd catalysts supported on CeO$_2$ nanorods exposed by (100) and (110) (calcined at 500 ºC) are more

activated than that exposed by (111) (calcined at 700 ºC), which is related to the surface oxygen vacancies concentration and the strength of interface interaction. By performing density functional calculations, the surface oxygen activities and the binding strength of Pd clusters on these low-index surfaces of CeO_2 have been investigated. The results show that the oxygen vacancy formation energies of (100) and (110) are smaller than that of (111). The binding strength of Pd clusters on these surfaces follows the sequence: (100) > (110) > (111). Furthermore, CO oxidation routes on these surfaces proceeding through the LH, ER and MvK mechanism have been studied. Our studies not only reveal that the catalytic performance of Pd/CeO_2 can be tuned by controlling the exposed surface of oxide but also shed light on the interface structures and CO oxidation mechanism of Pd/CeO_2 system.

3:00pm SS+AS+EN-TuA3 *In Situ* Adsorption and Decomposition Studies of Dimethyl Methyl Phosphonate on Molybdenum Oxide Surfaces and Nanoparticles, *Ashley Head*, *L. Trotochaud, Y. Yu*, Lawrence Berkeley National Laboratory (LBNL), *Z. Hicks, X. Tang, K. Bowen,* Johns Hopkins University, *B. Eichhorn,* University of Maryland, College Park, *H. Bluhm*, LBNL

There is great interest in understanding the interaction between the nerve agent simulant dimethyl methyl phosphonate (DMMP) and metal oxide surfaces to further nerve agent filtration technology and decomposition methods. To this end, we have studied the room temperature adsorption of DMMP on MoO_2 and MoO_3 surfaces up to 30 mTorr using ambient pressure x-ray photoelectron spectroscopy (APXPS). On both surfaces, the majority of DMMP adsorbs intact, but differences in the behavior of DMMP on the two substrates are found upon heating. Two phosphorus species are seen on the MoO_2 surface and three are seen on the MoO_3; these species remain on both surfaces up to 450 ºC Additionally, carbon remains on the MoO_2 at high temperatures but is removed from MoO_3 by 420 ºC. The APXPS data were correlated with TPD measurements of DMMP adsorbed on MoO_3 clusters on HOPG, a model system closer to real filtration materials. Methanol was found as the major decomposition product in addition to trace amounts of dimethyl ether. The easily reducible MoO_3 is likely responsible for an oxidative cleavage of the $P-CH_3$ bond on both the surface and nanoparticles. These studies highlight how APXPS coupled with TPD yields chemical information relevant to real-world applications.

3:20pm SS+AS+EN-TuA4 Adsorption of Sterically Hindered Sulfur Containing Molecules on a Heterogeneous Model Catalyst, *Signe Sørensen, J.V. Lauritsen*, Aarhus University, Denmark

Cobalt promoted MoS2 nanoclusters (CoMoS) are the active phase of the hydrodesulfurization catalyst which enables sulfur removal from crude oil. New legislations on sulfur impurity levels in diesel in EU and US demands still lower sulfur content which increases the requirements for even more effective catalysts.

Previously catalysts were improved by costly trial-and-error experiments. To target the improvements attempts, understanding of the catalytic mechanism is crucial. In the hydrodesulfurization catalysis the main source to residual sulfur content is the sterically hindered sulfur containing molecules, as the reactivity towards these is very low. To targeted enhance the catalytic activity, atomic scale understanding of this catalytic mechanism is essential.

Scanning tunneling microscopy (STM) is an outstanding tool for real space, atomic-scale imaging of supported nano-scale systems. This makes it the optimal tool for investigating the interaction between the sulfur containing molecules and metal-supported CoMoS, as it offers the unique and powerful ability to directly observe the catalytic active site by imaging single molecules adsorbing on the nanoparticles.

In this study STM is used on a model system of Co-promoted MoS2 on a gold substrate under ultrahigh vacuum conditions. To study the adsorption of the strongly steric hindered sulfur containing molecule 4,6-dimethyl-dibenzothiophene the molecule is dosed directly onto the nanoparticles which means that their location, orientation and the dynamics of single molecules can successfully be revealed through atom-resolved STM images and films. All observed adsorption modes are either associated with a sulfur vacancy on the corner site of the nanoclusters or with the one-dimensional metallic edge state associate with the edge of the Co-promoted MoS2 nanoclusters. These observations strongly indicate that these sites are important active sites of the catalyst and enable targeting the attempts for enhanced activity to optimization of the number of these apparent active sites in the industrial catalyst.

4:20pm SS+AS+EN-TuA7 Metal Nanoparticles on Thin Film Oxide Supports: Interaction and Reaction of Metals with Hydroxyls, *Martin Sterrer*, University of Graz, Austria **INVITED**

Water-oxide interaction is of great importance in a number of technologically relevant fields, among them heterogeneous catalysis. Several studies report on the promoting effect of water in catalytic reactions, the participation of surface hydroxyls in catalytic reactions, and the influence of hydroxylation on the binding of metals to oxide surfaces. Achieving a fundamental atomic scale understanding of water-oxide interaction at environmentally and catalytically relevant conditions (e.g. ambient pressure) represents, therefore, a challenge for surface science studies related to heterogeneous catalysis. In this contribution, I will present results of our recent studies related to the interaction of water with thin, single crystalline oxide films (Fe-oxides, alkaline earth oxides) carried out in a wide range of water chemical potential (from UHV to mbar water pressures). Topics that will be discussed are the characterization of ordered water monolayers, the dewetting of ice on oxide surfaces, hydroxylation of oxide surfaces at elevated pressure, the influence of hydroxyls on metal nucleation and sintering, and metal deposition onto oxide surfaces from aqueous solutions.

5:00pm SS+AS+EN-TuA9 Dynamics of Isolated Surface Complexes Formed Between a Chemisorbed Chiral Molecule and a Prochiral Reactant, *Jean-Christian Lemay*, *Y. Dong, P.H. McBreen*, Laval University, Canada

Adsorbed chiral molecules (chiral modifiers) can interact stereoselectively with prochiral co-adsorbates on reactive metal surfaces (1). This is used in one of the most common methods to perform asymmetric heterogeneous catalysis. The chiral modifier provides stereoselection through non-covalent assembly with a substrate, forming isolated complexes with well-defined geometries. We will present a variable temperature STM study of individual bimolecular complexes formed by enantiopure 1-(1-naphthyl)ethylamine and three representative prochiral substrates on Pt(111). The results reveal sub-molecularly resolved and time-resolved stereospecific data for competing complexation geometries. Time-lapsed STM measurements of individual substrate molecules sampling a set of interaction geometries provide new insight on the dynamics of stereocontrol. The results reveal that a single prochiral substrate can probe various sites on the surface due to diffusion and prochiral switching. This shows the importance of considering interconversion between complexation geometries to fully understand the stereocontrol operated by the chiral modifier. The results will be discussed in the context of proposed mechanisms for enantioselective hydrogenation.

5:20pm SS+AS+EN-TuA10 Density Functional Theory Study of CO Assisted Water Dissociation, *Liney Arnadottir, L. Halberstadt*, Oregon State University

Previous computational studies of methanol oxidation reaction intermediates (H-C=O and C-OH) have shown significant effects of water on both adsorbate adsorption energy as well as activation energies of interconversion between the two. On a clean Pt(111) surface the interconversion between the two forms goes through a very stable COads and Hads intermediates and the activation barriers of CO + H to from HCO or COH are high or 1.3 and 1.8 eV respectively. In the presence of a single coadsorbed water molecule the activation barrier for this interconversion from HCO to COH was found to be much lower or 0.62 eV. These studies were motivated by experimental studies of methanol oxidation on Pt which found CO_2 formation at potentials lower then typically required for CO oxidation. Here we investigate Pt-water interactions and the effects of co-adsorbate CO on water dissociation as a possible CO assisted water dissection as an alternative reaction pathway on Pt surfaces.

6:00pm SS+AS+EN-TuA12 Crystalline Growth of Ice - Studying the Transition from the First Wetting Layer to Multilayers with Scanning Tunneling Microscopy, *Barbara Lechner, S. Maier, M.B. Salmeron*, Lawrence Berkeley National Laboratory

The growth of water layers on model substrates has been studied intensively, yet many questions still remain [1,2]. After many years of research, the structure of the first wetting layer on metal surfaces has been determined in comprehensive experimental and theoretical studies [3-5]. A surprisingly complex behavior was revealed, showing that the strain caused by the mismatch of the hexagonal planes in the ice crystal structure and the lattice of the substrate is released by forming structures that include rotated hexagons, pentagons and heptagons of molecules, in addition to strongly bound hexagonal rings commensurate with the substrate. A range of experimental and theoretical investigations showed that, on many substrates, the water monolayer does not expose any dangling hydrogen bonds as all water molecules adsorb either flat-lying or with a hydrogen atom pointing towards the surface [1,6]. Growth of multilayer water films that preserve the "down-pointing" average dipole orientation of water has been proposed to occur in some cases, resulting in the formation of

"ferroelectric ice" [7]. However, the growth of the entropically more favorable, proton-disordered ice requires flipping some of the molecules in the first layer to expose dangling hydrogen bonds. Such molecular reorientation may be kinetically hindered, and has been invoked to be the reason for the hydrophobic character of many water monolayer films at low temperatures [6].

Here, we present high-resolution scanning tunneling microscopy (STM) measurements of water layers adsorbed on Pt(111) and Ru(0001) to study the transition from the first layer to multilayers. We observe that a second water layer initially grows in an amorphous structure when grown on the crystalline monolayer containing pentagons, hexagons and heptagons of water molecules. To facilitate the growth of ice in a bulk-like hexagonal arrangement, the first wetting layer needs to rearrange into a hexagonal structure commensurate with the surface.

[1] Hodgson, A.; Haq, S. *Surf. Sci. Rep.* **2009**, *64*, 381–451.

[2] Carrasco, J.; Hodgson, A.; Michaelides, A. *Nat. Mater.* **2012**, *11*, 667–674.

[3] Maier, S.; Stass, I.; Cerdá, J. I.; Salmeron, M. *Phys. Rev. Lett.* **2014**, *112*, 126101.

[4] Tatarkhanov, M.; Ogletree, D. F.; Rose, F.; Mitsui, T.; Fomin, E.; Maier, S.; Rose, M.; Cerdá, J. I. *J. Am. Chem. Soc.* **2009**, *131*, 18425–18434.

[5] Nie, S.; Feibelman, P. J.; Bartelt, N. C.; Thürmer, K. *Phys. Rev. Lett.* **2010**, *105*, 026102.

[6] Kimmel, G. A.; Petrik, N. G.; Dohnálek, Z.; Kay, B. D.; Kimmel, G. A.; Petrik, N. G.; Dohnálek, Z.; Kay, B. D. *J. Chem. Phys.* **2007**, *126*, 114702.

[7] Su, X.; Lianos, L.; Shen, Y. R.; Somorjai, G. A. **1998**, 1533–1536.

Surface Science
Room: 112 - Session SS+EN-TuA

Photocatalysis, Photochemistry, and Chirality at Surfaces
Moderator: Arthur Utz, Tufts University

2:20pm SS+EN-TuA1 Photoemission of Electron from Diamond Into Water: Enabling Novel Electrochemical Reduction Reactions, *Robert Hamers*, D. Zhu, L.H. Zhang, University of Wisconsin-Madison, *J. Bandy*, University of Wisconsin-Madson, *G.M. Nathanson, J.R. Schmidt*, University of Wisconsin-Madison

Diamond's unusual property of negative electron affinity has long been used to enhance electron emission in vacuum. Recently we have demonstrated that diamond's facile electron emission properties can also be extended to solid-liquid interfaces. Electron photoemitted from diamond into water lead to formation of solvated electrons, widely regarded as the chemist's perfect reducing agent. We demonstrate the inexpensive diamond thin films and diamond powder can be used as solid-state sources of electrons able to induce the reduction of N2 to NH3 and the selective reduction of CO2 to CO. In this talk we will discuss the factors that influence electron emission into liquids, differences from emission into vacuum, and how electrons emitted into liquids can induce novel reduced chemistry not possible with traditional photocatalysts.

2:40pm SS+EN-TuA2 STM Tip-Induced Desorption of TMAA from TiO₂(110): Model Study of a Photocatalytic Process, *Denis Potapenko*, R.M. Osgood, Jr., Columbia University

Titanium oxide is a versatile photocatalytic material with numerous applications in the areas related to utilization of solar energy. Scanning Tunneling Microscopy (STM) allows explorations on the single molecule basis thus providing important insight into the physical phenomena involved in photocatalysis. Our experiments examine the tip-induced chemistry of trimethyl acetic acid (TMAA) molecules adsorbed on TiO₂ rutile(110) surface;this systems was chosen as a model for light-driven catalysis since it is easily imaged with STM and since this system has been the subject of many earlier studies of photo and thermal chemistry. In present work we study the electrical hole-driven desorption of TMAA molecules, initiated by the charges, injected from the STM tip. Different values of the flux and the energy of the excitation charges were achieved by the simultaneous control of the setpoint current and the bias voltage of the STM tunneling junction. The dynamics of the tip-induced desorption of TMAA was compared with the photo-induced dynamics of the same reaction. In the latter experiments the monochromated light from a UV lamp was used as the source of excitation. We show that there is a threshold energy for a hot hole below the edge of the TiO₂ valence band that is required for TMAA photo-desorption.

3:00pm SS+EN-TuA3 Ultrafast Time-resolved Photoelectron Spectroscopy of Photocatalytic Surfaces, *Hrvoje Petek*, S. Tan, A. Argondizzo, University of Pittsburgh **INVITED**

We investigate the ultrafast optical excitation and electron relaxation pathways for the clean and molecule covered rutile TiO₂(110) surface. Using high power, broadly tunable (2.9-4.6 eV), 20 fs noncollinear parametric amplifier excitation source, we perform multiphoton photoemission (mPP) spectroscopy of TiO₂ surface. The energy, momentum, and pump-probe delay time resolved mPP spectra provide information on the occupied and unoccupied density of states that participate in photoemission from the valence band or the Ti-3d defect states on reduced TiO₂ surfaces. We find a new bulk transition between the Ti-3d bands of t_{2g} and e_g symmetry, which dominates the photoemission process form the Ti-3d defect states below the conduction band minimum of TiO₂.[1] The 3D mPP spectra provide information on the phase and energy relaxation of photoexcited electrons and holes.[2] Adsorption of molecules introduces adsorbate-induced resonances,[3,4] which can be excited by charge transfer excitation from the Ti-3d defect states. Metal nanoparticles grown on TiO₂ also open new photoemission pathways. We map out the energy and momentum distributions of the adsorbate and nanoparticle resonances as well as their relaxation dynamics.

1. Argondizzo, A.; Cui, X.; Wang, C.; Sun, H.; Shang, H.; Zhao, J.; Petek, H., Ultrafast multiphoton pump-probe photoemission excitation pathways in rutile TiO₂(110). *Phys. Rev. B* **91**, 155429 (2015).

2. Cui, X.; Wang, C.; Argondizzo, A.; Garrett-Roe, S.; Gumhalter, B.; Petek, H., Transient excitons at metal surfaces. *Nat. Phys* **10**, 505 (2014).

3. Onda, K.; Li, B.; Zhao, J.; Jordan, K. D.; Yang, J.; Petek, H., Wet Electrons at the H₂O/TiO₂(110) Surface. *Science* **308**, 1154 (2005).

4. Li, B.; Zhao, J.; Onda, K.; Jordan, K. D.; Yang, J.; Petek, H., Ultrafast interfacial proton-coupled electron transfer. *Science* **311**, 1436 (2006).

4:20pm SS+EN-TuA7 Surface and Interface Properties of Photoelectrocatalysts for Solar Fuels, *Bruce Koel*, C.X. Kronawitter, P. Zhao, Z. Chen, Princeton University

Experiments using well-defined model catalysts under controlled conditions and utilizing a range of spectroscopic techniques for characterization of surface and interface properties and the nature and reactivity of surface-bound species can greatly advance understanding of the structure and reactivity of photoelectrocatalysts for solar fuels. We report on several of our recent studies, which include investigations of the effects of dopant incorporation on the structural and chemical properties of the α-Fe₂O₃(0001) surface for water oxidation catalysis, facet-dependent activity and stability of Co₃O₄ nanocrystals towards OER, and the interaction of water with GaP(110), a semiconductor that is known to enable selective CO₂ reduction to methanol in aqueous solutions of CO₂ and nitrogen-containing heteroaromatics. For water oxidation on α-Fe₂O₃, we found that Ni doping in thin films of model catalysts caused a new termination for the films and induced formation of more stable surface-bound OH groups. For the Co₃O₄ system, we used the well-defined morphologies of nanocubes and nanooctahedra to demonstrate that the (111) surfaces vastly out-perform the (100) surfaces for OER activity (overpotential and current density). Finally we have spectroscopically identified *in situ* the surface-bound species on GaP(110) associated with exposure to water using ambient pressure photoelectron spectroscopy (APPES). These observations on model systems afford further analysis and discussion of the role of surface-bound species in mechanisms for catalyzed water oxidation and CO₂ reduction.

4:40pm SS+EN-TuA8 Improving Hematite-Based Solar Water Splitting by Surface Modification with Sn, Ti, and FeOOH, *Anjli Patel*, A.J. Abel, Drexel University, *I. Garcia-Torregrosa*, Utrecht University, Netherlands, *B. Opasanont, J.B. Baxter*, Drexel University

Photoelectrochemical (PEC) water splitting with hematite (α-Fe₂O₃) photoanodes presents a promising route to sustainable energy production due to hematite's favorable bandgap, chemical stability, and widespread abundance. However, limitations arise from sluggish oxygen evolution reaction (OER) kinetics at the hematite-electrolyte interface, requiring a significant overpotential to induce photocatalysis. We report on the effects of Sn, Ti, and FeOOH surface treatments on hematite photoanodes to improve PEC performance by overcoming surface kinetic limitations. Thin film hematite photoanodes were fabricated by successive ionic layer adsorption and reaction (SILAR) of FeOOH on F:SnO₂–coated glass substrates, followed by annealing at 450 C to induce phase transition of FeOOH into hematite. Subsequent annealing at 775 C caused diffusion of Sn from the F:SnO₂ substrate through the hematite, resulting in 0.5at% Sn concentration at the photoanode surface. Current-voltage testing revealed that the presence of Sn in the hematite film significantly reduced the photocurrent onset potential, suggesting improved hole injection efficiency. Electrochemical impedance spectroscopy (EIS) revealed a reduction in the surface state charge transfer resistance ($R_{ct,ss}$) by 2 orders of magnitude,

supporting the importance of interfacial kinetics. Hematite photoanodes doped with up to 10% Ti were also prepared by incorporating titanium into the SILAR deposition bath. Ti doping decreased the onset potential by 600 mV and significantly increased the plateau photocurrent density from 0.01 mA/cm^2 at 1.23 V vs. RHE for undoped hematite to nearly 0.6 mA/cm^2 for Ti-doped photoanodes. EIS showed that Ti-doping reduced the $R_{ct,ss}$ at applied potentials ranging from 0.8 to 1.6 V vs. RHE, indicating a possible catalytic effect on the OER reaction at the photoanode surface. FeOOH films were deposited on the hematite photoanodes by an additional SILAR step, which reduced the photocurrent onset potential and increased the plateau photocurrent density by 20%. Unlike Ti, the FeOOH surface treatment exhibited little to no effect on the $R_{ct,ss}$, suggesting that FeOOH does not directly catalyze the OER. However, both the FeOOH treatment and Ti doping significantly increased the peak surface state capacitance, which may be attributed to an increase in density of charged states at the hematite surface, resulting in higher plateau photocurrent. Together, these treatments yield photocurrents that are 3x larger than previous reports using SILAR-deposited planar hematite films, offering promising opportunities to overcome challenges in PEC water splitting with hematite photoanodes.

5:00pm SS+EN-TuA9 Metalation of a Polypyridine Macrocycle on Au(111): Preparation of a Water Reduction Catalyst on a Solid Substrate, *Gerson Mette*, *D. Sutter, S. Schnidrig, B. Probst, R. Alberto, J. Osterwalder*, Universität Zürich, Switzerland
Within the search for new materials and methods for renewable energy resources, photocatalytic water splitting is a very promising field of study. In this framework, a polypyridine macrocycle was investigated which was already described in 1984 but only superficially examined [1]. It shares some similarities to porphyrins but with pyridyl subunits instead of pyrrol, hence the given trivial name: *pyrphyrin*. A high stability of the pyrphyrin and corresponding complexes is indicated due to its conjugation, planarity and cyclic nature. Furthermore, metal complexes based on pyrphyrin show promise as water reduction catalysts.

In this study, we examined the preparation of a pyrphyrin metal complex on a single crystalline surface in ultrahigh vacuum. In a first step, pyrphyrin coverages of approximately one monolayer and less, as determined by XPS measurements, were obtained by sublimation of the molecules on a Au(111) surface at room-temperature. By means of Low-Energy Electron Diffraction (LEED) and Scanning Tunneling Microscopy (STM), two distinct phases depending on the surface coverage were identified and structurally characterized. In a second step, deposition of Co metal at the level of 5% of a monolayer and subsequent annealing led to the formation of an almost complete monolayer of Co-ligated pyrphyrin molecules.

[1] S. Ogawa et al., J. Am. Chem. Soc. **1984**, 106, 5760-5762.

5:20pm SS+EN-TuA10 Chiral Selective Chemistry Induced by Natural Selection of Spin-Polarized Electrons by DNA, *Richard Rosenberg*, Argonne National Laboratory, *D. Mishra, R. Naaman*, Weizmann Institute of Science, Israel
Most biomolecules can be synthesized in two different mirror-image (chiral) shapes, namely two enantiomers. The enantiomers are recognized by their ability to rotate the polarization of linear polarized light either to the left (L) or to the right (D). In bio-organisms, sugars are always D and amino acids are always L. How this enantiomeric preference originated remains a mystery. Investigations into possible avenues of prebiotic chiral selectivity have been pursued since the time of Pasteur. Many investigations in this area have been devoted to pathways that involve preferential destruction of a particular isomer in an initially racemic (equal quantities of both enantiomers) mixture, through the interactions of chiral particles such as circularly polarized UV radiation or longitudinally spin polarized electrons. It has been shown that low energy (0 – 10 eV) spin polarized secondary electrons, produced by irradiation of a magnetic substrate, can induce chiral-selective chemistry in an adsorbed adlayer.[1] Additional work has demonstrated that organized, double-stranded (ds) DNA, adsorbed on a gold substrate, acts as a natural spin filter for initially unpolarized, low energy (0 – 1.2 eV) electrons produced by UV irradiation of the substrate, resulting in net polarizations as high as 60%.[2] Experiment and theory indicates that this spin filtering effect should be effective for higher energy (E < 15 eV) electrons as well.[3] In the present study, we probe if low energy secondary electrons, produced by x-ray irradiation of a gold substrate, and transferred through the chiral monolayer, induce enantiomeric selective chemistry in an adsorbed adlayer. To test this, (R)- or (S)-epichloroydrin (C_3H_5ClO, Epi) was adsorbed on a self-assembled monolayer of 70 base pair long dsDNA. The secondary electron-induced reaction was monitored by following changes in the Cl 2p x-ray photoelectron spectroscopy spectra. By kinetic modeling of the reaction, quantum yields (QYs) were determined. For S-Epi the QY was ~16 % greater than for the (R) enantiomer, while the QYs were the same for the two enantiomers when they were adsorbed on bare Au.

[1] R. A. Rosenberg, M. Abu Haija, P. J. Ryan, Phys. Rev. Lett. **2008**, 101, 178301.

[2] a) B. Gohler, V. Hamelbeck, T. Z. Markus, M. Kettner, G. F. Hanne, Z. Vager, R. Naaman, H. Zacharias, Science **2011**, 331, 894-897; b) S. G. Ray, S. S. Daube, G. Leitus, Z. Vager, R. Naaman, Phys. Rev. Lett. **2006**, 96, 036101.

[3] R. A. Rosenberg, J. M. Symonds, V. Kalyanaraman, T. Markus, T. M. Orlando, R. Naaman, E. A. Medina, F. A. López, V. Mujica, J. Phys. Chem. C **2013**, 117, 22307-22313.

5:40pm SS+EN-TuA11 Creating Enantioselective Surfaces; Templating and One-to-one Interactions, *Wilfred Tysoe*, University of Wisconsin-Milwaukee
The mode of operation of heterogeneous chiral modifiers can be classified into those operating as templates, where several modifier molecules act in concert to define a chiral adsorption site, or one-to-one modifiers that form a docking complex between the modifier and a prochiral reactant.

Enantioselectivity is measured by adsorbing chiral probe molecules onto chirally modified surfaces. Templating is illustrated using aminoacids on Pd(111). Scanning tunneling microscopy (STM) reveals that some aminoacids form tetrameric units, and others form dimers. Only those aminoacids that form tetramers are enantioselective implying that the tetramers act as templates.

Naphthylethylamine (NEA) is proposed to acts as a one-to-one modifier. The interaction between NEA and a prochiral reactant, methyl pyruvate, is explored using STM. Possible docking complexes are identified using density functional theory and the simulated images are compared with experimental images. Finally, it is shown the tartaric acid on Pd(111) acts as a one-to-one modifier for glycidol and is controlled by hydrogen-bonding interactions.

6:00pm SS+EN-TuA12 Single-Molecule and Single-Active-Site Studies of Stereocontrol by Chemisorbed Chiral Molecules, *Peter McBreen, Y. Dong, J.C. Lemay, G. Goubert,* Laval University, Canada, *M.N. Groves, B. Hammer,* Aarhus University, Denmark
Isolated adsorbed chiral molecules can stereodirect prochiral co-adsorbates on reactive metal surfaces and the application of this phenomenon underpins a method to perform asymmetric heterogeneous catalytic reactions. Typically, the stereochemical action is attributed to intermolecular interactions in complexes formed by docking the prochiral substrate in a chiral pocket created by the chemisorbed chiral molecule. We will present results from combined variable temperature STM and optB88-vdW DFT studies of individual bimolecular docking complexes formed by enantiopure 1-(1-naphthyl)ethylamine and selected prochiral molecules on Pt(111). The experiments reveal sub-molecularly resolved and time-resolved site-specific and stereospecific data. The results show that a single chemisorbed enanantiomer simultaneously presents several chiral pockets, each displaying a specific prochiral ratio for a given substrate molecule. A hierarchy of metal-molecule and molecule-molecule interactions is found to control prochiral selection at each site. Time-lapsed STM measurements of individual substrate molecules sampling a set of chiral pockets provide new insight on the dynamics of stereocontrol.

Energy Frontiers Focus Topic
Room: Hall 3 - Session EN-TuP

Energy Frontiers Poster Session

EN-TuP1 Effect of Ultra-violet Light on the Degradation in Organic Solar Cells, *Kenji Harafuji,* Ritsumeikan University, Japan, *H. Sato,* Ritsumeikan University

Organic solar cells (OSCs) offer many desirable properties such as flexibility, low cost, and easy fabrication. The lifetime is, however, still short. The degradation may be driven by light illumination, exposure to external air, and high temperature.

The degradation phenomenon under repetitive light illumination and high-vacuum is experimentally investigated in small molecular OSCs. The OSC has a structure of an indium tin oxide (anode)/copper phthalocyanine (donor, 20 nm)/fullerene (acceptor, 40 nm)/bathocuproine (buffer, 10 nm)/Ag (cathode, 100 nm). Xenon lamp illumination with an intensity of 100 mW/cm^2 is performed, and an air mass 1.5 global spectrum is obtained using a solar simulator. The repetitive illumination with the period of 30 s is composed of 100 repetitions of 3 s illumination followed by 27 s in the dark. The effect of light wavelength on the degradation is studied with the use of a long-pass filter of cut-wavelength λ_c. The filter allows the transmission of light into the OSC only with its wavelength longer than λ_c. Six kinds of filter with λ_c=0, 320, 370, 400, 550 and 665 nm are used.

It is found that the OSC degradation is dominated by the UV (ultra-violet) light with wavelength less than 400 nm. The short-circuit current density J_{sc}, open-circuit voltage V_{oc}, and fill factor FF in the case of λ_c=0 nm (without the filter) are decreased approximately 20%, 40%, and 60% compared with the case of λ_c greater than 400 nm at the 100th illumination, respectively. Resultantly, power conversion efficiency η_p is decreased 80%. The η_p value is decreased 60% with the filter of λ_c =320 nm, whereas initial η_p is almost kept even at 100th illumination with the filter of λ_c =400 nm. An S-shaped kink appears near the V_{oc} region in the current-voltage (J-V) characteristics at 100th illumination in the case of λ_c shorter than 400 nm. This shows the increase of series resistance in the OSC. The origin may be due to the disorder of crystal structure at the anode/donor interface. There are no appreciable changes of J-V characteristics between at 1st and 100th illuminations in the case of λ_c longer than 400 nm.

On the other hand, the initial η_p value at the first illumination is much smaller as λ_c is increased in the range of λ_c longer than 400 nm, accompanied by the large decrease of J_{sc}. This is because the total amount of light energy transmitted into active organic layers is decreased as λ_c is longer.

The origin of the degradation by illumination is revealed to be the UV light component with its wavelength shorter than 400 nm. The optimum λ_c value is 400 nm from the compromise between initial efficiency η_p and OSC degradation.

EN-TuP2 Characteristics of DSSC Fabricated at Low Temperature, *EunChang Choi, J.U. Wie, B.Y. Hong,* Sungkyunkwan University, Republic of Korea

Dye-sensitized solar cells (DSSCs) have been widely investigated as a next-generation solar cell because of their simple structure and low manufacturing cost. To realize a commercially competitive technology of DSSCs, it is imperative to employ a technique to prepare nanocrystalline thin film on flexible organic substrate, aiming at increasing the flexibility and reducing the weight as well as the overall device thickness of DSSCs. The key operation of glass-to-plastic substrates conversion is to prepare mesoporous TiO2 thin film at low temperature with a high surface area for dye adsorption and a high degree of crystallinity for fast transport of electrons. However, the electron transport in the TiO2 film synthesized at low temperature is very poor. So, in this study, TiO2 films synthesized at high temperature were transferred on the selective substrate. We fabricated DSSCs at low temperature using this method. So, we confirmed that the performance of DSSCs using TiO2 films synthesized at high temperature was improved.

EN-TuP3 Conductivity Enhancement Effect of Sodium Dodecyl Sulfate on PEDOT:PSS for Organic Solar Cell Application, *K.-H. Hwang, H.J. Seo, S.-H. Nam, Y.J. Kim, C.Y. Park,* **Jin-Hyo Boo**, Sungkyunkwan University, Republic of Korea

There are many researches on PEDOT:PSS treatment for application to flexible device electrode. Almost PEDOT:PSS treatment is consisted with step adding little bit surfactant to enhancement of adhesion between PEDOT:PSS and substrate or TCO materials. But basic research about surfactant effect is lacking. We study on the effects of sodium dodecyl sulfate (SDS) with controlling the concentration in aqueous PEDOT:PSS solution, and we confirm the conductivity enhancement of the mixture thin films with surfactant and PEDOT:PSS. Thin films are firstly prepared by spin coating method and then fabricated organic solar cells. To study the structural effects on the resulted electrical properties, thin films are mainly investigated by FE-SEM (Field Emission Scanning Electron Microscopy), AFM (Atomic Force Microscopy), respectively. At the same time, electric properties are also investigated by both 4-point probe and solar simulator.

Keywords: PEDOT, SDS, Surfactant, Organic solar cell, Electrical conductivity

EN-TuP4 Study of the Synthesis of Cu$_2$ZnSnS$_4$ Thin Films by Reactive Magnetron Co-Sputtering, *P.-A. Cormier,* **Rony Snyders**, University of Mons, Belgium

Cu$_2$ZnSnS$_4$(CZTS) has attracted significant attention for thin film solar cells because it is composed on earth abundant and non-toxic elements and, has an optimal band gap of 1.5 eV. The control of the film stoichiometry is critical during the growth of CZTS thin films. We previously demonstrated the possibility to grow close to stoichiometric and phase pure crystallized CZTS thin films by reactive magnetron co-sputtering [1]. The films were close to stoichiometric (Zn/Sn=1.1-1.4, Cu/[Zn+Sn]=0.9-1.1). Nevertheless, it has been suggested that Cu-poor Zn-rich CZTS have would present the best solar cell performances [2].

Therefore, in the present work, aiming to better control the film stoichiometry and to deeper understand the relationship between the chemical composition of the deposited film and its phase constitution and ultimately to reach the best performances of the cell, two Cu poor CuSn targets presenting Cu/Sn ratio of 1.5 (CuSn1.5) and 1 (CuSn1) have been utilized. In both case, the effect of the sputtering power (P$_{CuSn}$) on the material properties has been studied. The films were characterized by multiwavelength Raman spectroscopy (785 and 325 nm), by X-Ray Diffraction (XRD), and by Energy-dispersive X-ray spectroscopy (EDX).

As expected, the phase constitution is affected by increasing P$_{CuSn}$. Using the CuSn1.5 target, its evolution is similar than the one observed using the CuSn2 target [1]: at low P$_{CuSn}$, the films mainly contain CZTS, with a low content of ZnS. Increasing the power, CZTS disappears to the profit of SnS, Cu$_4$Zn clusters, S$_6$ and ZnS. On the contrary, using the CuSn1 target does not allow the formation of CZTS dominated films. Indeed, even for the low P$_{CuSn}$ conditions, ZnS dominates the Raman spectra. For medium power (P$_{CuSn}$ = 45W), the film is composed by SnS, S$_6$, ZnS and CZTS while for higher powers, the films are similar than the one obtained with the CuSn1.5 and CuSn2 targets and the CZTS is replaced by Cu$_4$Zn clusters. For all sets of data, the concentration in Zn is stable. Therefore, the decomposition of the CZTS material seems to be related to the increase of the Cu and Sn concentrations and to the decrease of the S one, which deviates from the theoretical values in CZTS. Based on these data, a phase diagram can be built.

Finally, one film of each region was synthesized and used in solar cell devices in order to investigate the influence of the phase constitution on the cell performance with efficiency up to 1.8%.

[1] Cormier et al., Acta Materiallia, accepted for publication subjected to minor revisions (2015)

[2] Mitzi et al., Solar Energy Materials & Solar Cells 95 (2011)

EN-TuP5 Development of Low Cost, Solution Deposition Method for High Efficiency Cu$_2$ZnSn S$_x$Se$_{4-X}$(CZTSSe) Thin Film Solar Cells, *Cheik Sana, S. Shahriar, J. Galindo, D. Kava, D.R. Hodges,* University of Texas at El Paso

Non-vacuum, solution based processing of earth abundant Cu$_2$ZnSnS$_x$Se$_{4-x}$ (CZTSSe) has attracted considerable interest as a material capable of driving economical and terawatt capacity photovoltaic module production. It has already shown promising results with solar cells efficiency up to 12.6%. The interest to CZTSSe as an absorber layer for thin film solar cells is due to its large absorption coefficient of over 10^4 cm^{-1} in the visible range, its tunable optical band on-vacuum solution based method to deposit Cu$_2$ZnSnS$_x$Se$_{4-x}$ (CZTSSe) was investigated. In this approach, a precursor solution of CZTSSe is formed by reacting metal sources copper (II) acetate monohydrate, zinc (II) acetate dehydrate, tin (II) chloride dehydrate and elemental powders of sulfur and selenium powders in a solution of 2-metoxyethanol. The slurry was then spincoated followed by annealing at different temperatures. Optical, structural and electronic characterization of thin films were performed using scanning electron microscope (SEM), X-ray diffractometer (XRD), raman spectrometer, UV-Vis spectrophotometer,

4 point probe and Hall Effect Measurement System. Film thickness was measured using Dektak 150 surface profilometer. X-Ray diffragtograms show different shifts of the kesterite/stannite (112) peak, which indicates the presence of CZTSSe. The three major peaks of the (1112, (220), and (312) planes had respective 2θ in the vicinity of 28°, 47.5° and 56°. The shift of the peaks depends on the ratios of S/Se in the synthetized material. The lattice constants decrease linearly with increasing contents of S in the precursor solution. Raman spectroscopy showed traces of both quaternary CZTS and CZTSe.

EN-TuP7 Synthesis and Characterization of Electron Beam Deposited $Cu_2ZnSn_{1-x}Si_xS_4$ Thin Films, *Alejandro Alvarez Barragan*, *S. Exarhos, J. Hernandez, L. Mangolini*, University of California - Riverside

Nowadays, $Cu_2In_xGa_{1-x}Se_4$ (CIGS) and CdTe are the leading commercially available compounds in thin film photovoltaics technology. Nevertheless, the scarcity of In and Te, and the toxicity of Cd, are considerable threats that may hinder the production and increase the cost of these materials in the near future. Replacement of In, Ga, and Se in CIGS with Zn, Sn, and S yields the promising quaternary compound Cu_2ZnSnS_4 (CZTS). This material has a favorable direct band gap of 1.5 ev. Further, each of its constituent elements is earth abundant and non-toxic. These two attractive characteristics make it plausible to launch CZTS as the wave of the future in thin film PV. We now present the synthesis process of CZTS by electron beam evaporation and a subsequent sulfurization step[1]. A thin film of Zn, Cu, and Sn stacked layers was obtained upon localized heating of their respective metallic sources. The as-deposited layers were subsequently sulfurized under a vacuum inside a sealed quartz tube at temperatures ranging from 500°C to 600°C. One of the main difficulties that has been reported for CZTS synthesis is the stoichiometric control of the material. Secondary, unwanted phases such as CuS, SnS_2, ZnS, and Cu_2SnS_3 may nucleate if the initial atomic percentage of the layers or the sulfurization parameters are off a small window in which CZTS can be produced[2,3]. Extreme care was taken to prevent this issue. Characterization techniques such as Energy Dispersive Spectroscopy (EDS), X-ray Diffraction (XRD), and Raman Spectroscopy were heavily employed to confirm the presence of CZTS crystals. We are also presenting preliminary results regarding the synthesis of a $Cu_2ZnSn_{1-x}Si_xS_4$ structure. To the best of our knowledge, synthesis of this compound by the E-beam evaporation and sulfurization process is yet to be reported. Previous theoretical and experimental data regarding its wide band gap add up to the interest of engineering this material for optoelectronic applications[4].

1. Cheng, a.-J. *et al.* Imaging and phase identification of Cu2ZnSnS4 thin films using confocal Raman spectroscopy. *J. Vac. Sci. Technol. A Vacuum, Surfaces, Film.***29,** 051203 (2011).

2. Nagoya, A., Asahi, R., Wahl, R. & Kresse, G. Defect formation and phase stability of Cu2ZnSnS4 photovoltaic material. *Phys. Rev. B***81,** 113202 (2010).

3. Polizzotti, A., Repins, I. L., Noufi, R., Wei, S.-H. & Mitzi, D. B. The state and future prospects of kesterite photovoltaics. *Energy Environ. Sci.***6,** 3171 (2013).

4. Nakamura, S., Maeda, T. & Wada, T. Phase Stability and Electronic Structure of In-Free Photovoltaic Materials: Cu2ZnSiSe4 , Cu2ZnGeSe4 , and Cu2ZnSnSe4. *Jpn. J. Appl. Phys.***49,** 121203 (2010).

EN-TuP8 Optical and Photocatalytic Properties of Nanostructured Ce-TiO_2 Mixed Oxides, *R. Ramirez-Lopez,* Escuela Superior de Ingenieria Quimica e Industrias Extractivas-IPN, Mexico, *Isaias Hernandez-Perez,* Universidad Autonoma Metropolitana- Azcapotzalco, CBI, Mexico, *R. Suarez-Parra,* Instituto de Energias Renovables, UNAM, Mexico, *RT. Hernandez-Lopez,* Universidad Autonoma Metropolitana- Azcapotzalco, CBI, Mexico, *A. Garcia-Sotelo, E. Campos, M. Melendez-Lira,* Cinvestav-IPN, Mexico

The use of nano-crystalline TiO_2 is a promising strategy for photocatalytic remediation of wastewater due to its broad ability to remove various pollutants in aqueous media. In order to use a major part of the spectral solar distribution it would be necessary to reduce the bandgap of TiO_2 based materials. In this study, a series of nanocrystalline CeO_2-TiO_2 powders were successfully synthesized by sol-gel at room temperature, employing titanium isopropoxide and cerium nitrate as precursors, with nominal 2, 5, 10, 20 and 50 % of CeO_2:TiO_2 molar ratio. The crystalline structure, surface morphology and optical properties of synthesized samples were characterized using powder XRD, TEM, SEM, XPS. The optical band gap was determined by DR-UV-Vis spectroscopy and the emission spectrum by photoluminescence spectroscopy. Photocatalytic activity was evaluated by the photodegradation of Orange II azo dye, employing two different sources of irradiation 365 and 425 nm. Structural characterization showed that the Ce-TiO_2 particles crystallized into the anatase phase. TEM micrographies shown clearly the formation of nanocrystals. The optical bandgap energy shows a red shift for all synthesized samples compared with pure TiO_2. The

results shown that the incorporation of 5 % CeO_2 effectively improves the photocatalytic activity comnpared wit pure TiO_2 at UV; while Ce incorporation activates it for 425 nm excitation still the nominal 5% shows the best performance. The results are discussed in terms of the electronic structure modification by Ce incorporation in the TiO2 matrix.

EN-TuP9 Hybrid Photoelectrode Based on Two-Dimensional Materials Decorated $BiFeO_3$ Thin Films for Efficient Solar Water Splitting, *C.M. Youn, H. Lee, J. Lee, H. Lee, **Taekjib Choi***, Sejong University, Republic of Korea

Semiconducting metal oxides have been attracted much interest as photoelectrodes for solar water splitting because of their stable photochemical activity in aqueous solutions. However, photoelectrochemical performance is usually limited by poor charge carrier separation. Thus, hybrid photoelectrodes combined with semiconducting ferroelectric materials offer promising potential for achieving efficient solar water splitting by promoting photogenerated-charge carrier separation due to spontaneous electric polarization leading to an increase in the elective electric field. In this study, we have fabricated two-dimensional materials decorated $BiFeO_3$ thin films as hybrid electrodes. The structural and optical properties of single and hybrid electrodes were comparatively characterized. The hybrid electrodes exhibited a stronger absorption of visible light and produced a higher photocurrent than that of single electrode. For hybrid electrodes, photoelectrochemical characterization demonstrated a large enhancement of the interfacial charge transfer kinetics as well as an efficient charge carrier separation, which greatly contributed to the improved photoelectrochemical performances. In addition, we will discuss poling effect of electric polarization on interface reduction/oxidation (REDOX) through electrolyte ions. Therefore, our results provide useful information for developing highly efficient hybrid photoelectrodes for solar water splitting.

EN-TuP11 Improvement in Photovoltaic Response of PLZT Thin Film Capacitors with ITO Electrodes, *Sushma Kotru*, *V.N. Harshan, V. Batra*, The University of Alabama

Ferroelectric thin films of perovskite-type structure are of practical interest because of their excellent ferroelectric, dielectric and optical properties. Recently these materials have generated lot of research interest for photovoltaic applications (PV) . Photovoltaic properties of $Pb_{0.95}La_{0.05}Zr_{0.54}Ti_{0.46}O_3$ (PLZT) thin film capacitors prepared using solution based method with various top electrodes having different work functions are investigated. The results demonstrate that ITO (Sn doped In_2O_3), a transparent conducting oxide, as top electrode, enhances the magnitude of photo voltage and photo current as compared to metal electrodes. The photovoltaic efficiency is enhanced by orders of magnitude with ITO as top electrode when compared to metal electrode devices. Thus the choice of transparent conducting oxide as an electrode holds potential for improving the photovoltaic response of ferroelectric thin film capacitors.

EN-TuP14 Rational Design of Battery Architecture at Nanoscale: Self-Aligned Batteries Inside Nanopores via Atomic Layer Deposition, *C. Liu, E. Gillette, **Xinyi Chen**, A.J. Pearse, A.C. Kozen, M. Schroeder, K. Gregorczyk, S.B. Lee, G.W. Rubloff*, University of Maryland, College Park

A self-aligned nanostructured battery entirely confined within a single nanopore offers a powerful platform to investigate the rate performance and cyclability limits of nanostructured storage devices. Atomic layer deposition (ALD) has enabled such a structure that embeds coaxial nanotubular electrodes and electrolyte confined inside a single anodic aluminum oxide (AAO) nanopore, realizing an ultrasmall full cell battery with ~$1\mu m^3$ volume (~1fL). These nanopore batteries display exceptional power-energy performance and cyclability when tested as massively parallel devices (~2billion/cm^2). The extraordinary thickness and conformality control of ALD and the highly self-aligned nanoporous structure of AAO are crucial to fabrication of precise, self-aligned, regular nanopore batteries. Using controlled-conformality ALD processes, we optimized metal nanotube current collector (Ru or Pt) length at two ends of AAO nanopores to provide fast electron transport to overlying anode and cathode materials, while keeping them spatially and electrically isolated. Crystalline V_2O_5 was deposited as lithium ion storage material inside the metal nanotubes using O_3 as the oxidant. . Subsequently, the V_2O_5 was electrochemically prelithiated at one end to serve as anode while pristine V_2O_5 without Li at the other end served as cathode, enabling the battery to be cycled between 0.2V and 1.8V. Capacity retention of this full cell is 95% at 5C rate and 46% at 150C, with more than 1000 charge/discharge cycles. Further increase of full cell output potential is also demonstrated for SnO_2 and TiO_2 anodes in asymmetric full cells with V_2O_5 cathodes. These results reveal the potential of ultrasmall, self-aligned/regular, densely packed nanobattery structures as a building block for high performance energy storage systems and as a test bed to study ionics and electrodics at nanoscale with a variety of geometrical modifications.

[1] Liu, C.; Gillette, E. I.; Chen, X.; Pearse, A. J.; Kozen, A. C.; Schroeder, M. A.; Gregorczyk, K. E.; Lee, S. B.; Rubloff, G. W., An all-in-one nanopore battery array. *Nature Nanotechnology* **2014,** *9* (12), 1031-1039.

Thin Film
Room: 111 - Session TF+EN-WeM

ALD for Energy
Moderator: Jesse Jur, North Carolina State University,
Angel Yanguas-Gil, Argonne National Lab

8:00am TF+EN-WeM1 Photovoltage Design for ALD Metal Oxide Protected Solar-Water-Splitting Photoanodes, *Andrew Scheuermann*, *J.P. Lawrence, K.W. Kemp, O.L. Hendricks*, Stanford University, *A. Walsh, I. Povey, M.E. Pemble, P.K. Hurley*, Tyndall National Institute, *C.E.D. Chidsey, P.C. McIntyre*, Stanford University

Metal oxide protection layers for photoanodes may enable the development of large-scale solar fuel and chemical synthesis. ALD-TiO_2 is the most widely used material because of its excellent stability under water oxidation conditions and potential for high electrical conductivity both as an ultrathin film and with thicknesses exceeding 100 nm [1-3]. However, the most conductive ALD-TiO_2 films exhibit poor photovoltages of ~ 400 mV and less [3]. Even assuming near-ideal fill factors, these voltages fall far short of the values needed for viable water splitting devices. Photovoltage optimization is especially difficult to achieve in MOS photoanodes because of the presence of a defective metal oxide protection layer and a defective semiconductor/oxide interface in the device structure. Therefore, understanding how to optimize photovoltage and stability is of utmost concern for the advancement of the field.

Here we report a novel observation of photovoltage loss associated with charge transfer in these metal-oxide protected devices, and by eliminating it, achieve photovoltages as high as 630 mV, the maximum reported to date for single-junction water-splitting silicon cells. The loss mechanism is systematically probed in MOS Schottky junction cells compared to buried junction p+n cells, revealing the need to maintain a characteristic hole density at the semiconductor/insulator interface. A capacitor model that predicts this loss is developed, and is related to the dielectric properties of the protective oxide, achieving excellent agreement with the data. From these findings, we extract design principles for simultaneous optimization of charge transfer resistance and interface quality to maximize the photovoltage of metal-oxide protected MOS water splitting devices.

[1] Y.W. Chen, et al. *Nature Mat.* 2011, **10**, 539-544.

[2] A. G. Scheuermann, et al. Energy Environ. Sci. 2013, **6**, 2487–2496.

[3] S. Hu, et al. Science 2014, **344**, 1005−1009.

Supplemental Figure 1 | Charge transfer in three cell types for water splitting applied to silicon: Shows the Type 0 Semiconductor-Liquid (SL), Type 1 Metal-Insulator-Semicondcutor (MIS), and Type 2 p+n junction. The density of states on either side of the oxides and the exciton splitting position with respect to these layers play a crucial role in mediating efficient charge transfer. These effects are so strong that Type 0 protected silicon cells exhibit essentially no photovoltage, Type 1 nSi cells show a linear photovoltage loss with oxide thickness, and Type 2 cells--where the hole concentration on the Si/SiO_2 interface is always high--exhibit record photovoltages at all oxide thicknesses and pH values studied.

8:20am TF+EN-WeM2 Activity and Thermal Stability Enhanced Platinum catalysts with Nano-scale Oxide Coating via Atomic Layer Deposition, *Kun Cao, J.M. Cai, B. Shan, R. Chen*, Huazhong University of Science and Technology, Wuhan, China

Platinum nanoparticles (NPs) play an important role in the catalytic applications such as conversion of automotive exhaust, fuel cells, nano sensing and so on. For most catalytic applications, sintering of Pt NPs is undesired since the coalescence decreases the number of active sites of the catalyst. Herein we report the utilization of active oxide layers to encapsulate Pt NPs for CO oxidation. The active oxide coated catalysts have additional metal-oxide interfaces which may further improve the catalytic activity besides good sintering resistance. We use cobalt oxide, cerium oxide and nickel oxide as the active oxide encapsulations. Compared with aluminum oxide reference samples, these active oxides have been reported as much better materials with synergetic effect for Pt catalysts. The thickness of the metal oxide film is controlled by varying the number of ALD cycles. CO oxidation measurements were carried out in a micro flow reactor designed for planar model catalysts. Our results indicate that cobalt oxide coated Pt nanoparticles demonstrating the highest activity towards CO oxidation, and the optimal coating thickness is around 1nm. At the same time the coated catalysts have good thermal stability up to 750°C under

atmospheric conditions. The enhancement of catalytic activity may originate from the active oxygen at the Pt/cobalt oxide interface, further Co (II) sites show better synergetic effect compared with Co (III) sites.

8:40am TF+EN-WeM3 Passivation of Highly-doped c-Si Solar Cell Surfaces by Atomic Layer Deposition, *Bas van de Loo*, Eindhoven University of Technology, Netherlands, *J. Melskens*, Eindhoven University of Technology, *G.J.M. Janssen*, ECN Solar Energy, *K.R.C. Mok, L.K. Nanver*, Delft University of Technology, *A.H.G. Vlooswijk*, Tempress Systems, *W.M.M. Kessels*, Eindhoven University of Technology, Netherlands

Atomic layer deposition (ALD) of Al_2O_3 has been successfully implemented in silicon solar cell manufacturing, predominantly to passivate defects at the lowly-doped back surface of *p*-type solar cells. However, also for the passivation of highly-doped n^+ or p^+ type surfaces, present in e.g., high efficiency *n*-type solar cells, ALD films and stacks might become feasible. Yet, for such surfaces, the level of passivation strongly depends on the doping concentration and surface conditions. To allow for an even wider implementation of ALD-based passivation schemes in industrial solar cells, the work presented in this contribution aims to understand the passivation of highly-doped n^+ and p^+ type regions.

First of all, we observed that the passivation of boron-doped (p^+) Si surfaces highly depends on the doping process and the fixed charge density Q_f in the passivation layer. For instance, when a boron-rich layer (a B_xSi_y compound) was remained after the doping process, the surface passivation by ALD Al_2O_3 severely deteriorated. The formation of this undesirable layer could be avoided by using an oxidizing ambient during the drive-in of boron, although this results in a significant reduction in boron doping density at the surface. The latter impaired the level of passivation when Q_f was virtually zero, such as for ALD SiO_2/ Al_2O_3 stacks. Importantly, the level of surface passivation offered by ALD Al_2O_3 films remained high under these circumstances, due to the strong negative Q_f.

Next, for phosphorous doped (n^+) Si surfaces having surfaces densities of 10^{18}-10^{20} cm^{-3}, the passivation by dielectrics containing a negative Q_f such as ALD Al_2O_3, can be severely compromised, as the negative Q_f increases the minority carrier (i.e., hole-) concentration at and near the surface. Moreover, the negative Q_f can invert the n^+ Si surface, which triggers (undesirable) increased recombination at low injection levels and parasitic shunting. For those n^+ Si surfaces, it is demonstrated that ALD stacks such as SiO_2/ Al_2O_3 and HfO_2/ Al_2O_3 are promising alternatives to Al_2O_3 single layers, due to the absence of a negative Q_f. These stacks are particularly interesting from an industrial point of view, as they can make ALD viable for the passivation n^+ Si surfaces.

Lastly, ALD-based passivation schemes also have the potential to fully replace the heavily-doped n^+ and p^+ Si regions in solar cells. In this new field of 'passivating contacts', the significant recombination losses in the highly-doped regions can be avoided due to accurate band-alignment. Preliminary but promising results on novel electron-selective, passivating stacks of HfO_2 and TiO_2 by ALD will also be presented.

9:00am TF+EN-WeM4 Low Temperature Plasma-Assisted Atomic Layer Deposition of TiO_2 Blocking Layers for Organo-Metal Halide Perovskite Solar Cells, *V. Zardetto*, Eindhoven University of Technology, The Netherlands, *F. di Giacomo, G. Lucarelli, T.M. Brown, A. di Carlo, S. Licoccia, A. D'Epifanio*, University of Rome "Tor Vergata", Italy, *W.M.M. Kessels, Mariadriana Creatore*, Eindhoven University of Technology, The Netherlands

Atomic layer deposition (ALD) offers accurate control in terms of film thickness, chemical and opto-electrical properties. This is extremely appealing for the novel class of mesoscopic solar cells (SCs), where the several interfaces between the absorber, charge transport layers and electrical contacts require the control of selected charge transfer and charge recombination processes.

Organo-metal halide perovskite SCs presently catalyze the interest in the PV community due to the remarkable increase in device performance in the last three years. Recently, thermal ALD processes have been applied for the deposition of TiO_2 blocking layers (BLs) in glass- based perovskite SCs[1]. Plasma-assisted ALD allows to extend the process window down to temperatures compatible with conductive plastic substrates. Therefore, in this work we investigate the role of plasma-assisted ALD TiO_2 BLs deposited on ITO/PET substrates for a $CH_3NH_3PbI_{3-x}Cl_x$ perovskite SC. The BLs are required to avoid the charge recombination process at the interface between the transparent conductive oxide layer and the perovskite and/or the hole transport layer. They have been prepared [2] in a remote plasma reactor (FlexAL^{TM}) at 150 °C using an heteroleptic alkylamido precursor Ti(Cp^{Me})(NMe$_2$)$_3$ exposure step alternated with an O$_2$ plasma exposure.

Very low open circuit voltage (V_{OC} = 50mV) and efficiency (η = 0.01%) have been measured in the absence of the blocking layer. In this case, the analysis of dark current-voltage measurements revealed the lack of diode-like behavior and a significant exchange current (7 mA·cm^{-2}). The introduction of thin TiO_2 layers brought to an increment in all the photovoltaic parameters (J_{SC}, V_{OC} and FF), with a saturation in electrical efficiency for a TiO_2 thickness above 5.5 nm. The saturation in the anodic branch of the JV curve (V> 0) for ALD layers thicker than 5.5 nm points out that at this thickness the ALD layer is compact and therefore it suppresses the charge recombination processes. Dark current-voltage measurements have highlighted the decrease of exchange current and dark reverse current (V<0) up to three orders of magnitude with respect to the device without BL. The maximum performance of 9.2% on ITO-PET and 12.9% on ITO-Glass was achieved with 11 nm- thick TiO_2 BL, overcoming the efficiency achieved with conventional sol gel- deposited TiO_2 BLs (respectively, 4% and 8% on the two substrates).

[1] M. Grätzel, Nature Materials, 13, 838–842 (2014).

[2] F. Di Giacomo and V. Zardetto et al, Adv. Energy. Mater. 1401808 (2015)

9:20am TF+EN-WeM5 Ultra-thin transition Metal Oxide-titania Alloy Coatings for Water Oxidation by Atomic Layer Deposition, *Olivia Hendricks*, C.E.D. Chidsey, P.C. McIntyre, Stanford University
Synthesizing chemical fuels from solar energy requires a source of electrons. The most obvious choice for generating these electrons is the oxidation of water. The oxygen evolution reaction, however, is kinetically challenging, requiring significant overpotentials even with the best noble metal catalysts. At these positive potentials, preserving catalyst stability becomes a key concern. In industrial chlor-alkali electrolysis, which requires similarly positive potentials, the issue of catalyst durability was solved with the development of the dimensionally stable anode (DSA). Today's DSAs consist of a mixed TiO_2/RuO_2 coating prepared by thermal decomposition of appropriate precursors on a Ti substrate (Over, H. *Chem. Rev.*, 2012, 112, 3356). The TiO_2 imparts stability by preventing Ru dissolution, while the RuO_2 imparts sufficient activity and conductivity to the electrode. We report on the fabrication of an ultra-thin analogue to the DSA by atomic layer deposition (ALD) of ruthenium and TiO_2. We hypothesize that a conformal ALD coating of this type on nanostructured electrodes can optimize both the catalytic activity and durability for water oxidation while minimizing the use of transition metal components that have very limited Earth-abundance.

Both TiO_2 and Ru can be deposited simultaneously in our ALD reactor. Thus, by changing the relative number of ALD cycles for each precursor, we can achieve precise control of the catalyst content within the films. Preliminary results suggest that enhanced stability is achieved through the alloying process after annealing. The alloyed films also exhibit overpotentials that are competitive with pure ALD-Ru films deposited on a TiO_2 protective layer, even at relatively low Ru content. By decorating the TiO_2 surface with Ru ions at an optimal areal density, ALD alloying has the potential to achieve efficient catalysis of oxygen evolution from water while minimizing usage of the noble metal catalyst.

9:40am TF+EN-WeM6 Atomic Layer Deposition of Nickel-Iron-Oxide Catalysts for Photoelectrochemical Splitting of Water, *Adrie Mackus*, K.L. Pickrahn, J.G. Baker, S.F. Bent, Stanford University
The splitting of water to form hydrogen using sunlight as the source of energy has been actively researched in recent years to enable the production of green alternatives to fossil fuels. One of the main challenges in this technology is to develop a photoanode that (*i*) absorbs sunlight, (*ii*) has the ability to catalyze the oxygen evolution reaction (OER), (*iii*) is chemically stable in the aqueous electrolyte, and (*iv*) is made of earth-abundant materials. A strategy to synthesize an improved photoelectrochemical cell is to decouple these functions by conformally coating (e.g. by atomic layer deposition, ALD) a catalytic and protective layer on a nanostructured light-adsorbing material.[1]

In this work, we investigate ALD of NiO and $NiFe_xO_y$ films and their use as catalysts for the OER. The material $NiFe_xO_y$ was chosen because it is one of the most promising OER catalysts. The $NiFe_xO_y$ films were deposited using an ALD process that combines NiO ALD ($NiCp_2$, O_3) with Fe_2O_3 ALD ($FeCp_2$, O_3) in a supercycle. Alternatively, $NiFe_xO_y$ films were prepared by soaking ALD-grown NiO films in Fe-containing KOH electrolyte.[2] Using the latter approach, the best results were obtained when the electrode was preconditioned in Fe-poor KOH, causing the smooth and compact NiO film to partly exfoliate, which increases the number of electrochemically accessible Ni sites. Synchrotron-radiation X-ray diffraction was employed to investigate the phase of the material as a function of the deposition conditions. Moreover, the catalytic activity of the films for the OER was investigated by cyclic voltammetry (CV). It was found that incorporating Fe

in the NiO films enhances the activity for OER significantly with a 10-fold increase of the turnover frequency.

1. T.M. Gür, S.F. Bent, and F.B. Prinz, *J. Phys. Chem. C* **118**, 21301 (2014)
2. Y.T. Chong, E.M.Y. Yau, K. Nielsch, and J. Bachmann, *Chem. Mater.* **22**, 6506 (2010)

11:00am TF+EN-WeM10 From Atom to Solid: The Structure of Amorphous ALD Thin Films and Nanolaminates, *Angel Yanguas-Gil*, Argonne National Laboratory   **INVITED**
Atomic Layer Deposition is currently being used for a wide range of energy applications, such as photovoltaics, artificial photosynthesis, energy storage, and power semiconductor devices. In many cases the films are either very thin, well below 10 nm, or either doped or laminate materials, in which a second constituent is intercalated every few cycles.

Given the low deposition temperatures compared to other thin film processes, one of the key questions is how the microstructure of ALD materials differs from their bulk counterparts. This fundamental question of how atoms transition from isolated clusters or single monolayers to a local coordination environment characteristic of the bulk has important technological implications. Answering this question will allow us to better understand the performance of these materials as well as what makes ALD materials different, and in some cases better, to materials synthesized using other techniques.

In this talk I will discuss the impact that chemistry has on the properties and microstructure of very thin ALD films and nanolaminates of oxide dielectrics, semiconductors, and transparent conductors, comprising ZnO, HfO_2, and $M:Al_2O_3$ nanolaminates. By combining synchrotron X-ray characterization techniques such as X-ray Absorption Fine Structure (XAFS) and Pair Distribution Function (PDF) with in-situ techniques such as QCM and FTIR, my talk will focus on two particular problems: the evolution of coordination environment and the emergence of long-range order from the first monolayer and during the early stages of growth, and the impact that the interaction between dopant and host have in the microstructure of doped and laminate materials.

11:40am TF+EN-WeM12 Inorganic Functionalization of Colloidal Quantum Dot Solar Cells through ALD Infilling, *Axel Palmstrom*, P. Santra, S.F. Bent, Stanford University
Colloidal quantum dot (CQD) solar cells are of great interest due to the tunable nature of the quantum dot light absorbers through size, composition and interface engineering, together with the potential for low-cost fabrication through solution processing techniques. Lead chalcogenide CQD devices have recently gained traction with rapidly improving efficiencies (>9%). Great strides have been made with organic ligand functionalization of the quantum dot surfaces to enhance CQD transport properties; however, these devices often suffer from poor long-term stability and are still limited by carrier lifetime and mobility. Atomic layer deposition (ALD), a technique that allows for conformal coating of nanostructured surfaces, has been used to improve stability and mobility of CQD solar cells by growing oxides within the quantum dot film. In this work, we explore the inorganic functionalization of CQD solar cells through combinations of ALD materials, including Al_2O_3, ZnO, NiO and other oxide materials, in thin (~30 nm) devices to ensure infilling throughout the entire device. With the proper choice of ALD oxide, short circuit current density and overall efficiency could be enhanced by 70% and 10% respectively relative to the non-infilled control CQD device. We will discuss the effects of ALD inorganic functionalization on surface passivation and carrier mobility as well as methods to implement ALD infilling on thicker devices in order to ultimately push the limits of CQD solar cell performance.

12:00pm TF+EN-WeM13 Integrating Atomic Layer Deposited Lithium-Containing Thin Films for Lithium-ion Battery Applications, J. Cho, *Trevor Seegmiller*, J. Lau, L. Smith, J. Hur, B. Dunn, J.P. Chang, University of California at Los Angeles
Lithium-ion (Li-ion) batteries have demonstrated their performance in portable electronics for many years. Li-ion batteries also have the potential to be miniature power sources for microelectromechanical systems (MEMS) through 3-dimensional (3D) battery architectures. In order to fabricate a fully functional 3D Li-ion microbattery, an ultra-thin, highly conformal electrolyte layer is required to fully coat 3D electrodes. Lithium aluminosilicate ($Li_xAl_ySi_zO$, LASO), a solid oxide Li-ion conductor, synthesized by atomic layer deposition (ALD) is a promising electrolyte material for 3D battery applications due to its adequate ionic conductivity (1×10^{-7} S/cm) in thin film applications as well as improved electrode stability.

The self-limiting nature of ALD allows precise thickness and composition control when applied to complex metal oxides. This results in a highly conformal and pinhole-free coating on complex structures, including high

aspect ratio 3D electrodes. Lithium tert-butoxide (LTB), trimethylaluminum (TMA), tris(tert-butoxy)silanol (TTBS), and tetraethylorthosilicate (TEOS) were precursors used to synthesize LASO by ALD. LASO films ranging in thickness from 6 to 12 nm exhibited Li-ion conductivity from 8.2×10^{-8} to 1.4×10^{-9} S/cm. The LASO films were also deposited on anode and cathode materials for evaluating their integration into solid state Li-ion batteries. A Li-ion half-cell consisting of LASO-coated 2D carbon anode showed reversible electrochemical behavior with coulombic efficiency reaching 98%.

Current research on Li-ion batteries is directed at creating next generation anode materials. Both silicon and germanium have received considerable study due to their high theoretical volumetric capacity (8444 A h L^{-1} for $Li_{15}Si_4$ and 7366 A h L^{-1} for $Li_{15}Ge_4$ respectively). Upon lithium intercalation, however, these anode materials undergo large volumetric expansion (~300% for Si) which compromises their mechanical integrity. We have started to carry out *in situ* transmission electron microscopy (TEM) studies in which the structural effects of lithium intercalation and deintercalation on silicon/germanium (Si/Ge) alloy nanowires conformally coated with LASO electrolyte are characterized . These *in* situ TEM studies show 40% radial expansion of the $Si_{0.4}Ge_{0.6}$ alloy upon lithium intercalation, and morphological changes upon deintercalation, with the LASO film preserved on the nanowire.

Wednesday Afternoon, October 21, 2015

Nanometer-scale Science and Technology
Room: 212B - Session NS+EN+MG+SS+TF-WeA

Nanoscale Catalysis and Surface Chemistry
Moderator: Sidney Cohen, Weizmann Institute of Science, Israel

2:20pm NS+EN+MG+SS+TF-WeA1 Effects of γ-Al₂O₃ Support on the Geometry and Electronic Structure of H-covered Pt Nanoparticles, *Sampyo Hong*, G. Shafai, T.S. Rahman, University of Central Florida

We have studied the effects of γ-Al$_2$O$_3$(110) support on the geometry and electronic structures of H-covered Pt$_x$ (x=22,44) nanoparticles (NP) using density functional theory (DFT). We find that the unoccupied d-band center of γ-Al$_2$O$_3$(110) supported Pt NPs exhibits a blue shift with decreasing Pt size similarly as the measured XANES absorption peak energy of Pt NP samples. In fact, our DFT results reveal that the shift of the unoccupied d-band center of Pt NPs is dependent of surface hydroxylation level on γ-Al$_2$O$_3$(110). At higher hydroxylation the calculated unoccupied d-band center can even show red shift. Thus, consideration of hydroxylation level on γ-Al$_2$O$_3$(110) is needed to properly interpret support effect from XANES spectra. Overall, the strength of Pt- γ-Al$_2$O$_3$(110) binding seems to be a reasonable measure of the shift of unoccupied d-band center as a result of metal-support interaction: the stronger the interaction the more the blue shift. In the light of these results, it is plausible to postulate that the adsorption energy shift of XANES spectra represent the strength of metal-support interaction (support effect). A remarkable example of such hydroxylation tuned metal-support interaction is structural transition of Pt$_{22}$ from a biplanar to a 3D-like geometry as a function of support hydroxylation.

3:00pm NS+EN+MG+SS+TF-WeA3 Fabrication and SERS Activity of Metal-loaded TiO₂ Nanometer ScaleParticles, *Paolo Reyes*, J.C. Hemminger, University of California Irvine

Our current research focuses on the fabrication and study of metallic loaded titanium dioxide (TiO$_2$) nanoparticles supported by highly oriented pyrolitic graphite (HOPG). Highly dispersed TiO$_2$ particles are formed via physical vapor deposition (PVD) under high vacuum settings with an average pseudo-diameter of 11.6 ± 2.65 nm. Metallic loading is completed by an ex-situ photo-deposition method by exposure to precursor metal salt solutions under TiO$_2$ bandgap UV irradiation. We have attempted to fabricate Pt-, Ag-, Au-, and Pt-Au-TiO$_2$ particles and observed photocatalytic enhancement with the inclusion of Pt nanoparticles deposited onto TiO$_2$ surfaces. We believe this enhancement is a result of Pt nanoparticles harboring free excited electrons and preventing electron-hole recombination. We have developed a technique to increase the density of TiO$_2$ particles by creating site defects on the surface of HOPG through plasma mild oxygen plasma exposure. Highly dispersed TiO$_2$ nanoparticle distributions allow an increase of metal nanoparticle formation on TiO$_2$ for surface and intrinsic property observations. Ag nanoparticles have been fabricated in order to observe Surface Enhanced Raman Spectroscopy (SERS) Ag nanoparticles were observed to be an average pseudo-diameter of 2.6 ± 1.4 nm. A probe molecule was used to determine Raman intensity enhancement factor (EF) and we believe that the EF can be affected by the spacing and size of Ag-TiO$_2$ nanoparticles. We will present our studies of bi-metallic loading of TiO$_2$.

4:20pm NS+EN+MG+SS+TF-WeA7 Pyridine Coordination Chemistry for Molecular Assemblies, *Milko Van der Boom*, Weizmann Institute of Science, Israel **INVITED**

Many types of metal-ligand interactions have creatively been used in the chemical sciences since the description of coordination complexes. The rich coordination chemistry of pyridine-type ligands has contributed significantly to the incorporation of metal ions into functional materials on surfaces. We will discuss molecular assemblies formed with a variety of pyridine-based compounds. These assemblies are formed by layer-by-layer deposition from solution that allows for precise fitting of the assembly properties. The degree of intermolecular interactions can be controlled by varying the degree of π-conjugation and the availability of coordination sites. Unlike molecular assemblies that are constructed with organic ligands, assemblies with polypyridyl complexes are active participants in their own

formation and amplify the growth of the incoming molecular layers. Such a self-propagating behavior for molecular systems is rare and the mechanism of their formation will be presented. Incorporating multiple metal complexes into a single assembly give rise to composite materials that exhibit unique electrochemical and electrochromic properties that are dependent on the arrangement of these metal complexes. We will also discuss the coordination chemistry of pyridine-based compounds with nanoparticles, the formation of metal-organic frameworks and their practical applications.

5:00pm NS+EN+MG+SS+TF-WeA9 Atomic Scale Iron Carbide Films on Au(111) and Cu(111) as a Iron Fischer-Tropsch Model Catalyst, *Gilbère Mannie*, X. Wen, Y.W. Li, SynCat@Beijing, China, *J.V. Lauritsen*, Interdisciplinary Nanoscience Center (iNANO), Denmark, *H.J.W. Niemantsverdriet*, SynCat@Beijing, China

Iron-based Fischer-Tropsch synthesis (FTS) is one of the most investigated catalytic systems in the world due to the ability to convert any form of hydrocarbons like coal, natural gas or biomass into diesel, gasoline and chemicals [1]. Although investigated for more than 50+ years, fundamental surface reactions involved in this process are not known or fully understood. Within the FTS community, iron carbide is seen as the active phase in the catalytic process but the atomic-scale surface structure and even the stoichiometry of the bulk phase is a matter of debate [1,2]. In order to fundamentally investigate the active phase, to for example verify molecular modeling studies on iron carbide surfaces (like [3,4]), we successfully synthesized highly-crystalline iron carbide monolayer islands (on Au(111)) and multilayer islands (on Cu(111)). Obtained carbidic films are suitable for analysis with scanning tunneling microscopy (STM) and other surface science techniques. Our atomically-resolved STM results, together with preliminary density functional theory (DFT) results show that we can characterize our iron carbide (Fe$_x$C$_y$) islands as iron layer with interstitial carbon atoms, based on the increase of the inter-atomic Fe-Fe distance [5]. During the synthesis of the Fe$_x$C$_y$ islands we were able to record some STM movies showing the formation of the carbidic phase out of the metallic phase but we could also record movies during dosing experiments of several gasses (H$_2$, O$_2$) to the pure iron carbide islands. During the presentation we will explain how we synthesized these crystalline iron carbide films and how these films can act as a model system for fundamental Fischer-Tropsch catalyst research.

[1] E. de Smit, B. M. Weckhuysen, *Chem. Soc. Rev.,***2008,** *37,* 2758

[2] J. W. Niemantsverdriet, A. M. van der Kraan, W. L. van Dijk, H. S. van der Baan, *J. Phys.,* **1980,** *84,* 3363

[3] J. M. Gracia, F. F. Prinsloo, J. W. Niemantsverdriet, *Catal. Lett.,***2009,** *133,* 257

[4] M. O. Ozbek, J. W. Niemantsverdriet, *J. Catal.,***2014,** *317,* 158

[5] G. J. A. Mannie, L. Lammich, Y. W. Li, J. W. Niemantsverdriet, J. V. Lauritsen, *ACS Catal.,***2014,***4,* 3255

5:20pm NS+EN+MG+SS+TF-WeA10 Fullerene Interaction with W Surfaces: Synthesis of Nanospheres with Tunable Bandgap, *Ehsan Monazami*, University of Virginia, *J.B. McClimon*, University of Pennsylvania, *P. Reinke*, University of Virginia

The interaction of f C$_{60}$ molecules with metal surfaces is a topic of considerable interest and discussed in the context of molecular electronics and organic solar cell applications. Our work focuses on the interaction of C$_{60}$ with W, which is a carbide forming transition metal. It has generally been assumed that the C$_{60}$ cage breaks up readily on a W surface, but our observations reveal a more complex, temperature induced reaction sequence leading to the formation of nanospheres with variable bandgap, which has been studied with in-situ STM and STS analysis.

The nanospheres are synthesized by initiating the reaction between C$_{60}$ deposited on a W-thin film surface grown on MgO(001) at about 450 K. In contrast to previous reports, the molecules do not collapse but the spherical shape is retained up to 800 K and the electronic structure changes gradually from wide bandgap C$_{60}$ to fully metallic nanospheres. The size distribution of the nanospheres is centered at 1.5 nm (600 K) and shifts for higher temperatures to about 2 nm with a concurrent decrease in height resulting in an ellipsoidal shape. These nanosheres present an exceptional resistance to sintering which is a unique feature for metallic nanoparticles. The densely packed C$_{60}$ and isolated C$_{60}$ molecules show the same transition in shape and electronic structure which confirms that the transformation is controlled by the reaction with the W substrate.

The transition in the electronic structure progresses gradually from the wide-bandgap molecule (2.3 eV) to a bandgap of ~1eV at 700 K, and a metallic surface at 800 K. We will illustrate this progression with a series of

ST spectra and maps. The bandgap variation offers for the first time a pathway to the formation of nanoscale clusters (nanospheres) with variable bandgap while retaining the surface curvature in narrow range. The detailed structure of the nanospheres is, however, still subject to discussion. We currently favor, based on our experimental results, a substitution model where the W-atoms from the substrate react with the C_{60} cage which acts as a scaffold. The W atoms are incorporated substitutionally forming a carbide type bonding, whose presence is indicated by XPS analysis. The variation in bandgap is then driven by the degree of substitution and the fullerene molecule acts as a scaffold. We predict that other carbon scaffolds such as nanotubes and carbide forming transition metals can react in the same manner leading to a new class of nanostructures with unique adaptability of the electronic structure. The nanospheres are an excellent testbed for the physics and chemistry of highly curved surfaces.

Supported by NSF-DMR Ceramics DMR-100580.

5:40pm **NS+EN+MG+SS+TF-WeA11** **Enantiomeric Separations of Chiral Pharmaceuticals using Chiral Tetrahexahedral Au Nanoparticles**, *Nisha Shukla*, *D. Yang*, *A.J. Gellman*, Carnegie Mellon University

Chiral tetrahexahedral (24-sided) Au nanoparticles are tested for their use as chiral separators of pharmaceutical drugs in solution phase. Tetrahexahedral Au nanoparticles were chirally modified with either D- or L-cysteine. They show enantioselective adsorption of pharmaceuticals such as propranolol hydrochloride (used for anxiety and high blood pressure) from a solution of racemic propranolol hydrochloride, thus leaving an enantiomeric excess in the solution phase. This work suggests that chiral nanoparticles can be used for enantiomeric separation of real pharmaceutical drugs. A simple robust model has also been developed that allows extraction of the enantiospecific equilibrium constants for R- and S-propranolol hydrochloride adsorption on the chiral tetrahexahedral Au nanoparticles. The model obviates the need for experimental determination of the surface area of absorbent Au nanoparticles which is extremely difficult to measure.

6:00pm **NS+EN+MG+SS+TF-WeA12** **Electroreduction Catalysis with Defect-Rich Metal Nanoparticles**, *Xiaofeng Feng*, *M. Kanan*, Stanford University

New design principles for electroreduction catalysts are essential for CO_2 recycling using renewable electricity. Au is one of the most active catalysts for CO_2 reduction to CO, and numerous efforts have been made to optimize Au catalysts by tuning the size, composition, and shape of Au nanostructures. Here we show that grain boundaries (GBs) in Au nanoparticles create highly active surface sites for CO_2 electroreduction (1). Defect-rich Au nanoparticles were synthesized by vapor deposition of Au onto a carbon nanotube thin film, which enables direct TEM characterization without further processing. We compared the CO_2 reduction activity of the as-deposited catalysts to those annealed at different temperatures. While the annealing process has little impact on the distribution of Au surface facets, it reduces the GB density, which is quantified by measuring GB lengths and particle areas from high-resolution TEM images. We found that the surface-area-normalized activity for CO_2 reduction is linearly correlated with GB density in Au nanoparticles in the low overpotential regime. Similarly, GB-density was also found to correlate with catalytic activity for the electroreduction of CO to multi-carbon oxygenates on Cu nanoparticles. Our studies show that grain boundary engineering is a general strategy for improving electrocatalytic activity for carbon fuel synthesis.

References:

(1) Feng, X.; Jiang, K.; Fan, S.; Kanan, M. W. *J. Am. Chem. Soc.* **2015**, *137*, 4606–4609.

Surface Science
Room: 113 - Session SS+AS+EN-WeA

Metals, Alloys & Oxides: Reactivity and Catalysis
Moderator: Daniel Killelea, Loyola University Chicago

2:20pm **SS+AS+EN-WeA1** **Understanding Chemical Activity in Pt-Re Bimetallic Systems**, *Donna Chen*, *R.P. Galhenage*, *K. Xie*, *A.S. Duke*, University of South Carolina, *H. Yan*, Brookhaven National Laboratory **INVITED**

The nucleation, growth and chemical activity of bimetallic Pt-Re clusters on titania have been investigated as model systems for understanding Pt-Re catalysts for oxidation reactions. Scanning tunneling microscopy studies demonstrate that exclusively bimetallic clusters can be grown from the sequential deposition of Pt on Re or Re on Pt, provided that the deposition of the first metal creates a high enough cluster density for the nucleation of the second metal. Low energy ion scattering experiments indicate that the bimetallic clusters are Pt-rich regardless of the order of deposition. However, X-ray photoelectron spectroscopy (XPS) suggest that a Pt-Re alloy is formed from deposition of Re on Pt but not from Pt on Re. Furthermore, Re interacts more strongly with the titania support than Pt, resulting in reduction of titania. Temperature programmed desorption studies for CO desorption and methanol reaction confirm that the Re clusters have lower activity than Pt despite their higher surface area, and this behavior is attributed to oxidation of Re by the titania support. The alloyed clusters exhibit new activity for CO and H_2 evolution that is not observed for the pure or unalloyed clusters. Methanol oxidation activity of these model surfaces are studied in a microreactor attached to an ultrahigh vacuum chamber so that the surfaces can be characterized by XPS before and after reaction. Specifically, changes in the oxidation states of Re in the bimetallic and pure Re clusters are investigated.

3:00pm **SS+AS+EN-WeA3** **Removal of Surface Carbon from Pt(111) by Hydrogenation via an Ethylidyne Intermediate**, *J.D. Krooswyk*, *C.M. Kruppe*, *Michael Trenary*, University of Illinois at Chicago

Transition metals that are used to catalyze reactions of hydrocarbons are often deactivated by the deposition of unreactive carbon on the catalyst surface. The structure and properties of the deposited carbon are often poorly defined. We have investigated the reactivity of carbon deposited onto a Pt(111) surface through exposure to acetylene at 750 K. At this temperature the acetylene is completely dehydrogenated leaving only carbon the surface. Earlier work had shown that the carbon deposited in this way largely consists of C_2 molecules. We have used reflection absorption infrared spectroscopy (RAIRS) to characterize the reactivity of the deposited carbon under ambient pressures of $H_2(g)$ up to 10 torr. The results show that C_2 can be hydrogenated to ethylidyne (CCH_3) and that the ethylidyne is slowly hydrogenated to ethane, which desorbs thus removing carbon from the surface. The maximum coverage of the C_2 molecules can be deduced from comparison with the peak areas measured with RAIRS for ethylidyne formed from ethylene exposure, which is known to give an ethylidyne coverage of 0.25 monolayer. Auger electron spectroscopy confirms that surface carbon is removed by hydrogenation under these conditions. In separate experiments based on comparisons of s- and p-polarized RAIR spectra in which both surface and gas phase species can be simultaneously monitored, we have shown that surface ethylidyne is a spectator species as gas phase acetylene is converted first to gas phase ethylene and then to gas phase ethane. Although ethylidyne is a spectator species in the hydrogenation of ethylene and acetylene to ethane over Pt(111), in the case of C_2 hydrogenation, ethylidyne plays the role of a reaction intermediate.

3:20pm **SS+AS+EN-WeA4** **Density Functional Study of the Oxygen Chemistry and NO Oxidation Mechanism on Low-index Surfaces of SmMn$_2$O$_5$ mullite**, *X. Liu*, *Z.Z. Chen*, Huazhong University of Science and Technology, China, *K.J. Cho*, The University of Texas at Dallas, *R. Chen*, *Bin Shan*, Huazhong University of Science and Technology, China

$SmMn_2O_5$ mullite has recently been reported to be a promising alternative to traditional Pt-based catalysts for environmental and energy applications. By performing density functional calculations, we systematically investigated lattice oxygen reactivity and oxygen adsorption/dissociation/migration behaviors on low index surfaces of $SmMn_2O_5$ mullite with different terminations. The (001), (010) and (100)surfaces have lowest barriers against exchanging O species with environments and thus are expected to be active surfaces.Furthermore, we have calculated the reaction routes along different channels on these three surfaces. Our results show that both ER and MvK mechanisms co-exist in NO oxidation by $SmMn_2O_5$. The most active surface is the (010) facet with Mn^{4+} ions in the surface layer where oxidation can be realized by a synergetic mechanism involving ER processes along bridge-MnO channels. The (001) surface with Mn^{4+} ions in the surface layer is also expected to be active for oxidation via the MvK mechanism. On the other hand, despite the low oxygen vacancy formation energy, the (110) surface could easily undergo surface reconstruction and quickly lose active sites. Our calculations also suggest that the rate determining step of oxidation reaction on $SmMn_2O_5$ surfaces is the desorption of NO_2 on both (010) and (001) facets. Our study presents systematic pictures on catalytic activities of $SmMn_2O_5$, which are important to the full understanding and improvement of $SmMn_2O_5$ performance. The comprehensive micro-kinetic model on the reaction dynamics of $SmMn_2O_5$ is under construction.

4:20pm SS+AS+EN-WeA7 Medard W. Welch Award Lecture - Thermodynamics and Kinetics of Elementary Reaction Steps on Late Transition Metal Catalysts, *Charles Campbell**, University of Washington **INVITED**
Experimental and theoretical results concerning the thermodynamics and kinetics of surface chemical reactions of importance in late transition metal catalysis will be reviewed. Topics include: (1) calorimetric measurements of the adsorption energies of small molecules and molecular fragments on single crystal surfaces, and their comparison to different DFT methods; (2) measurements of the entropies of adsorbates and their trends, (3) using these together with elementary-step rate measurements to build microkinetic models for multi-step catalytic reactions, and a method for analyzing these that quantifies the extent to which each elementary step and intermediate controls the net rate; and, (4) measurements of the energies of transition metal atoms in nanoparticle catalysts as a function of particle size and support, which correlate with catalytic activity and sintering rates.

· Work supported by NSF and DOE-OBES Chemical Sciences Division.

5:00pm SS+AS+EN-WeA9 Bridging Hydroxyl Formation from Water on Reduced TiO₂(110), *Nikolay Petrik*, G.A. Kimmel, Pacific Northwest National Laboratory
TiO_2 is an important photocatalyst with many practical applications. It is also a good model system for fundamental studies of thermal and non-thermal reactions, including photocatalytic water splitting. Our understanding of water's reactions on TiO_2 surface is limited. In this paper, we have investigated temperature-dependent reaction of water molecules with bridging oxygen vacancy (V_O) on rutile $TiO_2(110)$ surface using three independent methods: i) infrared reflection absorption spectroscopy (IRAS) to monitor the bridging hydroxyl (OH_B or OD_B) formation, ii) electron-stimulated desorption (ESD) of molecular water to monitor the water coverage,[1] and iii) photon-stimulated desorption (PSD) of CO_2 – which is a product of CO photooxidation – to monitor the unoccupied V_O coverage.[2] Narrow, distinct peaks for isolated OD_B and OH_B at ~2736.5 cm^{-1} and ~3711.5 cm^{-1} are detected in P-polarized mode for the samples exposed to D_2O and H_2O, respectively. If water is dosed at low temperature and annealed, bridging hydroxyl peaks appear above 150 K, growing with temperature until ~ 250 K, then saturate. In the same temperature range, molecular water and V_O coverages from the ESD and PSD data decrease in correlated fashion according to the reaction $H_2O_{Ti} + V_O \rightarrow 2OH_B$. The temperature range for this conversion appears to be too broad to be fitted with a single Arrhenius term and a reasonable pre-factor. On the other hand, the data can be fitted well using a "normal" prefactor ($v = 10^{12}$ s^{-1}) and a distribution of activation energy (E_a) centered at 0.545 eV with $\Delta E_a(FWHM) = 0.125$ eV. These parameters are close to those obtained from STM data[3] and theory[4] for the water monomer diffusivity on Ti sites, which most likely controls the water – vacancy reaction. This work was supported by the US Department of Energy, Office of Science, Office of Basic Energy Sciences, Division of Chemical Sciences, Geosciences & Biosciences.

(1) Zhang, Z.; Du, Y.; Petrik, N. G.; Kimmel, G. A.; Lyubinetsky, I.; Dohnalek, Z. Water as a Catalyst: Imaging Reactions of O_2 with Partially and Fully Hydroxylated $TiO_2(110)$ Surfaces. *J. Phys. Chem. C* 2009,113, 1908-1916.

(2) Petrik, N. G.; Kimmel, G. A. Off-Normal CO_2 Desorption from the Photooxidation of CO on Reduced $TiO_2(110)$. *J. Phys. Chem. Lett.* 2010,1, 2508-2513.

(3) Matthiesen, J.; Hansen, J. O.; Wendt, S.; Lira, E.; Schaub, R.; Laegsgaard, E.; Besenbacher, F.; Hammer, B. Formation and Diffusion of Water Dimers on Rutile $TiO_2(110)$. *Phys. Rev. Lett.* 2009, 102, 226101.

(4) Hammer, B.; Wendt, S.; Besenbacher, F. Water Adsorption on TiO_2. Top. Catal. 2010, 53, 423–430.

5:20pm SS+AS+EN-WeA10 The Adsorption and Desorption of Small Hydrocarbons on Rutile TiO₂(110), *Long Chen*, R.S. Smith, B.D. Kay, Z. Dohnalek, Pacific Northwest National Laboratory
The interaction of small hydrocarbons with metal and metal oxide surfaces is important for a wide range of applications including heterogeneous catalysis, atmospheric chemistry, geochemistry and chemical sensing. In this work, temperature programmed desorption (TPD) and molecular beam techniques are used to study the adsorption and desorption kinetics of small hydrocarbons (C_1 - C_4) on rutile $TiO_2(110)$ surface. In addition to n-alkanes, 1-alkenes (ethylene, propylene and 1-butylene) and 1-alkynes (acetylene, propyne and 1-butyne) were included to follow the effect of the nature of the carbon-carbon bond on hydrocarbon binding. We show that the sticking coefficients for all the hydrocarbons studied here are close to unity (> 0.95) at an adsorption temperature of 60 K. Similar to previous studies on metal

and metal oxide surfaces, for n-alkanes on $TiO_2(110)$ we find a linear increase in desorption energy with chain length. In contrast, for 1-alkenes and 1-alkynes, a roughly linear relationship between desorption energy and chain length is also observed at low coverages, but with a much smaller slope, suggesting that the additional CH_x segments either interact less efficiently with the substrate or destabilize the bonding of the unsaturated carbon-carbon bond. Further, we also determined the absolute saturation coverages of each hydrocarbon on the five-fold coordinated titanium sites (Ti_{5c}). We show that except for CH_4, the saturation coverages of the same type of hydrocarbons on Ti_{5c} sites are nearly independent of the chain length, and that the saturation coverages of 1-alkynes consistently exceed those of n-alkanes and 1-alkenes, contrary to what one would expect based on their sizes.

5:40pm SS+AS+EN-WeA11 Pd-Au *Single Atom Alloys* for the Activation of Diatomic Molecules, *Felicia Lucci*, E.C.H. Sykes, Tufts University Department of Chemistry
Pd-Au alloys are known to catalyze a wide range of hydrogenation and oxidation reactions; however, the size of Pd ensembles in Au required for small molecule activation is not well understood. On the atomic scale, we investigate size effects of Pd atoms in Au for the catalytic activation of H_2 and O_2. We show that isolated Pd atoms are capable of catalyzing the dissociative adsorption of H_2, a process which was previously thought to require contiguous Pd sites. H spillover from active Pd sites to the Au surface can be induced the adsorption of CO. Conversely, single Pd atoms are not capable of O_2 dissociation. Small Pd clusters on Au enable O_2 activation and adsorption at Pd-Au interface sites. Since weakly bound H and O atoms are capable of enhancing reaction selectivity on Au substrates, this Pd-Au system serves as an ideal model system with which to probe selective hydrogenation and oxidation reactions at both single and ensemble active sites.

6:00pm SS+AS+EN-WeA12 Pt/Cu Single Atom Alloys for Highly Selective Formic Acid Dehydrogenation, *Matthew Marcinkowski*, C.J. Murphy, M.L. Liriano, N.A. Wasio, F.R. Lucci, E.C.H. Sykes, Tufts University Department of Chemistry
Selective decomposition on metal catalysts is a critical step in formic acid's application as a hydrogen storage molecule and for its use in direct formic acid fuel cells. Depending on the metal, formic acid can decompose via a dehydrogenation pathway to produce CO_2 and H_2, or a dehydration pathway to produce CO and H_2O. For most applications, very high selectivity to dehydrogenation is preferred as reactively formed CO from dehydration can poison the catalyst. The Cu(110) surface is known to selectively decompose formic acid via dehydrogenation, however, despite being the most dominate facet of nanoparticles, Cu(111) has received little study. Pt surfaces exhibit greater reactivity to decomposition, but are not as selective resulting in increased catalyst poisoning. We report that formic acid on Cu(111) and Pt/Cu(111) selectively decomposes via dehydrogenation. We find the bare Cu(111) surface to be 100% selective towards dehydrogenation, but not very active. Substitution of 1% of a monolayer of Pt into the Cu(111) surface results in a single atom alloy (SAA) that maintains this high selectivity and is ~six times more reactive than Cu(111). Higher coverages of Pt improve reactivity further, but beyond the single atom regime the selectivity towards dehydrogenation decreases and dehydration is observed. Our results show that Pt/Cu SAAs significantly improve the reactivity of Cu, while also maintaining high selectivity towards dehydrogenation, therefore avoiding catalyst poisoning by CO. Based on our results, real nanoparticle catalysts designed on the SAA principle are expected to be promising candidates for formic acid dehydrogenation.

Thin Film
Room: 111 - Session TF+AS+EM+EN+MN-WeA

CV Infiltration Methods and Energetic and Thermal Properties of Thin Films
Moderator: Richard Vanfleet, Brigham Young University, David Allred, Brigham Young University

2:20pm TF+AS+EM+EN+MN-WeA1 The Many Avatars of PVD, *Murali Narasimhan*, Applied Materials, Inc. **INVITED**
Physical Vapor Deposition has been used for many years for depositing thin film coatings for diverse uses ranging from jewelry to industrial cutting tools. PVD has found usage in the manufacture of advanced semiconductor manufacturing for depositing various metals and some specialty dielectrics as well. The majority of high purity metal deposition for semiconductor use has been done using PVD although the use of CVD and ALD has increased

---

* Medard W. Welch Award Winner

over the years because of requirements of conformality and gap fill where conventional planar PVD has not been adequate. However, breakthroughs in PVD technology have been successful in extending the use of PVD to advanced semiconductor manufacturing nodes by changing the geometry of PVD sources and reactors and the nature of the plasma involved. Collimated and long-throw sources developed by the semiconductor equipment industry in the early '90s enabled the deposition of high-purity Ti to lower contact resistance for transistors. Reactive sputtering of TiN enabled a robust barrier for CVD W plugs used at the 0.5um node. Further, use of electromagnetic fields to ionize and then guide the plasma and sputtered ionized atoms has been successful in improving the conformality of PVD Ti films. Ionized Metal Plasma (IMP), Hollow-Cathode Magnetron (HCM) and Self-Ionized Plasma (SIP) were innovations in ionized PVD reactor design that led to widespread adoption of PVD TaN and PVD Cu for Cu interconnect barrier and seed layer production from the 90nm node to the present. The application of thermal energy on the substrate during PVD Al and Cu has been useful in improving the flow of deposited material and subsequent gap-fill of sub-micron features. The use of Radio Frequency (RF) energy to power the target has allowed for more efficient ionization at lower power levels. The application of a capacitive tuner to modulate the ion bombardment on the wafer and tailor the film properties of TiN for hard mask applications has enabled the realization of etched features at the 22nm node. Pulsed DC magnetrons enable sputtering of dielectric materials, thus opening up the controlled deposition of thin films of insulating films for various applications such as improving the brightness of high-efficiency LEDs. Multi-cathode off-axis PVD magnetrons have enabled the deposition of multi-layers of ultra-thin films for magnetic devices such as advanced in-plane and out-of plane MRAM and the manufacture of EUV mask blanks for sub 10nm manufacturing. This talk will present the above listed progression of PVD technology over the years and its use for many applications in semiconductor manufacturing.

3:00pm TF+AS+EM+EN+MN-WeA3 Reactive Foil Ignition by Laser Irradiation: Experimental and Modeling Results, *Ryan Murphy, C.D. Yarrington,* Sandia National Laboratories*, R.V. Reeves,* Lawrence Livermore National Laboratory*, D.P. Adams*, Sandia National Laboratories
It has been shown that forced mixing of reactive layers (foils) leads to an exothermic release of energy after initiation by pulsed laser irradiation. In order to understand the ignition of foils initiated by laser irradiation, we study the interaction of laser pulses with Al/Pt multilayer reactive foils prepared by sputter deposition. It will be shown that the single-pulse ignition threshold and dynamics are dependent on the length of the laser pulse as the pulse length is varied from 150 fs to 100 ms. The dependence of the ignition threshold on pulse length is a combination of laser-material interactions such as the size of the heat affected zone and the onset of ablation for ultrafast irradiation. Simulations of single-pulse laser heating were performed with Aria, the thermal package of the SIERRA finite element computational framework. Three-dimensional geometries were subjected to laser flux boundary conditions equal to those measured from the experimental conditions. Modeling and experimental results are correlated to show the effects of the heat affected zone size and shape on ignition thresholds and onset times.

3:20pm TF+AS+EM+EN+MN-WeA4 The Effects of a Heat Sink on Self-Sustained Propagating Reactions in Sputter-Deposited Bimetallic Multilayers, *David Adams, R.V. Reeves, M. Hobbs,* Sandia National Laboratories
Reactive multilayers grown by sputter deposition have recently attracted interest for applications including material joining (soldering, brazing) and energy sources. For these applications, a metal-metal multilayer is typically designed to have many discrete reactant layers and a composition that corresponds to the peak enthalpy for a given material system. A thickness of reactive multilayers as small as 1.6 microns has recently been demonstrated for microelectronics joining (Braeuer et al. ECS Transactions, 2012). However, little is known about the minimal multilayer thickness required for ensuring a self-sustained, high temperature synthesis (SHS) reaction.

With this presentation, we describe the behavior of thin reactive Al/Pt multilayers tested as freestanding foils and as adhered films. For multilayers having a total thickness of 1.6 microns, self-sustained, high temperature reactions readily occur when the multilayer is tested as a freestanding foil. When coupled to a semi-infinite substrate, the likelihood of reaction is reduced depending on the multilayer design.

5:00pm TF+AS+EM+EN+MN-WeA9 Beyond Deep Silicon Etching – Generating High Aspect Ratio Microstructures by Infiltration of Carbon Nanotube Frameworks, *Robert Davis*, Brigham Young University **INVITED**
In addition to being the anchor material for microelectronics, silicon is widely used as the basis of high aspect ratio microfabrication for MEMS with applications ranging from inertial sensors to neural probe arrays. Carbon nanotube templated microfabrication (CNT-M), extends the palate of materials and structures for high aspect ratio microfabrication beyond those achievable with vertically etched bulk silicon. In CNT-M, 3-D forests of patterned vertically-aligned carbon nanotubes are grown as a high aspect ratio framework and then the "forests" are infiltrated with a secondary material by chemical vapor deposition. Precision structures (including nanoporous structures) with very high aspect ratios (greater than 400:1) can be generated with CNT-M. The infiltration materials range from ceramics to metals and include silicon dioxide, silicon nitride, carbon, nickel, and yes silicon. We are using CNT-M to fabricate functional structures for applications including mechanical actuation, chemical separations and detection, and electrochemical energy storage.

5:40pm TF+AS+EM+EN+MN-WeA11 The Influence of Thin Binder Films on Reaction Behavior in Reactive Powder Complexes, *Robert Reeves, K.T. Sullivan, A.E. Gash,* Lawrence Livermore National Laboratory
With the recently renewed interest in additive manufacturing (AM), there has been a recent upswell in the number of AM processes available. One such process that could be useful for reactive materials utilizes a curable liquid binder to adhere loose powders into coherent solid forms. In this process, tap-density powders are nearly saturated with binder, so the resulting film of binder present on each particle can represent a significant contaminant to the reaction system. In this work, the effect of the binder on reaction behavior in the Ni-Al system is explored. First, the distribution of binder and its elemental constituents are studied by electron microscopy and energy dispersive spectroscopy for powders with varying levels of binder saturation. Then, the effect of binder on the reaction kinetics and overall behavior is investigated. The change in overall heat release and apparent activation energy are quantified through differential scanning calorimetry, and the bulk reaction propagation rate is measured by high speed photography as a function of the weight fraction of binder in the compact. Finally, the reaction products are identified through x-ray diffraction. In all tests, comparisons are made to the neat Ni-Al system.

6:00pm TF+AS+EM+EN+MN-WeA12 Carbon Nanotube Sheets from Horizontally Aligned Carbon Nanotubes, *Nathan Boyer, D.B. Syme, J.T. Rowley,* Brigham Young University*, M. Harker, R. Creighton, S. Cornaby,* Moxtek Inc.*, R. Vanfleet, B.D. Iverson,* Brigham Young University*, L. Pei,* Johns Hopkins University*, R.C. Davis,* Brigham Young University
Carbon sheets comprised of horizontally aligned carbon nanotubes (CNT) were prepared by rolling vertically aligned CNTs into a thin-film. A subsequent infiltration step to coat the rolled CNTs with amorphous carbon or polymer has also been performed to improve adhesion of neighboring CNTs. Amorphous carbon infiltration was achieved using chemical vapor deposition and polymer infiltration was performed by dipping the sheet into a solvent-mediated, polymer solution. The typical failure mode of the CNT thin-films is to tear parallel to the alignment of the CNTs. Infiltration of the aligned CNT film with additional materials strengthens the film against tearing and increases burst pressure. Non-infiltrated CNT thin-films have sustained a differential pressure of 1.4 atm over a circular area of 7 mm2 on a bulge test apparatus. Both carbon and polymer infiltrated sheets could be used in many applications including micromechanical sensing and actuation.

Thursday Morning, October 22, 2015

Spectroscopic Ellipsometry Focus Topic
Room: 112 - Session EL+EM+EN-ThM

Spectroscopic Ellipsometry: Novel Applications and Theoretical Approaches
Moderator: Tino Hofmann, University of Nebraska - Lincoln, Vimal Kamineni, Globalfoundries, Ny, Usa

8:00am EL+EM+EN-ThM1 Multi-Spectral Polarimetric Imaging and Biomedical Applications, *Bernard Drevillon, A. Pierangelo*, LPICM-CNRS, Ecole Polytechnique, France **INVITED**
In the last years Polarimetric Imaging has received considerable attention in the literature thanks to its tremendous potential for the assessment of biological tissues in biomedical diagnostics. Light Polarization allows obtaining morphological information on tissues microscopic structure, potentially improving the diagnosis and treatment of several pathologies. Moreover, polarimetric imaging can be implemented using conventional light sources, like LED or halogen lamps, making it a cheap alternative to current standards. For several years the PICM Laboratory has designed and built innovative polarimetric imagers for biomedical applications. In particular, the development of the *eigenvalue calibration method* [1], led to the design of several polarimeters for macroscopic and microscopic analysis (in real and Fourier space) of *ex vivo* samples and for *in vivo* diagnoses. The development of such new instruments ranged from the simple measurement of polarization degree to the complete Mueller polarimetry. Several studies were devoted to the early detection and staging of uterine cervix cancer and to show that polarimetric imaging is effective for the visualisation and first grading of cervical dysplastic regions for patients with anomalous Pap smear [2]. Mueller matrix imaging polarimetry also provides enhanced contrast to differentiate types of cancer of colon and their stage of progress and penetration, which is currently detectable only by histological examination [3]. Moreover, this technique may also be useful to quickly verify the presence of residual cancer in the rectum after treatment with radiochemotherapy [4]. Finally, as a complementary development to experimental techniques, the set-up of Monte-Carlo detailed modelling of polarized light scattering in tissues has been carried out in the last few years and provides fundamental insight on the origin of observed polarimetric contrasts [5]. In conclusion the synergy of new experimental techniques based on polarimetry with the biomedical analysis and theoretical computer models, led to significant advances in the field of biological tissues characterization and diagnosis of related pathologies.

[1] E. Compain et al., Appl. Opt. 38, 3490-3502 (1999).

[2] A. Pierangelo et al., Opt. Express, 21, 14120 -14130 (2013).

[3] A. Pierangelo et al., Opt. Express 19, 1582 (2011).

[4] A. Pierangelo et al., J. Biomed. Opt., 18 (04), 046014 (2013).

[5] M.R. Antonelli et al., Opt. Express 18, 10201 (2010).

8:40am EL+EM+EN-ThM3 Anisotropic Optical Properties of Rhombohedral and Tetragonal BiFeO$_3$ Phases, *Daniel Schmidt*, National University of Singapore, *L. You,* Nanyang Technological University, Singapore, *X. Chi,* National University of Singapore, *J. Wang,* Nanyang Technological University, Singapore, *A. Rusydi*, National University of Singapore
Single crystalline bismuth ferrite (BiFeO$_3$) is a multiferroic perovskite structure and exhibits magnetic as well as strong ferroelectric behaviour at room-temperature. Since about a decade BiFeO$_3$ is of strong research interest due to its potential applicability in ferroelectric memory devices and spintronics, for example [1].

While the lattice system of bulk BiFeO$_3$ is rhombohedral, the crystal structure of thin films can be engineered by introducing epitaxial strain. Depending on the choice of single crystalline substrate materials the thin film BiFeO$_3$ crystal structure and associated physical properties can be modified.

Here, we present the anisotropic optical properties of high-quality multiferroic BiFeO$_3$ thin films determined with Mueller matrix ellipsometry at room-temperature within the spectral range of 0.6 and 6.5 eV. The full dielectric function tensors of tetragonal-like and rhombohedral-like BiFeO$_3$ phases epitaxially grown on LaAlO$_3$ and SrTiO$_3$ single crystal substrates, respectively, are discussed. Significant birefringence and dichroism are observed as well as strain-induced differences in critical point energies between both phases.

The importance of careful optical analysis of anisotropic Mueller matrix data will be discussed, which allows for characterization of subtle sub-band gap crystal field transitions and reveals indications of an indirect band gap. Such transitions have been observed before by means of other techniques but not by ellipsometry. Additionally, the analysis of Mueller matrix data revealed that an unintentional substrate miscut can introduce an overall polarization tilt of the ferroelectric thin films. This tilt was confirmed by extensive in- and out-of-plane piezoelectric force microscopy studies.

An accurate determination of the dielectric function tensor is of high importance to verify or, if necessary, improve and correct ab-inito calculations, which are crucial for understanding the driving physical principles in such complex materials. A comparison of the experimental results with state-of-the art first-principle calculations will be presented.

[1] G. Catalan and J.F. Scott, Adv. Mater. 21, 2463 (2009).

9:00am EL+EM+EN-ThM4 Temperature Dependent Structural and Optical Properties of SnO$_2$ Thin Film, *Junbo Gong, R.C. Dai, Z.P. Wang, Z.M. Zhang, Z.J. Ding*, University of Science and Technology of China
SnO$_2$, which is an n-type semiconducting material with a wide band gap 4 eV, is an interesting material due to its high electrical conductivity and optical transparency. SnO$_2$ film is attractive for many applications such as optoelectronic devices, gas sensors, thin film transistors, transparent electrodes, anti-reflecting coating, and as catalyst support.

In this work, the ellipsometric parameters of SnO$_2$ films on quartz glass are measured by spectra ellipsometer(J. A. Woollam M-2000U) in the wavelength range of 300 to 1000 nm at different temperature from room temperature to 600 °C. By using a semitransparent model, the precise thickness and optical constants of SnO$_2$ thin film depending on the temperature were obtained and the evolution process was studied. The film thickness significantly decreased with increased temperature from 100 °C to 300 °C and the absorption edge has an obvious blue shift which means an increased band gap. The result reveals that this process is not reversible. Combined with XRD measurement, we identified that the change of thickness and optical properties of SnO$_2$ film was due to a phase transition from rutile structure to columbite structure.

9:20am EL+EM+EN-ThM5 Determining Curvature Radius of a Curved Surface by use of Mueller Matrix Ellipsometry, *Weiqi Li, H. Jiang, C.W. Zhang, X.G. Chen, S.Y. Liu*, Huazhong University of Science and Technology, China
Determining curvature radius of a curved surface by use of Mueller matrix ellipsometry

Weiqi Li, Hao Jiang, Chuanwei Zhang, Xiuguo Chen, and Shiyuan Liu*

State Key Laboratory of Digital Manufacturing Equipment and Technology, Huazhong University of Science and Technology, Wuhan 430074, China.

* Corresponding author: shyliu@hust.edu.cn

Ellipsometry is a powerful metrology tool for the characterization of surfaces and thin films. Generally, the basic principle of conventional ellipsometry is based on the assumption that the studied film or structure is on a planar surface [1], in another word, the conventional ellipsometry works the best for a flat surface. When the studied surface is tilted or curved, the measurement accuracy of the conventional ellipsometry will be significantly degraded, or even be incorrect. It is thus important to develop a method to deal with the cases when the surface for characterization is tilted or curved. Comparing with the conventional ellipsometry, the Mueller matrix ellipsometry (MME) can provide all 16 elements of a 4 by 4 Mueller matrix, and consequently can acquire much more useful information about the curved surface and thereby shows great potential in the curved surface metrology.

In this work, we propose an optical model that is able to process curved surface based on our in-house developed dual rotating-compensator MME [2] to characterize the surface layer of a single crystal silicon sphere crown with a radius of about 51 mm for demonstration. Focus probe accessory is used in the MME to achieve sufficient small spot on the curved surface so that the detected area on the spherical surface can be approximately regarded as a tilted one. We found that some of the measured off-diagonal Mueller matrix elements are very sensitive to the offset between the actual detected spot and the surface vertex, which is proportional to the deviation angle α of the surface normal across the surface vertex. An optical model of the spherical layer is proposed by considering the curved surface of the silicon sphere crown and the offset. With the proposed model, the deviation angle α as well as the surface layer thickness can be extracted from the measured Mueller matrix spectrum, and then the curvature radius of the sphere crown can be achieved. Experiments are performed on the silicon

sphere crown show that not only the accuracy of measurement can be improved but also the curvature radius of the sphere crown is capable to be measured using the proposed optical model.

[1] R. M. A. Azzam and N. M. Bashara, *Ellipsometry and Polarized Light* (North-Holland, 1992).

[2] S. Y. Liu, X. G. Chen, and C. W. Zhang, *Thin Solid Films* **584**, 176-185 (2015).

9:40am EL+EM+EN-ThM6 Cavity-Enhanced Optical Hall Effect in AlInN/GaN-based HEMT Structures Detected at Terahertz Frequencies, *Sean Knight*, University of Nebraska-Lincoln, *S. Schöche*, J.A. Woollam Co. Inc., *V. Darakchieva, P. Kühne*, Linköping University, Sweden, *J.-F. Carlin, N. Grandjean*, Ecole Polytechnique Fédérale de Lausanne (EPFL), Switzerland, *C.M. Herzinger*, J.A. Woollam Co. Inc., *M. Schubert, T. Hofmann*, University of Nebraska-Lincoln

The terahertz optical Hall effect (THz-OHE) has been established as a non-contact and therefore valuable tool for the investigation of free charge carrier properties in semiconductor heterostructures [1-4]. In this work, we demonstrate that the THz-OHE signal for samples grown on THz transparent substrates can be controlled and enhanced by a tunable, externally coupled Fabry-Pérot cavity mode [5]. An AlInN/GaN-based high electron mobility transistor structure (HEMT) grown on a sapphire substrate is investigated as an example, while the cavity enhancement phenomenon discussed here is generally applicable to situations when a layered sample is deposited onto a THz transparent substrate. We show that in the vicinity of an externally coupled-cavity mode, a strong enhancement of the OHE signatures of up to one order of magnitude can be achieved by optimizing the cavity geometry, which is very useful for small magnetic field strengths. This signal enhancement allows the determination of free charge carrier effective mass, mobility, and density parameters using OHE measurements in low magnetic fields. Previously, high-field electromagnets needed to be employed for THz-OHE measurement for the determination of free charge carrier parameters in semiconductor heterostructures. Tuning the external cavity allows an enhancement of the THz-OHE signatures by as much as one order of magnitude. We propose to employ this enhancement effect to reliably and accurately determine free charge carrier properties in semiconductor structures at small magnetic fields dispensing with the need for expensive high magnetic fields. Cavity-enhanced THz-OHE may therefore enable the wide spread contactless measurement of free charge carrier properties at THz frequencies and which is indispensable for the development of the next generation of group-III nitride-based high frequency devices.

11:00am EL+EM+EN-ThM10 Biosensor based on Imaging Ellipsometry and its Biomedical Applications, *Y. Niu, Gang Jin*, Institute of Mechanics, Chinese Academy of Sciences, China **INVITED**

The concept of biosensor based on imaging ellipsometry (BIE) was proposed in 1995 [1, 2]. With the development in recent 20 years, it has been formed an automatic analysis technique for detecting biomolecule detection interaction with merits of rapid, label-free, quantitative, high throughput and real-time. Its principle, methodology, biosensor system and biomedical applications are reviewed in this report.

A BIE system can be divided into four parts: the microfluidic array reactor, the imaging ellipsometer, the control system, and the biosensor database. The microfluidic array reactor serves to fabricate the protein microarray and accommodate biomolecular interactions. Using the microfluidic array reactor, various ligands are immobilized to different cells to form a sensing array, and each sensing surface can be prepared homogeneously under the flow condition. The imaging ellipsometer acts as a reader for data acquisition from the microarray. Since imaging ellipsometry is sensitive to slight variations of optical thickness, it can be used to visualize ultra-thin films and the change of molecular mass surface concentration. The control system combines the reactor with the imaging ellipsometer and functions to control the hardware's mechanical motion and obtain results in images, while the biosensor database is to aid BIE users in determining optimized experimental conditions and comparing previous test data.

The sensitivity and flexibility of the biosensor is very important for practical purpose, especially in biomedical fields. The sensitivity depends not only upon the resolution of imaging ellipsometry but also upon the bio-system of ligand-receptor on the microarray that is the bioactivity and its act related to the ligand screen, ligand immobilization, unspecific blocking and interaction conditions, etc. The flexibility mainly depends on the mechanical, electrical, informatics and biological control. So far, a serviceable engineering system of the biosensor and some bio-systems is installed available for more applications, especially for high throughput protein analysis, such as antibody screening [3], disease markers serological detection [4] and joint detection of tumor markers [5] as well as virus infection identification [6-7].

References

[1] G. Jin, et al., *Anal. Biochem.* **232**, 69 (1995).

[2] G. Jin, R. Jansson, and H. Arwin, *Rev. Sci. Instrum.* **67**, 2930 (1996).

[3] Y. Niu, et al., *Thin Solid Films* **519** 2768 (2011).

[4] C. Qi, et al., *J. Viral Hepatitis* **16**, 822 (2009).

[5] Y. Niu , et al., *Thin Solid Films* **571**, 453 (2014).

[6] C. Qi, et al., *Biosensors & Bioelectronics* **25**, 1530 (2010).

[7] C. Qi, et al., *Virus Res.* **140**, 79 (2009).

11:40am EL+EM+EN-ThM12 Screening Breast Cancer by Joint Detection of Tumor Marker Carbohydrate Antigen 15-3 and Carbohydrate Antigen 242 with Biosensor Based on Imaging Ellipsometry, *Yu Niu, G. Jin*, Institute of Mechanics, Chinese Academy of Sciences, China

Breast cancer which develops from breast tissue is the leading type of cancer in women worldwide, accounting for more than 25% of all carcinogenesis [1]. Compared with other common cancers, the survival rate of breast cancer is remarkably positive and optimistic that between 80% and 90% of those in developed country could be alive for at least 5 years. Therefore, screening high risk population and further concluding a clinical diagnosis in the early stage act as a pivotal factor to cure breast cancer, because it can provide overwhelming contribution to carry out essential therapy in time. Carbohydrate Antigen 15-3 (CA 15-3) and Carbohydrate Antigen 242 (CA 242) are widely-used tumor markers for breast cancer in clinic and their concentrations in serum vary sensitively with breast cancer genesis. The biosensor based on imaging ellipsometry (BIE) for visualization of biomolecular interactions was reported in 1995 [2] and now it is composed of a 48 protein unit array and imaging ellipsometry reader with a field of view (20 x 30 mm) and good resolution for protein adsorption layer on a silicon substrate (lateral and vertical is 1 μm and 0.1 nm, respectively) [3]. In this investigation, joint detection of these two tumor markers simultaneously has been performed with BIE as a trial for screening breast cancer for clinical purpose.

To realize the joint detection, a series of design and optimization has been performed, including the ellipsometric setting, ligand immobilization strategy, ligand surface density, as well as the blocking and rinsing procedures. The test concentration range calibration and the detection limit for quantitative detection have been established by standard samples, which meet the standards of clinical test. By diluting sera to the detection range fitting to the calibration curves, joint quantitative detection of CA 15-3 and CA 242 can be achieved simultaneously.

149 serum samples composed of both the healthy and patients have been performed with BIE. Compared with the results obtained by standard approaches in clinic, the correlation analysis indicates the BIE are highly consistent with clinical methods. In order to estimate the BIE performance for tumor markers detection, ROC curve analysis has been introduced. Its result suggests that the single marker detection by BIE presents good capability to distinguish the normal from patients and the joint detection of CA 15-3 and CA 242 plays a positive role in the improvement of the diagnosis specificity and accuracy.

Reference

[1] A. Jemal, et al., *CA Cancer J. Clin.* **61**, 69 (2011).

[2] G. Jin, et al., *Anal. Biochem.* **232**, 69 (1995).

[3] G. Jin, et al., *Thin Solid Films* **519,** 2750 (2011).

12:00pm EL+EM+EN-ThM13 Decomposition of Angle Resolved Spectroscopic Mueller Matrices from Scarabaeidae Beetles, *Roger Magnusson*, Linköping University, Sweden, *R. Ossikovski, E. Garcia-Caurel*, LPICM-CNRS, Ecole Polytechnique, France, *K. Järrendahl, H. Arwin*, Linköping University, Sweden

We use angle-dependent Mueller-matrix spectroscopic ellipsometry (MMSE) to determine Mueller matrices of Scarabaeidae beetles which show fascinating reflection properties due to structural phenomena in the exocuticle which are often depolarizing. It has been shown by Cloude [1] that a depolarizing matrix can be decomposed into a sum of up to four non-depolarizing matrices according to $M = aM_1 + bM_2 + cM_3 + dM_4$, where a, b, c and d are eigenvalues of the covariance matrix of M. Using the same eigenvalues the matrices M_i can be calculated. This method provides the full solution to the decomposition with both the non-depolarizing matrices and the weight of each of them in the sum.

An alternative to Cloude decomposition is *regression decomposition*. Here any Mueller matrix can be decomposed into a set of matrices M_i which are specified beforehand. Whereas in Cloude decomposition the only constraint on the matrices is that they are physically realizable non-depolarizing Mueller matrices, we can now limit the constraint and only use Mueller matrices representing pure optical devices having direct physical meaning, such as polarizers, retarders, etc. This leaves a, b, c, d as fit parameters to

minimize the Frobenius norm $\mathbf{M}^{exp}$ -$\mathbf{M}^{reg}$ where $\mathbf{M}^{exp}$ is the experimentally determined Mueller matrix to be decomposed and $\mathbf{M}^{reg}$ is the sum of all $\mathbf{M}_i$. Depending on $\mathbf{M}^{exp}$ an appropriate choice of $\mathbf{M}^{reg}$ matrices has to be made and different values of a, b, c and d are obtained through regression analysis.

We have previously shown that regression decomposition can be used to show that the Mueller matrix of *Cetonia aurata* can be decomposed into a sum of a circular polarizer and a mirror [2]. Here we expand the analysis to include angle-resolved spectral Mueller matrices, and also include more species of Scarabaeidae beetles.

One effect of the decomposition is that when depolarization is caused by an inhomogeneous sample with regions of different optical properties the Mueller matrices of the different regions can be retrieved under certain conditions. Regression decomposition also has potential to be a classification tool for biological samples where a set of standard matrices are used in the decomposition and the parameters a, b, c, d are used to quantify the polarizing properties of the sample.

[1] Cloude S.R. 1989. Conditions for the physical realisability of matrix operators in polarimetry. Proc. SPIE 1166, Polarization Considerations for Optical Systems II, pp. 177-185

[2] Arwin H, Magnusson R, Garcia-Caurel E, Fallet C, Järrendahl K, De Martino A, Ossikovski R, 2015. Sum decomposition of Mueller-matrix images and spectra of beetle cuticles. Opt. Express, vol. 23, no. 3, pp. 1951–1966

Surface Science
Room: 113 - Session SS+AS+EM+EN-ThM

Semiconductor Surfaces and Interfaces - I
Moderator: Yves J. Chabal, University of Texas at Dallas

8:00am SS+AS+EM+EN-ThM1 Reaction of 1,2,3-Benzenetriol with the Ge(100)-2x1 Surface, *Tania Sandoval, S.F. Bent*, Stanford University
Functionalization of semiconductor surfaces can provide tunable control of interfacial properties in organic-inorganic hybrid devices. In particular, multifunctional molecules have the potential to change the surface chemistry by leaving unreacted functional groups available after adsorption. Understanding the adsorption of these complex molecules could lead to various applications as sensors, selective film deposition, and molecular electronics.

In this work, the reaction of 1,2,3-benzenetriol on Ge(100)-2x1 surface was investigated. While the reaction of hydroxyl groups has been previously studied, differences in selectivity can be expected due to the position of the functional groups along the ring. The purpose of this study is to determine the extent of these differences and the effect on product distribution.

An analysis of the adsorption energetics was carried out by density functional theory. As expected, a proton transfer reaction was shown to be the most stable adsorbate configuration. However, after the adsorbate reacts with the surface through its first OH group, the energetics of the second OH dissociation showed differences based on two factors: (i) surface configuration (cross or diagonal trench and end or cross bridge) and more interestingly (ii) which two of the OH groups (1 and 2 or 1 and 3) are reacting with Ge. The latter constraint affects the adsorption energy of the second dissociation, where adsorption regardless of the surface configuration is less stable when the OH groups are next to each other. Finally, transition states for dissociation of the third OH were found to be limited by the configuration of the second dissociation, and in some cases were not possible to find without unrealistic distortions of the molecule.

Chemisorbed and physisorbed O(1s) and C(1s) spectra were obtained by X-ray photoelectron spectra. Differences between these spectra can be used to identify the reaction products. No change in the C(1s) spectra was observed, suggesting that no carbon forms a bond directly with the Ge surface. On the other hand, clear differences between the chemisorbed and physisorbed O(1s) spectra are observed. The presence of a second peak with a lower binding energy only in the chemisorbed spectra, assigned to oxygen bonded to Ge, confirms that 1,2,3-benzenetriol reacts with the Ge surface through OH dissociation. Quantitative analysis of the chemisorbed O(1s) spectra provides information on the fraction of OH groups reacting with the surface. Interestingly, about 66% of the total hydroxyl groups in 1,2,3-benzenetriol are involved in reaction with Ge, indicating that there is a significant fraction of unreacted OH groups.

8:20am SS+AS+EM+EN-ThM2 Ethylenediamine Grafting on Oxide-free H-, F-, and Cl- terminated Si(111) Surfaces, *Tatiana P. Chopra*, R.C. Longo, K.J. Cho*, University of Texas at Dallas, *M.D. Halls*, Schrodinger, Inc., *P. Thissen*, Karlsruhe Institute of Technology, Germany, *Y.J. Chabal*, University of Texas at Dallas
Amine termination of surfaces constitutes a core platform for fields as diverse as microelectronics and bioengineering, and for nanotechnology in general. Diamines are particularly attractive for surface amination because, unlike ammonia or simple amine molecules, they have a metal chelating capability useful in fabricating heterostructures. They can act as a linker molecule between inorganic electronic materials and biomolecules or photoactive quantum dots for applications in microlectronic, photonics and biosensing. Most work in the field utilizes self-assembled monolayers (SAMs) on oxidized substrates to present an amine termination of the surface. However, grafting on oxides through silanes or phosphonates is not robust. Moreover, several applications require as short a distance between the substrate and the amine group, which is hindered by the thickness of the oxide. Therefore, diamine grafting directly on oxide-free substrates is important, yet remains unexplored.

In this work, the attachment of liquid and vapor-phase ethylenediamine on three types of oxide-free (H-, F- and Cl-terminated) Si(111) surfaces is examined by infrared absorption spectroscopy and X-ray photoelectron spectroscopy in conjunction with first-principles calculations. We find that chemisorption is only possible on F- and Cl-terminated Si surfaces, with H-terminated Si surfaces yielding only physisorbed diamine molecules. On Cl-terminated Si surfaces, diamines adsorb in a mixture of monodentate and bridging configurations (chemical reaction of both amine endgroups), while on partially F-terminated Si surfaces the adsorption occurs primarily at one end of the molecule. The reaction of ethylenediamine with Cl-terminated Si surfaces is also characterized by complete removal of Cl and partial Si-H (~25% ML) formation on the surface. This unexpected result suggests that a proton-chlorine exchange may take place, with the endothermic barrier possibly reduced via a silicon lattice assisted process after an initial attachment of ethylenediamine to the surface.

8:40am SS+AS+EM+EN-ThM3 Reaction of Phenylhydrazine with Cl-Si(111) Surface by Wet Chemistry and with Clean Silicon Surface in UHV, *A.V. Teplyakov, Fei Gao*, University of Delaware
The monolayer coatings with aromatic functional groups can be used to tune mechanical, electronic, and chemical properties of semiconductor surfaces. This work focuses on obtaining well-defined surface of silicon functionalized with phenylhydrazine to produce an oxygen-free platform for further functionalization. Single crystalline Si(111) surface has been prepared using modified RCA procedure to produce well-ordered H-Si(111) surface. Next, Cl-terminated Si(111) surface is prepared from H-terminated Si(111) surface using PCl_5 in chlorobenzene solvent with trace amount of benzoyl peroxide as a reaction initiator under nitrogen atmosphere following previously established procedures. Phenylhydrazine-functionalized Si(111) sample is obtained from Cl-Si (111) surface with phenylhydrazine at 38°C under N_2 atmosphere. To confirm the presence of Si-N bonds following this procedure, establish the structures of surface species produced and to investigate the oxidation mechanism, we followed the reaction by Fourier-transform infrared spectroscopy, X-ray photoelectron spectroscopy, and time-of-flight secondary ion mass spectrometry. To study the formation of Si-NH_x groups, this result was compared with the results of phenylhydrazine reactions on clean silicon surface under ultra-high vacuum (UHV) conditions. Density functional theory (DFT) calculations were performed to infer the mechanisms of surface reactions and further oxidation steps, and to compare the predicted vibrational spectra and core-level energies with the results of experimental studies.

9:00am SS+AS+EM+EN-ThM4 Anomalously Low Surface Recombination Velocity for Fluorine Terminated Nanopatterned Si Surfaces, *W.N. Peng, Jonghan Park, L.-H. Liu, R.C. Longo*, University of Texas at Dallas, *D.J. Michalak*, Intel Corporation, *D.M. Pak, Y.J. Lee, J.X. Hsu, K.J. Cho, Y.J. Chabal*, University of Texas at Dallas
Recently, oxide-free and partially methoxy-terminated Si surfaces[1] have been developed as a novel platform for surface reactions because of their superior reactivity compared to hydrogen termination[2]. As a result, strong polar bonds such as Si-F could be stabilized on these surfaces. Since the electrical quality is critical for many applications (i.e. surface defects can degrade the device performance), we performed contactless surface recombination velocity measurements to examine the electronic quality of partially covered surfaces. Interestingly, we found that the carrier lifetime is significantly increased after fluorine termination, with the carrier lifetime 10 times higher than that of hydrogen terminated Si surfaces, approaching 1.5

---

* Morton S. Traum Award Finalist

ms. This anomalously long carrier lifetime can be explained either by a better surface passivation or by surface band bending effects. We therefore performed UPS and kelvin probe measurements to investigate the band structure of these surfaces after fluorine termination and found evidence for band bending. A potential model of a surface dipole layer induced band bending is supported by DFT calculations. Regardless of the mechanism controlling the recombination time, this method is well suited to explore the fluorination mechanism of H-terminated surfaces.

[1] D. Michalak, S. Amy, D. Aureau, M. Dai, A. Esteve, and Y. J. Chabal, *Nature Materials*, **9**, (2010)

[2] P. Thissen, T. Peixoto, R. Longo, W. Peng, W. Schmidt, K. Cho, and Y.J. Chabal, *JACS*, **134** (2012)

9:20am SS+AS+EM+EN-ThM5 Molecular Functionalization of Semiconductor Surfaces: From Single Crystals to Quantum Dots, *Stacey Bent*, Stanford University **INVITED**
Because the surfaces of small structures can dominate their properties, implementing functional nanoscale materials depends to a large extent upon understanding and controlling the surface reactivity. This talk will focus on studies of the adsorption of organic molecules at semiconductor surfaces, toward the ultimate goal of controlling the chemical and electrical properties of the substrate. We will describe model studies of molecular functionalization on both flat and nanostructured surfaces. The presentation will begin by examining adsorption on the Ge(100)-2×1 surface. Using a combination of experimental (infrared spectroscopy, X-ray photoelectron spectroscopy) and theoretical (density functional theory calculation, Monte Carlo simulation) methods, we will show how the molecular structure as well as the identity of the reactive moieties of organic molecules can affect the product distribution upon adsorption. We will then present results of a study in which the organic ligands bonded to semiconductor quantum dots (QDs) are used to tune the electronic properties of the QDs. We will describe experimental and theoretical studies of the effects of such interface engineering on the band gap and relative band positions in lead sulfide (PbS) QDs. These ligand-exchanged quantum dots are tested in multilayer colloidal QD solar cells, and the results show that molecular functionalization can be used to achieve enhanced photogenerated carrier collection in the devices.

11:00am SS+AS+EM+EN-ThM10 Periodic Trends in the Hydrogen Elimination Thermal Decomposition Reaction on Si(100)-2×1: Linear and Branched Alkyl Halides, Alcohols, and Amines, *Andrew Pohlman*, K.L. Romolino, N.J. Burgener, S.M. Casey, University of Nevada
The hydrogen elimination thermal decomposition reaction was studied on the Si(100)-2×1 surface using temperature programmed desorption mass spectrometry (TPDMS) and electronic structure methods for a selection of linear and branched alkyl halides, alcohols, and primary amines. Desorption activation energies and pre-exponential factors were determined using several analysis techniques from TPDMS spectra and compared to calculations based on ab initio canonical transition state theory using density functional theory (DFT). Values for activation energies and pre-exponential factors for dissociative desorption are compared within an adsorbate class based on a varying ratio of available alpha:beta:gamma hydrogens for elimination. Kinetic parameters are also compared between classes of adsorbates for general structure-activity periodic trends. TPDMS experiments reveal desorbing masses consistent with hydrogen elimination in all cases; however, the different elimination channels remain convoluted. Rate constants for each desorption channel were calculated using DFT and used to determine branching ratios for each dissociative desorption reaction. Reaction barrier trends are consistent with previous reports; however, numerical values were found to be much lower when considering inter-dimer reaction mechanisms.

11:20am SS+AS+EM+EN-ThM11 Diffusion of Arsenic Oxides During the Atomic Layer Deposition of Metal Oxide Films on GaAs(100) Surfaces, *Alex Henegar, T. Gougousi*, University of Maryland, Baltimore County
It is known that native oxides of III-V semiconductors are consumed during atomic layer deposition using certain subsets of precursors. It was believed these surface oxides were completely removed during the first few deposition cycles because once the surface was covered by a coalesced film the native oxides would be protected. It has been observed, however, that native oxide consumption in systems such as ALD TiO_2 on GaAs(100) and InAs(100) proceeds continuously well after the surface is completely covered. Therefore there must be a transport mechanism that continuously moves these oxides through the developing film in order to interact with the precursor at the surface and be removed.

The aim of this work was to find unequivocal evidence of the transport mechanism needed for continuous oxide removal during ALD at typical processing conditions. ALD processes using metal organics and H_2O were used to deposit TiO_2, Al_2O_3 and HfO_2 films on GaAs(100). The experiments were designed so as to decouple the native oxide consumption from the native oxide transport and provide convincing evidence for the existence of this unacknowledged thus far mechanism. We will provide results that solidify the hypothesis that native oxide diffusion is a critical component in the complete and continuous removal of the interfacial layer.

11:40am SS+AS+EM+EN-ThM12 Ultrafast Non-Equilibrium Effects in Ti Overlayers on P-Type GaAs(100) Investigated by Femtosecond XUV Photoemission Spectroscopy, *Mihai E. Vaida*, University of California, Berkeley, *S.R. Leone*, University of California, Berkeley and Lawrence Berkeley National Laboratory
Time resolution, surface sensitivity and element specificity are technical ingredients required to investigate ultrafast photoinduced processes and charge localization at semiconductor surfaces. All these requirements are fulfilled by a new experimental apparatus that consists of a tunable femtosecond high harmonics XUV source, a pump-probe setup, and an ultra-high vacuum surface science chamber for surface preparation and investigation.

The present contribution focuses on the charge carrier dynamics at the surface of a bare p-type GaAs(100) as well as Ti overlayers on p-type GaAs(100). The charge transfer between the bulk and the surface of the bare GaAs(100) is produced by the pump laser pulse at the central wavelength of 800 nm and is investigated by monitoring the surface photovoltage through the shift of the Ga 3d photoemission peak with the XUV probe laser pulse as a function of the pump-probe time delay. A transient shift of the Ga 3d photoemission peak to lower binding energy at early pump-probe time delay, with a magnitude of 0.3 eV, is observed and is attributed to transport of the electrons from the bulk to the surface. Upon increasing the pump-probe time delay, a restoration of the Ga 3d peak is observed, which corresponds to the recombination of the positive and negative carriers.

When a Ti overlayer is deposited on the p-type GaAs(100) surface, a Schottky diode is formed. If the 800 nm pump laser pulse has sufficient intensity to produce a photoemission process via multi-photon excitation, non-equilibrium effects occur at the Ti-GaAs interface independently from the presence of the surface photovoltage. In this case, positive charges accumulate at the surface and are not effectively screened by the electrons coming from the bulk, and the Schottky diode is transiently driven into a reversed bias mode. The formation of the reverse bias Schottky diode, which is studied in real time with the XUV probe laser pulse by monitoring the Ti Fermi level photoemission shift as a function of the pump-probe time delay will be presented and discussed.

12:00pm SS+AS+EM+EN-ThM13 Improving the Quality of p-type AlGaN Layers by Reactive-ion Etching, *Joy McNamara, K.L. Phumisithikul, A.A. Baski, M.A. Reshchikov*, Virginia Commonwealth University, *J. Marini, F. Shahedipour-Sandvik*, SUNY Polytechnic Institute
AlGaN layers prepared by metal-organic chemical vapor deposition, with varying composition of Al (6 – 17%), were studied using the surface photovoltage (SPV) technique. Previous SPV studies on both *n* and *p*-type GaN allowed us to calculate the value of the surface band bending, by applying a thermionic model to explain the transfer of charges over the near surface barrier in various conditions (air, vacuum, and for a wide range of temperatures, T = 80 – 600 K). [1,2] The band bending was estimated to be 1.0 eV and – 2.0 eV, for *n*-type GaN and *p*-type GaN, respectively. SPV measurements on *p*-type AlGaN layers were expected to have similar behaviors to their *p*-type GaN counterparts. However, numerous measurements showed that this was not the case. The SPV transients (upon turning on or off the excitation source) showed significantly slower transients and smaller values than expected from the thermionic model. Moreover, the restoration of the band bending, as indicated by the restoration of the SPV signal to its dark value, did not occur within a reasonable amount of time. The data could not be fit by the thermionic model, and thus we were unable to calculate the band bending. We attribute the slow transients and lack of restoration to a defective surface region which interferes with thermionic processes. To verify this assumption, the top 40 nm of the AlGaN layer was etched using a reactive-ion etch (RIE). After etching, the SPV behavior exhibited substantially different behavior. Fast transients and close-to-thermionic behavior was recovered. Additionally, the effect of annealing the samples after etching provided even closer values to what is predicted by the thermionic model. From this study, it can be concluded that a defective, near surface region is inhibiting the transfer of holes over the near surface barrier under illumination, and hole trapping may be occurring during restoration. In both cases, this behavior cannot be modeled by theory. Etching removes the defective layer, and reveals a region of presumably higher quality as evidenced by the subsequent thermionic behavior.

[1] M. A. Reshchikov, M. Foussekis, and A. A. Baski. *J. Appl. Phys*. **107**, 113535 (2010).

[2] M. Foussekis, J. D. McNamara, A. A. Baski, and M. A. Reshchikov, *Appl. Phys. Let.***101**, 082104 (2012).

Thursday Afternoon, October 22, 2015

Electronic Materials and Processing
Room: 211C - Session EM+EN-ThA

Materials for Light Management

Moderator: Michael Filler, Georgia Institute of Technology, Sang M. Han, University of New Mexico

2:20pm EM+EN-ThA1 III-V Nanowires for Photonics and Solar Energy Applications, *Anna Fontcuberta i Morral*, EPFL, Switzerland
INVITED

Semiconductor nanowires are filamentary crystals with a tailored diameter between few to few hundred nanometer. Their special shape and dimensions render them especially interesting for photonic applications. In my talk I will discuss several photonic applications of nanowires. I will start by showing how to modify light absorption and emission of nanowires by coupling them to plasmonic elements [1]. I will then follow by explaining the use of III-V nanowires for solar cell applications. I will show how, by choosing the adequate diameter and length, it is possible to obtain absorption cross-sections much larger than the nanowire physical size. This concentration effect can be used to increase the efficiency of nanowire-based solar cells and to reduce considerably the use of materials [2].

References

[1] A. Casadei et al , Scientific Reports 5, 7651 (2015)

[2] P. Krogstrup et al, Nature Photon. 7, 306 (2013) ; M. Heiss et al, Nanotech. 25, 014015 (2014)

3:00pm EM+EN-ThA3 Formation of Wurtzite Phase by Si Doping and its Effect on the Optical Properties of GaAs Nanowires grown on Si Substrates by a Catalyst-free MBE-VLS Technique, *Marina Nakano, K. Sugihara, D. Ohori, K. Sakai,* Univ. of Miyazaki, Japan, *H. Amano, Y. Honda,* Univ. of Nagoya, Japan, *T. Ikari, A. Fukuyama,* Univ. of Miyazaki, Japan

GaAs nanowires (NWs) are expected to applying to optoelectronic devices. However, material properties have not been understood yet due to a presence of impurity and defect level related to an involved catalyst which was inevitable for growing nanowires. Recently, we succeeded in fabricating the catalyst-free GaAs NWs on a (111) Si substrates using a combination of molecular beam epitaxy and vapor-liquid-solid method [1]. The NW had two kinds of crystalline phases, a zinc-blend (ZB) and a wurtzite (WZ) structures [2]. We found the amount of WZ phase increased with increasing the amount of Si-doping by using high-resolution X-ray diffraction and transmission electron microscope [3]. In this study, we investigate the electronic band structure of Si-doped GaAs NWs by using a photoreflectance (PR) and a photoluminescence (PL) techniques and discuss the effect of Si-doping on the optical properties.

Three kinds of samples with different Si cell temperatures at 1015, 1065, and 1150ºC were grown. The average diameter and length of NWs were 60 nm and 35 mm, respectively. The amount of Si doping was evaluated by a carrier concentration estimated from a Hall measurement. The lowest hole concentration was 5.5×10^{17} cm^{-3} for the sample grown at 1015 ºc and increased about an order by increasing the cell temperature. PR and the PL emission light were carried at 4 K.

The crystallographic investigations showed that the amount of secondary WZ phase increased with increasing the Si-doping. Three critical energies were observed at 1.51, 1.49 and 1.43 Ev in the PR. The first two signals were observed for all samples and attributed to band to band and band to Si acceptor transitions, respectively. Since the signal at 1.43 Ev appeared only in high Si-doping sample with high amount of WZ phases, this is due to the band to band transition at the interface between the two different crystalline phases. In the PL spectra, three other emission peaks were observed at 1.46, 1.42 and 1.37eV. The intensities of these peaks changed for the samples with different cell temperature, these may be due to impurity and defect levels in nanowires. Si dopant itself as well as different crystal structure affect the electron transition. Since the interface transition observed at 1.43 Ev becomes dominant, emissions through such impurities were hidden for the sample with highest Si-doping. Temperature dependences of the PR and PL spectra will be discussed for further understanding the effect of Si-doping.

[1] J. H. Paek et al., Phys. Stat. Sol. (c) 6, 1436 (2009).

[2] D. Spirkoska et al., Phys. Rev. B 80, 245325 (2009).

[3] A. Suzuki et al., Jpn. J. Appl. Phys. 54, 035001 (2015).

3:20pm EM+EN-ThA4 Nanowire Enabled 3-Dimensional Band Engineering for Efficient Next Generation Solar Cells, *Esther Alarcon Llado,* Ecole Polytechnique Fédérale de Lausanne (EPFL), Switzerland, *O. Demichel,* Universite de Bourgogne, France, *A. Fonctuberta i Morral,* Ecole Polytechnique Fédérale de Lausanne (EPFL), Switzerland

Next generation photovoltaics (PV) aim to achieve large currents at high voltage by new materials and device concepts that overcome the main efficiency losses in traditional solar cells. Intermediate band solar cells (IBSCs) are a class of next generation PV where multi-energy levels in the semiconductor enable the scavenging of low energy photons and converting them into high voltage electrons. IBSCs have only been recently proven with highly mismatched alloys, however with very little efficiencies. The main challenge is the short lifetime of electrons at intermediate band states.

In this regard, the nanowire (NW) geometry offers potential advantages in the solar energy conversion process. Due to their richness in structure and morphology combined with doping and bandgap engineering, NWs provide an opportunity for new charge separation mechanisms.

In this work we propose a new IB-based solar cell design that is advantageously benefited from nanostructuring. We propose the use of core-shell heterostructures in order to reduce the optical coupling between the different band states in a three-level IBSC. Taking advantage of the intrinsic anisotropy of the nanowire geometry, the fundamental idea here is that excitons are separated by the heterostructure along the radial direction, while carrier extraction is performed along the axial direction. As a result, mid-gap recombination rate is reduced by several orders of magnitude.

On the other hand, it is known that optical resonances in NWs result into light self-concentrating effects that allow high absorption with reduced material. What's more, light resonances in NWs leave a very specific spatial distribution of light inside the nanostructure. By tuning the geometrical parameters of the NW, one can guide light around different regions in the NW depending on the photon energy. A combination of both electrical and morphological engineering, can lead to high efficiency PV.

4:00pm EM+EN-ThA6 Effect of Internal Electric Field on the Miniband formation of Multi Quantum Well Solar Cell Structures Investigated by a Photoreflectance and a Photothermal Spectroscopy, *Tsubasa Nakamura, K. Matsuochi, T. Murakami, H. Suzuki,* University of Miyazaki, Japan, *K. Toprasertpong, M. Sugiyama, Y. Nakano,* The University of Tokyo, Japan, *T. Ikari, A. Fukuyama,* University of Miyazaki, Japan

Insertion of a multiple quantum-well (MQW) structure into the absorbing layer of solar cells is promising for accomplishing higher conversion efficiency. Recently, a MQW with a very thin barrier structure has been proposed to enhance the conversion efficiency [1]. The coupling of the wave functions between adjacent quantum wells causes a mini-Brillouin zone along the growth direction, which results in the formation of miniband. We have discussed carrier escaping mechanism in MQW by using photoreflectance (PR) and photothermal spectroscopy (PPT) and found that internal electric field in the QW region might affect the recombination probability [2]. In this study, we investigate the effect of internal electric filed on the miniband width.

Three kinds of MQW samples were grown by a metal-organic vapor phase epitaxy technique. Two GaAs p-i-n solar cell structure samples with MQWs in the i-layer were prepared. The doping levels in the p- and n-type layer were changed and this induced the different strength of the electric field in the absorbing layer. Another sample had GaAs n-n structures without any electric field in the absorbing layer. The thicknesses of the well barrier were changed from 2 to 6 nm for discussing the detailed miniband formation. PR and PPT measurements were carried out at room temperature. The miniband width was estimated from the difference of the peak energies of the PR modulus spectra. The lower and higher energy peak correspond to the energies of bottom and top of the miniband, respectively. The PPT method is used to detect the heat generated by non-radiative recombination of photo generated carriers. The miniband width was also calculated from the Gaussian decomposition technique of the observed PPT spectra [3].

Decrease of the miniband width by increasing the barrier width was observed for all samples. This is coincide with the theoretical prediction. The miniband width for n-n structure is considered to be larger than that of p-i-n structure. Applied electric filled may reduce the wave function overlapping between the adjacent wells. The increase of the miniband width by the electric field for the p-i-n structure sample was observed. However, the increase of the miniband widths for n-n structure could not be confirmed from the PR spectra. Since the PPT measurement is more sensitive for estimating the band edge transition, effect of the electric field may be more clearly observed by comparing the PR and PL spectra.

[1] Y. Wang, et al., J. Cryst. Growth 352, 194 (2012).

[2] T. Aihara et al., J. Appl. Phys. 116, 044509 (2014).

[3] T. Aihara et al., J. Appl. Phys. 117, 084307 (2015).

4:20pm EM+EN-ThA7 Controlling Light Absorption with Nanophotonics, *Vivian Ferry*, University of Minnesota **INVITED**
Luminescent solar concentrators (LSCs) offer many advantages over traditional concentrator geometries. As opposed to concentrators that rely on tracking, LSCs operate under both direct and diffuse illumination and require the solar cell to only be efficient at a small range of wavelengths. In practice, most LSCs suffer losses from reabsorption of emitted light, non-unity quantum yields, and incomplete light guiding to the solar cell. Here we combine tunable lumophores based on quantum dot heterostructures with photonic designs to improve the concentration efficiency of LSCs and study light propagation within the device.

To achieve high concentration ratios it is critical to have high effective Stokes shifts, high quantum yields, and to reduce escape cone losses. We synthesized a series of core-shell nanocrystal lumophores that exhibit tunable emission. We show how the narrow emission bandwidth of these nanocrystals enables the use of a 1D photonic mirror on the top surface of the device, designed to admit incident sunlight and trap luminesced light from the nanocrystal. In combination, the concentration ratios from these devices exceed the performance of dyes with higher quantum yields but broader emission. Another approach to photonic LSCs is to restrict the angle of emission from the lumophores to promote coupling to the total internal reflection modes of the LSC. This talk will discuss designs for the latter approach and compare achievable concentration factors.

The second portion of the talk will discuss light management strategies for solid-state lighting, and the incorporation of plasmonic nanostructures to enhance light outcoupling from solid-state devices. This section of the talk will compare and contrast plasmonic structures for solar cells and solid-state lighting, and discuss ways that design rules should be adjusted for different materials systems.

5:20pm EM+EN-ThA10 Symmetry-Breaking in Periodic Nanostructures for Enhanced Light Trapping in Organic Solar Cells, *Seok Jun Han, S. Ghosh, O.K. Abudayyeh, E.J. Martin, J.K. Grey, S.M. Han, S.E. Han*, University of New Mexico
In this study, we introduce a new light-trapping scheme for organic solar cells by systematically breaking the symmetry in periodic nanostructures on the bottom metal contact. To create symmetry-breaking metal nanostructures, we start by fabricating a mold from a crystalline silicon (c-Si) substrate. We intentionally misalign the etch mask with respect to [110] crystallographic orientation of the c-Si. Subsequently, silver is sputter-coated over the nanoscale recess created in the c-Si substrate to create the metal nanostructures, and an organic photoactive material, PCPDTBT, is spin-coated on the silver layer. The enhancement in light absorption is achieved at surface plasmon resonances at the polymer-metal interface. We demonstrate that surface plasmon band structure can be tailored by symmetry-breaking. In experiment, we increase the number of surface plasmon bands in the visible spectrum and locate the bands at the desired wavelengths by controlling the symmetry. In general, by patterning a flat film in symmetry-breaking structures, absorption is enhanced from 65% to 85% in a broad short wavelength spectrum. Moreover, the absorption spectrum is extended into long wavelengths by 20 nm. We expect that our low-cost, symmetry-breaking fabrication strategy would be scalable and lead to a manufacturable process for efficient light-trapping in organic photovoltaic devices.

5:40pm EM+EN-ThA11 Symmetry-Breaking in Light-Trapping Nanostructures on Silicon, *Sang Eon Han, S.J. Han, S. Ghosh, T. Cai, B. Hoard, S.M. Han*, University of New Mexico
In thin-film photovoltaics, highly absorptive materials are conventionally used. However, these materials have achieved efficiencies that are not comparable to those of thick crystalline silicon (c-Si) photovoltaics and, in some cases, suffer from their toxicity and low supply. A viable solution to these problems would be to use c-Si for thin-film photovoltaics. However, thin c-Si films absorb sunlight weakly because of its indirect band gap and strong light-trapping should be provided to achieve high efficiency. For thin-film photovoltaics, nanoscale structures are typically involved for light trapping because the film thickness becomes comparable to the wavelength of sun light. While diverse nanostructures have been studied to break the light-trapping limit of geometric optics, known as the Lambertian limit, highly efficient nanostructures that can be easily manufactured have not been demonstrated. We have previously predicted that symmetry-breaking in light-trapping periodic nanostructures on thin films can approach the Lambertian limit very closely. Herein, we will present how the systematic symmetry-lowering increases light-trapping in c-Si thin-film photovoltaics.

We will demonstrate the experimental realization of such low-symmetry structures using simple wet etching methods on c-Si(100) wafers without any off-cut, tilt angle. Further, we will discuss the optical characterization of our fabricated structures on thin c-Si films.

Surface Science
Room: 113 - Session SS+AS+EM+EN-ThA

Atomistic Modeling of Surface Phenomena & Semiconductor Surfaces and Interfaces - II
Moderator: Talat Rahman, University of Central Florida

2:20pm SS+AS+EM+EN-ThA1 Ideas Old and New Applied to Non-Ideal Surface Adsorption and Reaction, *William Schneider*, University of Notre Dame **INVITED**
Free energies of adsorption are arguably the most elementary quantities in heterogeneous catalysis. These free energies depend on the surface and adsorbate (reactant, intermediate, or product) of interest, system temperature and adsorbate coverage. The free energy represents a balance between the energetic driving force for creating bonds between an adsorbate and a surface and the entropic cost of moving an adsorbate from a fluid phase to a surface. Standard density functional theory (DFT) approaches generally begin by optimizing the location of an adsorbate on a surface, computing a binding energy, and approximating the internal, translational, and configurational contributions to the free energy. In this work we examine the reliability of standard approximations and describe easily applied improvements that give reliable free energy estimates. We describe applications to adsorption at metal surfaces and in the pores of zeolites.

3:00pm SS+AS+EM+EN-ThA3 Insights into the Oxidation of Stepped Cu Surfaces using Multiscale Investigations, *Q. Zhu, W.A. Saidi, Judith Yang*, University of Pittsburgh
Surface defects can induce non-canonical oxidation channels on metal surfaces that may lead to the formation of novel nanostructures. Recently, in situ environmental transmission electron microscopy (ETEM) experiments showed that the oxidation of stepped Cu surfaces promotes the formation of a flat metal-oxide interface through Cu adatoms detachment from steps and diffusion across the terraces. To bridge the gap between experiments and theory, we are investigating Cu oxidation using a multiscale computational approach. Our previous MD simulations based on a reactive force field (ReaxFF) demonstrated that the oxidation of stepped Cu(100) takes place on the upper terrace at a faster rate than the lower terrace due to a preferable oxygen diffusion from the lower to upper terraces. We have extended this study using first-principles density functional theory (DFT) and kinetic Monte Carlo (KMC), and performed a systematic study of all stepped Cu surfaces with a low Miller index. The DFT results show that the oxygen diffusion trend varies with the surface type, where in most cases the oxygen ascending diffusion is more favored. This result is confirmed also with ReaxFF MD and KMC simulations. The MD simulations, with a fine-tuned ReaxFF force field parametrization, have also indicated that oxygen adatoms on the upper terrace can enhance the interlayer Cu atom mass transport. These theoretical simulations provide essential fundamental understanding of the experimentally observed smoothing of the Cu surface during in situ oxidation.

3:20pm SS+AS+EM+EN-ThA4 Reconciling Complimentary Analyses of Epitaxial Growth: Role of Transient Mobility for para-Hexaphenyl on Mica, *Josue Morales-Cifuentes, T.L. Einstein*, University of Maryland, College Park, *A. Pimpinelli*, Rice University
In studies of epitaxial growth, a major goal is to assess the size of the smallest stable cluster (with $i + 1$ monomers, where i is the critical nucleus size). This is accomplished by analyzing either the capture zone distribution (CZD), the scaling of incident flux F to the density of stable islands N or the island-size distribution (ISD). For CZD, generalized Wigner distributions (GWD) have proven useful, [1,2] with successful applications to, non-comprehensively: polar-conjugated molecule Alq_3 on passivated Si(100), self-assembled Ge/Si(001) nanoislands and para-Hexaphenyl (6P) films on amorphous mica. [3] We concentrate on the last, for which the Winkler group found that $i \approx 3$.

Scaling of N usually follows $N \propto F^\alpha$, where α is the growth exponent. For 6P films, a difference in scaling behaviors at small and large F is attributed to DLA and ALA dynamics (i.e. $i = 5 \pm 2$, and $i = 7 \pm 2$, respectively). [4] This discrepancy motivates our current work, where transient mobility effects modify scaling non-trivially. [5]

Consider that monomers begin in a (ballistic) hot precursor state before thermalizing (random walk). The competing times of ballistic monomers

becoming thermalized vs. being captured by an island naturally define a "thermalization" scale for the system. We obtain an analytic solution and elaborate on the physical meaning behind the energies and dimensionless parameters used. Novel scaling regimes are retrieved for which power-law scaling applies, with non-monotonic crossovers between them and the growth exponent exclusively dependent on i. Applying the model to the 6P films results in good agreement for the scaling and the activation energies: experimental values of the activation energies of 0.26eV (high-T) and 0.04eV (low-T) match model predictions of 0.3eV (high-T) and 0.04eV (low-T). Furthermore, the high-flux regime is interpreted not as ALA (attachment-limited aggregation) or HMA (hot monomer aggregation) but rather as an intermediate scaling regime related to DLA (diffusion-limited aggregation). Lastly, we discuss a simplifying approximation for the model and connections to some capture zone distribution considerations of α. [6]

[1] T.L. Einstein, A. Pimpinelli, D. González, J. Cryst. Growth 401, 67 (2014)

[2] T.L. Einstein, A. Pimpinelli, D. González, and J. R. Morales-Cifuentes, Proc. CCP2014, J. Phys.: Conf. Series (2015), in press.

[3] T. Potocar, G. Lorbek, D. Nabok et al. 2011 Phys. Rev. B 83 075423

[4] L. Tumbek & A. Winkler, Surf. Sci. 606, L55 (2012)

[5] J. R. Morales-Cifuentes, T. L. Einstein, and A. Pimpinelli. Phys. Rev. Lett. 113, 246101(2014)

[6] J. R. Morales-Cifuentes, T. L. Einstein, and A. Pimpinelli (in preparation)

4:00pm SS+AS+EM+EN-ThA6 Probing 2-DEG at InN Surface by Electrolyte-Gated Raman Spectroscopy, *E. Alarcon Llado,* Ecole Polytechnique Fédérale de Lausanne (EPFL), Switzerland*, **Tommaso Brazzini**,* Lawrence Berkeley Lab, University of California, Berkeley, *J.W. Ager*, Lawrence Berkeley National Laboratory (LBNL)
Indium nitride has attracted much attention as its narrow bandgap (~0.67eV) expands the range of the direct gaps of the group III-N alloys into the visible and near-IR and thus offers an outstanding potential for solar energy conversion and optoelectronic applications. However, experimental demonstration of high efficiency In-rich III-V pn rectification junctions has been hampered by the existence of an intrinsic interface electron accumulation layer, which seems to persist regardless of surface treatment. The large capacitance of the Helmholtz double layer that forms on a surface of an object in contact with an electrolyte allows the 2-DEG at the surface of InN to be tuned and even depleted. Using this effect, we demonstrated the first pn rectification behavior in InN.[1]

In addition, the 2-DEG accumulation layer affects not only the electrical properties, but also has brought many controversies in the interpretation of optical experiments. Raman spectroscopy probes not only the lattice dynamics in a crystal, but also the electronic structure and free carriers. In particular, the interaction between the free electrons at the surface and the longitudinal optical (LO) phonon in InN has been addressed by several studies. However some questions still remain.

In this work, we present an in-situ micro-Raman study that confirms the presence of a surface related Raman mode in InN and shows its interaction with accumulated electrons at the surface. Electrolyte gated Raman spectroscopy (EGRS) on InN layers was performed in order to modulate and in-situ probe the surface electron accumulation region in InN. A reversible shift of the LO phonon with the applied gate potential is found (see figure 1). The peak position and shift depends on the probing light energy, however it is independent of bulk doping. We explain these findings by Martin's double scattering mechanism and bandgap narrowing at the surface tuned by the gate voltage. InN nanocolumns were also investigated by EGRS. The LO mode lies at higher frequencies in all nanocolumn samples. This fact corroborates the nature of the scattering mechanism, which is strongly dependent on the surface orientation. In summary, our results clearly demonstrate the surface origin of this feature and allow the fundamental study and understanding of the electronic structure of InN.

1.Alarcón-Lladó, E. et al. PN junction rectification in electrolyte gated Mg-doped InN. Appl. Phys. Lett. 99, 102106 (2011).

4:20pm SS+AS+EM+EN-ThA7 Surface Termination of Single Crystal Bi₂Se₃ Investigated by Low Energy Ion Scattering, *Weimin Zhou, J.A. Yarmoff*, UC Riverside
Bismuth Selenide (Bi_2Se_3) is a prototypical topological insulator (TI) with a two-dimensional layered structure that enables clean and well-ordered surfaces to be prepared by cleaving. Although some surface structure studies have concluded that the cleaved surface is terminated with Se, as is expected from the bulk crystal structure, there are other reports that show either a Bi- or mixed-termination [1]. Low Energy Ion Scattering (LEIS) and low energy electron diffraction (LEED) are used here to compare surfaces prepared by *ex-situ* cleaving, *in-situ* cleaving and Ar$^+$ ion

bombardment and annealing (IBA) in ultra-high vacuum. Surfaces prepared by *in-situ* cleaving always have a sharp 1x1 LEED patterns and are Se-terminated. Surfaces prepared by IBA show a transition from Bi- to Se-termination with increasing annealing temperature. Samples inserted into the vacuum chamber following *ex-situ* cleaving have much dimmer LEED patterns, show surface contamination with Auger electron spectroscopy, and could be terminated either with Se or Bi. The angular dependence of LEIS spectra, which is sensitive to the surface atomic structure, doesn't indicate any substantial differences between surfaces prepared by IBA or *in-situ* cleaving. Ion scattering simulations using Kalypso are compared to experimental angular data to obtain more details about the structure. Exposure of clean surfaces to gaseous species will also be discussed in an effort to determine the surface chemical reactions responsible for the termination change.

[1] X. He, W. Zhou, Z. Y. Wang, Y.N. Zhang, J. Shi, R.Q. Wu and J.A. Yarmoff, Phys. Rev. Lett. **110**, 156101 (2013).

4:40pm SS+AS+EM+EN-ThA8 Real-Time Imaging with Atomic-level Spatial Resolution of Silicon Oxidation, *Bryan Wiggins, L.G. Avila-Bront, R. Edel, S.J. Sibener*, University of Chicago
The investigation of the initial stages of molecular oxygen adsorption on Si(111)-7x7 with real-time and real-space visualization will be discussed in this presentation. We will present the first results from a newly built supersonic molecular beam paired with a scanning probe microscope instrument. The system is designed with an oil free differentially pumped supersonic beam and has a custom scanning probe microscope with the surface plane normal to the beam. This geometric arrangement allows us to perform real-time and real-space *in-situ* experiments. This study consists of exploring the potential energy surface for molecular oxygen adsorption on Si(111)-7x7. The questions that are being addressed are fundamental for issues relating to semiconductor oxidation as well as being of direct relevance to semiconductor processing. The site-specific locations of molecular oxygen reactivity on Si(111)-7x7 surfaces are not clear and remains a topic of current discussion. Recent spectroscopic studies show that by controlling the molecular beam energy (E_k) one can activate different adsorption pathways for molecules on surfaces. However, the effect of collimated and energy-selected beams impacting the surface at different incident angles has not been observed *in-situ* at the local molecular level until now. We will show high-resolution spatial images of the initial stages of oxygen adsorption on Si(111)-7x7 at different beam energies. The comparison of Si(111)-7x7 oxidation *via* thermal oxygen versus the specific adsorption sites that arise at different beam energies will also be discussed. The results indicate that using supersonic beams in this matter may provide enhanced control of semiconductor oxidation chemistry.

5:00pm SS+AS+EM+EN-ThA9 Surface Band-Bending Upon Oxidation of Wurtzite and Zincblende InAs Depending on Surface Orientation and atomic Structure, *Rainer Timm, M. Hjort, J. Knutsson, O. Persson, A. Troian, S. Lehmann, K.A. Dick, A. Mikkelsen*, Lund University, Sweden
InAs is known to typically show n-type behavior with an electron accumulation layer at the surface. Many studies have been performed for evaluating to which extend this behavior is due to adsorbates such as a native oxide layer, or to specific surface orientations and reconstructions of clean InAs. InAs nanowires (NWs) add an extra degree of complexity, since they can exist both in zincblende and wurtzite crystal structure, typically exhibiting unintended switching between both stacking orders during epitaxial growth. During recent years, a strong debate has been going on about how far such crystal phase mixing influences the conductivity of InAs NWs and therewith their suitability for high-mobility device application [1]. A staggered band alignment with band offsets in the range of up to 0.1 eV between zincblende and wurtzite conduction band edges has been reported, based on transport measurements in ambient atmosphere [2]. In contrast, our recent study of clean and unreconstructed InAs NW surfaces based on scanning tunneling microscopy and spectroscopy (STM/S) in ultrahigh vacuum showed aligned conduction band edges for zincblende [110[and wurtzite [11-20[surfaces [3].

Here, we present a systematic study of surface band-bending upon cleaning and oxidation of various InAs surfaces, including purely zincblende or purely wurtzite NWs, obtained by synchrotron-based X-ray photoemission spectroscopy (XPS). We were able to clean all investigated InAs surfaces from their native oxide by annealing them in the presence of atomic hydrogen [3]. Different rates of cleaning and re-oxidation were observed for the different surfaces. Even more importantly, from the energy shifts of the investigated core-levels upon oxidation, varying between 0.1 and 0.3 eV for various surfaces, we obtained significant differences in oxide-induced surface band-bending for different surface orientations. We will compare our XPS results with the atomic and local electronic structure of the specific surfaces as obtained by STM/S [4]. Our results indicate that the band alignment along InAs heterostructures, and therewith the transport

properties of InAs NWs, depend on the surface orientation, composition, and atomic structure rather than the crystal phase of the specific InAs segments.

[1] Thelander *et al.*, Nano Lett. **11**, 2424 (2011)

[2] Dayeh *et al.*, Adv. Funct. Mater. **19**, 2102 (2009)

[3] Hjort *et al.,* ACS Nano **12**, 12346 (2014)

[4] Knutsson *et al.*, ACS Appl. Mater. Interfaces **7**, 5748 (2015)

5:20pm **SS+AS+EM+EN-ThA10** **Control of Oxygen Defect Surface Injection in ZnO via Sub-Monolayer Sulfur Adsorption**, *Ming Li*, *E. Seebauer*, University of Illinois at Urbana-Champaign

Native oxygen defects within metal oxide semiconductors such as ZnO affect the material's performance in applications for photovoltaics, nanoelectronics, gas sensing, and photocatalysis. Previous work in this laboratory has shown that the semiconducting metal oxides surfaces can be used to manipulate the concentrations and spatial distributions of bulk oxygen defects, particularly oxygen vacancies. The interaction chemistry between bulk point defects and reactive sites on semiconductor surfaces is comparable in richness to the reactions of surfaces with gases. The present work discusses a novel mechanism of controlling oxygen defect injection in c-plane ZnO(0001) through surface active sites blocking with sub-monolayer sulfur adsorption. Oxygen diffusion rates were measured by exposing single-crystal ZnO to isotopically labeled oxygen ($^{18}O_2$) gas. Sulfur was deposited controllably via an electrochemical cell and characterized *in situ* by Auger Electron Spectroscopy (AES). The resulting diffusion profiles were measured by secondary ion mass spectrometry (SIMS). Kinetic parameters were extracted by fitting the diffusion profiles with a previously derived mass transport model. The preliminary data shows that sulfur adsorption decreases the oxygen defect injection rate by roughly three times through affecting the injection flux, which points to a site blocking model. Subsequent temperature and pressure dependence study will help us gain insights into detailed injection kinetic pathways.

5:40pm **SS+AS+EM+EN-ThA11** **Investigation of the Role of Electronic Defects and Grain Boundaries in Sputter Deposited CdS/CdTe Junctions and Solar Cells**, *Mohit Tuteja*, University of Illinois at Urbana Champaign, *P. Koirala*, University of Toledo, *J. Soares,* University of Illinois at Urbana Champaign, *R. Collins,* University of Toledo, *A. Rockett*, University of Illinois at Urbana Champaign

Device quality CdS/CdTe heterostructures and completed solar cells (~12% efficient) have been studied using low-temperature photoluminescence (PL) as a function of temperature (82-295 K) and laser excitation power (0.02-2 mW). The CdS/CdTe junctions were grown on transparent conducting oxide covered soda lime glass using rf-sputter deposition. It was found that the luminescence shifts from being dominated by sub-gap defect-mediated emission at lower excitation powers to near band edge excitonic emission at higher excitation powers. The effect of copper (Cu) used in making back contacts was studied in connection with the CdS/CdTe junction PL. It was found that the presence of Cu suppresses the sub-band gap PL emissions. This effect was concluded to be due either to Cu occupying cadmium vacancies (V_{Cd}) or forming acceptor complexes with them. This points to a potential role of Cu in plugging sub-band gap recombination routes and hence increasing charge separation ability of the device. An energy band diagram is presented indicating various observed transitions and their possible origins.

Electronic Materials and Processing
Room: 211C - Session EM+AS+EN+NS-FrM

Nanoparticles for Electronics and Photonics
Moderator: Jessica Hilton, Mantis Deposition, Joseph G. Tischler, U.S. Naval Research Laboratory

8:20am EM+AS+EN+NS-FrM1 Elimination of Bias-stress Effect in Ligand-free Quantum Dot Field-effect Transistors, *Matt Law*, UC Irvine **INVITED**

Colloidal quantum dot (QD) solids are the subject of active research with applications emerging in light-emitting diodes, field-effect transistors, and solar cells. In this talk, I describe the use of atomic layer deposition (ALD) infilling to engineer the surfaces and interfaces of PbSe QD films in order to produce high-performance QD field-effect transistors (FETs) that completely lack bias-stress effect (i.e., drain current transients caused by charge trapping near the dielectric/channel interface). This ALD "matrix engineering" approach includes steps designed to manage ligand concentrations, passivate surface states, and arrest ionic motion within the films, resulting in the first high-mobility (~14 cm V^{-1} s^{-1}), environmentally stable, and transient-free PbX QD transistors. Two bias-stress mechanisms in QD FETs are identified and discussed. The implications of these mechanisms for the operation of QD solar cells is highlighted.

9:00am EM+AS+EN+NS-FrM3 Ultra High Sensitive CO Sensors with Less Overhead: Influence of Doping Methods and Dopants on the CO Sensitivity of Cu, Pt and Pd Doped SnO_2 Pellets, *Karthik Tangirala*, M.A. Olvera, CINVESTAV-IPN, Mexico

In this work, we report the synthesis, characterization and manufacturing of Cu, Pt and Pd doped SnO_2 pellets with ultra high sensitivities for CO atmospheres. To the best of our knowledge, we have accounted for the first time the ultra high CO sensitivities for Cu doped than Pt and Pd doped SnO_2 pellets. In order to obtain high sensitivities, we have employed novel methods, which are the mixture of chemical and physical synthesis methods. Non-spherical SnO_2 structures were prepared via two chemical synthesis routes using Urea (R1) and ammonia (R2) as precipitation agents. The resultant SnO_2 powders were doped with transition metal, Cu, and noble metals like Pt and Pd via two doping methods D1 and D2. In D1, the powders were bulk doped and then ball milled, whereas in D2, the powders were ball milled and then surface doped. All the powders obtained were later pressed using manual pressing machine to manufacture the SnO_2 pellets. The effect of synthesis routes, doping methods and dopants, on the structural, morphological and also on CO sensing were studied by different characterization techniques and reported with their detailed explanations. Interestingly, the Cu-SnO_2 pellets manufactured from the powders obtained by method D1R1, showed highest sensitivity around 1783 due to various reasons like uniform and small particle size, necks formation, inter-particle conductance and high oxygen adsorption due to stacking faults. All the reasons mentioned above were demonstrated by comparing the established sensor theory with our different experimental results obtained using XRD, Raman, SEM, HRTEM and sensitivity analysis.

9:20am EM+AS+EN+NS-FrM4 Selective Nucleation of Quantum Dots on Spontaneously Nanopatterned Surfaces, *Davide Del Gaudio*, S. Huang, L. Aagesen, K. Thornton, R.S. Goldman, University of Michigan, Ann Arbor

Controlled lateral ordering of self-assembled semiconductor quantum dots (QDs) is desirable for a wide range of solid-state applications, including solar cells, lasers, and telecom devices. To date, lateral alignment of QDs has been demonstrated for multilayers of QDs.[1]

In these cases, the first layer of QDs is isotropically distributed; subsequently, during the growth of QD stacks, the accumulation of anisotropic strain often results in lateral QD alignment. However, a significant remaining question concerns the *direct* influence of spontaneous surface patterning on the selective nucleation of QDs.

In this work, we use a combined experimental-computational approach to directly examine correlations between buffer surface morphology and QD nucleation. For this purpose, we exploit a surface instability induced by the anisotropy of the surface diffusion constant of ad-atoms (the Ehrlich-Schwöbel effect[2]) which leads to the formation of elongated ripples, often termed "mounds". For epitaxial growth of InAs QDs on GaAs, Ye et al. reported a preference for in-plane QD alignment along the mound lengths[1]. Here, our one-dimensional phase-field model reveals a preference for QD nucleation in regions of positive curvature,[3] such as on the sides of the

mounds and/or in the "valleys" between the mounds. In our experiments, we explore the formation of InAs QDs on AlGaAs mounds using various substrate temperatures and indium exposure times.

We explore the use of fixed geometry indium evaporation as an approach to restrict QD nucleation to one side of the AlGaAs mounds, resulting in the formation of 1D QD chains.[4] Specifically, for substrate temperature of 580°C, a high density of AlGaAs mounds is observed along [0-11]. For 3 monolayer (ML) of InAs deposition, we achieved selective positioning of QDs, with an average diameter of 16nm, on one side of the mounds.

We will discuss the influence of the As species (As2 vs As4) and growth interrupts on the size, density, and spatial arrangement of QDs. We will also present a detailed analysis of the surface instabilities that induce ripple formation, and the As adsorption kinetics, which lead to the anisotropic nucleation.

References

[1] W. Ye, S. Hanson, M. Reason, X. Weng, and R. S. Goldman. (2005). *J. Vac. Sci. Technol.* B **23**, 1736-1740.

[2] Schwöbel, R. L., & Shipsey, E. J. (1966). *J. App. Phys.*, **37**(10), 3682–3686.

[3] Seol, D. J., Hu, S. Y., Liu, Z. K., Chen, L. Q., Kim, S. G., & Oh, K. H. (2005) *J. Appl. Phys.*, **98**(4), 044910.

[4] Arciprete, F., Placidi, E., Magri, R., Del Gaudio, D., Patella, F. (2013) *J. Mat. Res.***28**(23), 3201–3209

9:40am EM+AS+EN+NS-FrM5 Tailor-made Gas Phase based Nanoparticles with Functional Properties, *Gert ten Brink*, B. Kooi, G. Palasantzas, University of Groningen, The Netherlands **INVITED**

Using a home modified Mantis dedicated nanocluster© source we have the possibility to produce nanoparticles (NPs) of a great variety of materials with relatively small size dispersion and with properties that can be novel and different from their bulk counterpart. The system works on the principle of inert gas condensation and magnetron sputtering. We have produced a whole range of different NPs with size and motif control.

Covalent bonded NPs, in particular carbon;

Metallic NPs: Cu^1, Fe, Mg, Mo, Co, Al, Ag, Nb, Ti, Pd;

Semiconductor NPs, in particular Ge;

Bimetallic NPs: MgNi, MoCu, MgTi with several compositions;

Ternary alloy NPs, e.g. GeSbTe with several compositions and with amorphous and crystallinity control.

The particles can be deposited on most surfaces provided they have good vacuum compatibility.

The applications range from novel:

Wetting phenomena; Cu NPs covered surfaces giving rose petal effect[2];

Bimetallic Mo-Cu NPs which are bulk immiscible but in NPs fully miscible[3];

Bimetallic NPs for hydrogen storage[4]: MgNi, MgTi, MgCu;

Magnetic NPs: Fe-Fe_3O_4 core-shell particles for medical applications.

1. Brink, G. H. ten, Krishnan, G., Kooi, B. J. & Palasantzas, G. Copper nanoparticle formation in a reducing gas environment. *J. Appl. Phys.* **116**, 104302 (2014).

2. Ten Brink, G. H., Foley, N., Zwaan, D., Kooi, B. J. & Palasantzas, G. Roughness controlled superhydrophobicity on single nanometer length scale with metal nanoparticles. *RSC Adv.* **5**, 28696–28702 (2015).

3. G. Krishnan, M.A. Verheijen, G.H. ten Brink, G. Palasantzas, B.J. Kooi, Tuning structural motifs and alloying of bulk immiscible Mo-Cu bimetallic nanoparticles by gas-phase synthesis, *Nanoscale* **5**, 5375-5383 (2013).

4. Krishnan, G. *et al.* Synthesis and exceptional thermal stability of Mg-based bimetallic nanoparticles during hydrogenation. *Nanoscale* **6**, 11963-11970 (2014).

10:20am EM+AS+EN+NS-FrM7 A New Surfactant for Directed Deposition of Carbon Nanomaterials, *Hanna Nilsson*, University of Maryland, L. de Knoop, Chalmers University, J. Ticey, B. Meany, Y. Wang, University of Maryland, E. Olsson, Chalmers University, J. Cumings, University of Maryland

We show the results of using a new surfactant, ammonium laurate (AL), to suspend and deposit carbon nanostructures. In a recent publication[1], we show that multi-walled carbon nanotubes (MWCNTs) can be suspended in AL with much better shelf stability as compared with the common surfactant sodium dodecyl sulfate (SDS). AL differs from SDS only by the

choice of ionic species, but the deposition process with AL is more reliable and cleaner than with SDS. We use a process of producing a charged self-assembled monolayer on the substrate and then exposing the substrates to the aqueous surfactant solution of MWCNTs to achieve directed deposition of clean individual MWCNTs, which can then be used for fabrication of individual nanotube devices. In addition to these results, we show results for single-walled carbon nanotubes (SWCNTs) in AL, which show that nanotubes deposited from AL have lower electrical contact resistance as compared to those deposited from SDS. Photoluminescence results also show that SWCNTs with specific chirality are preferentially suspended in AL, which may present a separation and purification pathway. We will also present extensions of the work to single and few layer graphene sheets, where AL can be used to make clean depositions from aqueous solution onto sensitive substrates.

(1) Nilsson, H. M.; Meany, B.; Ticey, J.; Sun, C.-F.; Wang, Y.; Cumings, J. Ammonium Laurate Surfactant for Cleaner Deposition of Carbon Nanotubes. *Langmuir* **2015**, *31*, 6948-6955.

10:40am **EM+AS+EN+NS-FrM8 Compositional Control and Doping Uniformity in Spray Pyrolyzed CZTS Nanoparticles and Films**, *Stephen Exarhos, A. Alvarez, J. Hernandez, L. Mangolini*, University of California - Riverside

An innovative and scalable synthesis approach to the formation of stoichiometric Cu_2ZnSnS_4 (CZTS) nanocrystals has been developed using aerosol spray pyrolysis. This quaternary phase material is a potential replacement for currently commercialized semiconductors such as CdTe and CIGS that are used in photovoltaic devices. However, sustainability and environmental issues threaten long-term viability of these materials. Based upon earth abundant constituents and low chemical toxicity, CZTS, with a reported bandgap of ~1.5 eV[1], appears to be a superior alternative to these other materials. Additional research and development is necessary to increase the efficiency of CZTS-based cells from the current record (12.6% by Wang *et al*.[2]) to the >18% necessary to be considered commercially viable. Our work demonstrates the controllable, cost-effective, and reproducible synthesis of high-quality CZTS nanoparticles and films. A modified spray pyrolysis method involving decomposition of copper, zinc, and tin diethyldithiocarbamate precursors allows uniform incorporation of dopants (such as sodium) that are known to increase crystal grain growth during nanoparticle sintering[3]. Once formed, the nanoparticles are deposited onto a substrate from a methanol dispersion using an "ink-spray" process with an argon-driven airbrush. To form an efficient absorber layer in a photovoltaic device, the coating is then annealed in a sulfur-vapor atmosphere resulting in a thin film with uniformly large crystal grain morphology throughout the film thickness (~1-2 μm). The deposited films are characterized with respect to crystalline phase, stoichiometry, and overall film quality. Further preliminary results regarding the formation of $Cu_2ZnSn_{(1-x)}(IV)_xS_4$ by means of this processing approach will be reported.

[1] H. Wang. "Progress in Thin Film Solar Cells Based on Cu_2ZnSnS_4," International Journal of Photoenergy 2011 (2011).

[2] Wang, Wei, Mark T. Winkler, *et al*. "Device Characteristics of CZTSSe Thin-Film Solar Cells with 12.6% Efficiency." Advanced Energy Materials 4, no. 7 (2014).

[3] Johnson, M., S. V. Baryshev, *et al*. "Alkali-Metal-Enhanced Grain Growth in Cu2ZnSnS4 Thin Films." Energy & Environmental Science 7, no. 6 (2014): 1931–38.

Authors Index
Bold page numbers indicate the presenter